

UNCLASSIFIED

AD NUMBER
ADB017944
NEW LIMITATION CHANGE
TO Approved for public release, distribution unlimited
FROM Distribution authorized to U.S. Gov't. agencies only; Test and Evaluation; Dec 1976. Other requests shall be referred to the Air Force Flight Dynamics Laboratory, Attn: FBR, Wright-Patterson AFB, OH 45433
AUTHORITY
AFFDL ltr, 13 Jul 1979

THIS PAGE IS UNCLASSIFIED

AD BO 17944

AFFDL-TR-76-161 ✓

# A FINITE ELEMENT MACH BOX PROCEDURE FOR FLUTTER PREDICTION OF PANELS IN THREE-DIMENSIONAL SUPERSONIC UNSTEADY POTENTIAL FLOW

DECEMBER 1976

TECHNICAL REPORT AFFDL-TR-76-161  
FINAL REPORT FOR PERIOD JUNE 1976 - DECEMBER 1976

Distribution limited to U.S. Government agencies only; test and evaluation; statement applied in December 1976. Other requests for this document must be referred to AF Flight Dynamics Laboratory, (FBR), Wright-Patterson, AFB, Ohio 45433.

AU NU. \_\_\_\_\_  
DDG FILE COPY

AIR FORCE FLIGHT DYNAMICS LABORATORY  
AIR FORCE WRIGHT AERONAUTICAL LABORATORIES  
AIR FORCE SYSTEMS COMMAND  
WRIGHT-PATTERSON AIR FORCE BASE, OHIO 45433

7B D C  
MAY 9 1977

REPRODUCED FROM  
BEST AVAILABLE COPY

D

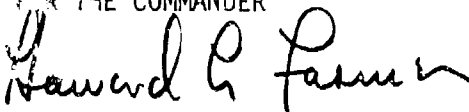
NOTICE

When Government drawings, specifications, or other data are used for any purpose other than in connection with a definitely related Government procurement operation, the United States Government thereby incurs no responsibility nor any obligation whatsoever; and the fact that the Government may have formulated, furnished, or in any way supplied the said drawings, specifications, or other data, is not to be regarded by implication or otherwise in any manner licensing the holder or any other person or corporation, or conveying any rights or permission to manufacture, use, or sell any patented invention that may in any way be related thereto.

This technical report has been reviewed and is approved for publication.

  
\_\_\_\_\_  
JAMES J. OLSEN  
Project Engineer

FOR THE COMMANDER

  
HOWARD L. FARMER, Colonel, USAF  
Chief, Structural Mechanics Division

Copies of this report should not be returned unless return is required by security considerations, contractual obligations, or notice on a specific document.

THIS REPORT HAS BEEN DELIMITED  
AND CLEARED FOR PUBLIC RELEASE  
UNDER DOD DIRECTIVE 5200.20 AND  
NO RESTRICTIONS ARE IMPOSED UPON  
ITS USE AND DISCLOSURE.

DISTRIBUTION STATEMENT A

APPROVED FOR PUBLIC RELEASE;  
DISTRIBUTION UNLIMITED.

Best Available Copy

UNCLASSIFIED

SECURITY CLASSIFICATION OF THIS PAGE (When Data Entered)

REPORT DOCUMENTATION PAGE		READ INSTRUCTIONS BEFORE COMPLETING FORM
1. REPORT NUMBER	2. GOVT ACCESSION NO.	3. RECIPIENT'S CATALOG NUMBER
1- ) AFFDL-TR-76-161		9 )
4. TITLE (and Subtitle)	5. TYPE OF REPORT & PERIOD COVERED	
6 ) A FINITE ELEMENT MACH BOX PROCEDURE FOR FLUTTER PREDICTIONS OF PANELS IN THREE-DIMENSIONAL SUPERSONIC UNSTEADY POTENTIAL FLOW.	Final Report June 1976-December 1976	
7. AUTHOR(S)	8. CONTRACT OR GRANT NUMBER(S)	
10 ) J. Y. YANG		
9. PERFORMING ORGANIZATION NAME AND ADDRESS	10. PROGRAM ELEMENT PROJECT TITLE AREA & WORK UNIT NUMBER(S)	
AFSC (AFWAL) AF Flight Dynamics Laboratory (FBR) Structural Mechanics Division, WPAFB, Ohio 45433	12-130705	
11. CONTROLLING OFFICE NAME AND ADDRESS	12. REPORT DATE	13. NUMBER OF PAGES
Air Force Flight Dynamics Laboratory Structural Mechanics Division Wright-Patterson AFB, Ohio 45433	11 ) December 1976	92
14. MONITORING AGENCY NAME & ADDRESS (if different from Controlling Office)	15. SECURITY CLASSIFICATION (including changes)	
	UNCLASSIFIED	
16. DISTRIBUTION STATEMENT (of this Report)		
Distribution limited to U.S. Government agencies only; test and evaluation; statement applied in December 1976. Other requests for this document must be referred to AF Flight Dynamics Laboratory, (FBR), Wright-Patterson AFB, Ohio 45433.		
17. DISTRIBUTION STATEMENT (of the abstract entered in Block 20, if different from Report)		
N/A		
18. SUPPLEMENTARY NOTES		
N/A		
19. KEY WORDS (Continue on reverse side if necessary and identify by block number)		
Aeroelasticity                      Finite Elements                      Mach Box Panel Flutter                      Supersonic Flow		
20. ABSTRACT (Continue on reverse side if necessary and identify by block number)		
A finite element formulation and solution procedure are developed for flutter predictions of rectangular panels with one surface exposed to three-dimensional supersonic unsteady potential flow. The effect of in-plane force is included. Each element is divided into several Mach boxes. The aerodynamic influence coefficients between each pair of sending and receiving boxes are computed by the method of Gaussian quadrature. The aerodynamic matrix is based on the numerically computed velocity potentials for all boxes.		

DD FORM 1 JAN 73 1473

EDITION OF 1 NOV 65 IS OBSOLETE

UNCLASSIFIED

SECURITY CLASSIFICATION OF THIS PAGE (When Data Entered)

012 570

**UNCLASSIFIED**

SECURITY CLASSIFICATION OF THIS PAGE (When Data Entered)

This development is particularly useful in the low supersonic range for panels with chord-span ratio less than about one, while the piston theory does not give satisfactory solution. Examples are demonstrated by using the 16 d.o.f. rectangular plate elements. Results for flutter boundaries for the unstressed panels agree well with an alternative Galerkin's modal solution. The examples demonstrate that flutter boundaries are dominated by higher modes for panels with higher chord-span ratio. They also demonstrate that the dominating flutter boundaries abruptly change modes as the Mach number is varied. The beneficial effect of in-plane tension is demonstrated.

**UNCLASSIFIED**

SECURITY CLASSIFICATION OF THIS PAGE (When Data Entered)



## TABLE OF CONTENTS

<u>SECTION</u>		<u>PAGE</u>
I	INTRODUCTION	1
II	FORMULATION OF EQUATIONS OF MOTION	5
	1. Principle of Virtual Work	5
	2. Aerodynamic Matrix and Aerodynamic Pressure	7
	3. Velocity Potential and Aerodynamic Influence Coefficient	9
III	FORMULATION FOR FLUTTER DETERMINANT IN TERMS OF FINITE ELEMENT SHAPE FUNCTIONS	12
IV	RESULTS	14
	Case 1 - Clamped panels with various chord-span ratios at $M = 1.3$	14
	Case 2 - Clamped panels with $Q/w = 2$ at various Mach numbers	24
	Case 3 - Pinned edge panels with various chord-span ratios at $M = 1.3$	31
	Case 4 - Clamped square panels with various tension parameters and Mach numbers	39
V	CONCLUDING REMARKS	57
	REFERENCES	59
	APPENDIX - THE COMPUTER PROGRAM	61



## ILLUSTRATIONS

<u>FIGURE</u>		<u>PAGE</u>
1	Panel divided into finite elements (solid lines) and boxes (dash lines) with coordinates, dimensions, and Mach cone	6
2	Three forms of integrals for computing the aerodynamic influence coefficients	6
3	Flutter boundaries for clamped panel with $l/w = 1/4$ and $M = 1.3$	16
4	The first mode shape (real part) for panel corresponding to point A in Fig. 3	17
5	The second mode shape (real part) for panel corresponding to point B in Fig. 3	17
6	Flutter boundaries for clamped panel with $l/w = 1/2$ and $M = 1.3$	18
7	The first mode shape (real part) for panel corresponding to point A in Fig. 6	20
8	The second mode shape (real part) for panel corresponding to point B in Fig. 6	20
9	Flutter boundaries for clamped panel with $l/w = 1$ and $M = 1.3$	21
10	The third mode shape (real part) for the center line of panel corresponding to point A in Fig. 9	22
11	The fourth mode shape (real part) for the center line of panel corresponding to point B in Fig. 9	22
12	Flutter boundaries for clamped panel with $l/w = 2$ and $M = 1.3$	23
13	The first mode shape (real part) for panel corresponding to point A in Fig. 12	25

LIST OF ILLUSTRATIONS (Continued)

<u>FIGURE</u>		<u>PAGE</u>
14	The fifth mode shape (real part) for the center line of panel corresponding to point B in Fig. 12	25
15	Flutter boundaries for clamped panel with $l/w = 4$ and $M = 1.3$	26
16	The second mode shape (real part) for panel corresponding to point A in Fig. 15	27
17	The tenth mode shape (real part) for the center line of panel corresponding to point B in Fig. 15	27
18	Flutter boundaries for clamped panel with $l/w = 2$ and $M = 1.05, 1.1$	28
19	Flutter boundaries for clamped panel with $l/w = 2$ and $M = 1.4, 1.5$	29
20	Flutter boundaries for clamped panel with $l/w = 2$ and $M = 2.0, 3.0$	30
21	Thickness required to prevent flutter for clamped aluminum panel with $l/w = 2$ at sea level	32
22	Flutter boundaries for pinned-edge panel with $l/w = 0.25$ and $M = 1.3$	33
23	The first mode shape (real part) for panel corresponding to point A in Fig. 22	34
24	Flutter boundaries for pinned-edge panel with $l/w = 0.5$ and $M = 1.3$	35
25	The first and second mode shapes (real part) corresponding to points A and B, respectively, in Fig. 24	36
26	Flutter boundaries for pinned-edge panel with $l/w = 1$ and $M = 1.3$	37
27	The first and third mode shapes (real part) corresponding to points A and B, respectively, in Fig. 26	38
28	Flutter boundaries for pinned-edge panel with $l/w = 2$ and $M = 1.3$	40

LIST OF ILLUSTRATIONS (Continued)

<u>FIGURE</u>		<u>PAGE</u>
29	The first and fifth mode shapes (real part) corresponding to points A and B, respectively in Fig. 28	41
30	Flutter boundaries for clamped panel of $l/w = 1$ , $M = 1.1$ , and various tension parameters F	42
31	The first mode shape (real part) for panel corresponding to point A in Fig. 30	43
32	The first mode shape (real part) for panel corresponding to point B in Fig. 30	43
33	Flutter boundaries for clamped panels of $l/w = 1$ , $M = 1.2$ , and various tension parameters F	44
34	The first mode shape (real part) for panel corresponding to point A in Fig. 33	45
35	The first mode shape (real part) for panel corresponding to point B in Fig. 33	45
36	The third mode shapes (real part) for the center line of panel with various tension parameter corresponding to points C, D, E, and F, respectively, in Fig. 33	47
37	Flutter boundaries for clamped panels with $l/w = 1$ , $M = 1.3, 1.32, 1.35$ , and various tension parameters F	48
38	Flutter boundaries for clamped panels with $l/w = 1$ , $M = 1.4, 1.45, 1.48$ , and various tension parameters F	49
39	Flutter boundaries for clamped panels with $l/w = 1$ , $M = 1.5$ , and various tension parameters F	50
40	Flutter boundaries for clamped panels with $l/w = 1$ , $M = 1.52$ , and various tension parameters F	51
41	Flutter boundaries for clamped panels with $l/w = 1$ , $M = 1.54$ , and various tension parameters F	52
42	Flutter boundaries for clamped panels with $l/w = 1$ , $M = 1.6$ , and various tension parameters F	53

LIST OF ILLUSTRATIONS (Continued)

<u>FIGURE</u>		<u>PAGE</u>
43	Flutter Boundaries for clamped panels with $Q/w = 1$ , $M = 2$ , and various tension parameters $F$	54
44	Thickness ratios required to prevent flutter for a square clamped aluminum panel at 25,000 feet above sea level and under various values of tension parameters $F$	56

## SYMBOLS

a, b	= length and width of the rectangular plate finite element as defined in Fig. 1.
[A]	= aerodynamic matrix of the panel system
$B_x, B_{xs}$	= number of boxes in the stream and cross-stream directions, respectively
D	= $Eh^3/12(1 - \gamma^2)$ , bending rigidity with $\gamma$ being Poisson's ratio
F	= $N_x/\ell^2\omega_1^2\sigma h$ , Initial in-plane tension parameter
$f_j(x,y)$	= shape function associated with degree of freedom "j"
g	= structural damping coefficient
h	= panel thickness
i, j	= subscripts indicate d.o.f. number
[K]	= stiffness matrix of the panel system
$k_\ell, k_\epsilon$	= $\omega\ell/V, \omega\epsilon/V$ , respectively, reduced frequency
$\ell$	= length of panel in stream direction
[M]	= mass matrix of the panel system
M	= Mach number
m, n	= receiving box index numbers in the stream and cross-stream directions, respectively
[N]	= incremental stiffness matrix of the panel system
$N_x, N_y, N_{xy}$	= panel in-plane line forces
r, s	= $(m - \lambda), (n - \nu)$ , respectively
u, v	= transformed variables of integration based on $\epsilon/2$ as reference length, $u\beta/2 = x_m - \epsilon, v/2 = y_n - \eta$
V	= speed of undisturbed airstream

LIST OF SYMBOLS (Continued)

$w$	= width of panel in cross-stream direction
$w_j$	= downwash velocity at panel surface for d.o.f. "j"
$x, y$	= panel coordinates as defined in Fig. 1
$\bar{x}, \bar{y}$	= $x/\ell, y/w$ , respectively
$x_m, y_n$	= values of $x/\epsilon$ and $y/\epsilon$ at center of box $m, n$
$\alpha_\phi$	= aerodynamic influence coefficient relating the velocity potential at a box to unit downwash on another box (Eq. 12)
$\beta$	= $(M^2 - 1)^{\frac{1}{2}}$
$\epsilon$	= $w/B_{XS}$ , box width
$\xi, \eta$	= values of $x/\epsilon$ and $y/\epsilon$ at any point in the sending box
$\mu$	= panel-air mass density ratio, $\sigma h/\rho \ell$
$\lambda, \nu$	= sending box index number in the stream and cross-stream directions, respectively
$\rho$	= density of undisturbed airstream
$\sigma$	= density of panel
$\tau$	= length-width ratio of box as defined in Fig. 1
$\phi_j(m, n)$	= velocity potential at center of box $m, n$ for d.o.f. "j"
$\bar{\phi}(m, n)$	= velocity potential at center of box $m, n$ due to unit downwash over box $\lambda, \nu$
$\omega$	= frequency of flutter motion
$\omega_1$	= first natural frequency of the panel
$\Omega$	= $(\omega_1/\omega)^2(1 + ig)$
$\bar{\Omega}$	= $M^2 k_\epsilon / \beta^2$

## SECTION I

### INTRODUCTION

Ever since the earliest days of manned flight, panel flutter has been known as one of the most important problems in the design of aircraft, missiles, launched vehicles, and spacecraft. Extensive progress in wind tunnel tests and theoretical studies has been achieved. The basic theories and an account of the developments on panel flutter can be found in, among other books, a recent text by Dowell (Reference 1). A list of keyed bibliography and collection of some significant survey papers and original papers were prepared by Garrick (Reference 2).

The theoretical solution for a panel flutter problem usually requires an accurate aerodynamic and structural theory to formulate a set of complex eigenvalue equations of motion interacted between the panel and the flow. One of the most common theoretical methods is the modal method where the aerodynamic pressure and the inertial and elastic forces of the panel are obtained by assuming the displacements as composed of a number of natural modes and generalized coordinates. The natural frequencies and corresponding normal mode shapes are obtained either theoretically or experimentally, or both. Since the finite element method is powerful and practical in the free vibration analysis of panels with arbitrary geometrical and boundary conditions, it is commonly used in obtaining natural frequencies and mode shapes in the modal method.

As an alternative approach, the finite element workers have formulated the matrix of aerodynamic pressure by using the

displacement functions as composed of the nodal degrees of freedom and shape functions rather than the generalized coordinates and natural mode shapes. Such approach can directly solve for the flutter frequencies and corresponding normal mode shapes without having to seek the natural frequencies and modes and choose the number of modes before the eigensolution, and also without having to compute the flutter mode shapes after the eigensolution. Such approach permits expression of the equations of motion in an elegant and straightforward form. Such approach also permits generality in panel configurations and boundary conditions, and allows for flexibility to accurately include physical effect such as in-plane forces.

The finite element method was first extended to the panel flutter problems by Olson (Reference 3). He formulated the aerodynamic matrix explicitly for an infinite plate element. Olson (Reference 4) later formulated the aerodynamic matrices for two rectangular (12 and 16 d.o.f.) and an 18 d.o.f. triangular plate elements. Simultaneously, but independently, Appa and Somashekar (Reference 5) formulated the aerodynamic matrix for a 12 d.o.f. rectangular plate element. Appa, Somashekar and Shah (Reference 6) later extended their work by accounting for skew panels and yawed flow by means of coordinate transformation. Sander, Bon, and Geradin (Reference 7) employed the CQ conforming quadrilateral plate finite element for flutter analysis of rectangular panels with yawed flow and in-plane stresses.



In all the above finite element works (References 3 - 7), Lighthill's linearized piston theory was employed. The Mach numbers considered were above approximately 1.6. Recently, Yang (Reference 8) developed a finite element procedure using the exact linearized two-dimensional theory (strip theory) for unsteady supersonic flow to formulate an infinite plate finite element by means of numerical integration. The flutter speed considered thus could be in the lower supersonic range. Such formulation cannot, however, be adequately applied to the more general case of rectangular panels with finite aspect ratios.

In this report, the three-dimensional supersonic unsteady potential flow theory is employed to formulate the plate finite elements so that the flutter problems of the finite panels in low supersonic range can be treated.

The aerodynamic matrix is derived by using the principle of virtual work. The aerodynamic forces or velocity potentials that produce the work are obtained for each d.o.f. by the Mach box method. Each finite element is divided into several boxes. The aerodynamic influence coefficients for each pair of sending and receiving boxes are evaluated, for each d.o.f., by the method of Gaussian quadrature. The velocity potential at each receiving box is obtained, for each d.o.f., by summation of the product of corresponding downwash and influence coefficients for all sending boxes. It should be noted that a similar box method was used by Cunningham (Reference 9) in conjunction with a Galerkin's modal method for panel flutter analysis. Such 3-D aerodynamic theory was also employed by Dowell and Voss (Reference 10) in a theoretical and experimental correlation study of panel flutter.

The 16 d.o.f. conforming rectangular plate element (Reference 11) was used for example demonstrations. Flutter boundaries were found for clamped rectangular panels with various aspect ratios. The thickness ratios required to prevent flutter of an aluminum panel at sea level were plotted for Mach numbers ranging from 1.05 to 3. Results found are in favorable agreement with Cunningham's solution (Reference 9).

The initial in-plane tensile stresses were then included in finding the flutter boundaries for a clamped aluminum panel. The thickness ratios required to prevent flutter of the panel at 25,000 feet altitude were obtained for Mach numbers ranging from 1.05 to 2.0 for various values of tension. It was found that the dominating flutter mode changed abruptly as Mach number was varied.

SECTION II  
FORMULATION OF EQUATIONS OF MOTION

The free vibration equations of motion for a finite element panel subjected to the effect of stiffness, in-plane force, inertia, and aerodynamic pressure may be written as

$$[K]\{q\} + [N]\{q\} + [M]\{\ddot{q}\} + [A]\{q\} = \{0\} \quad (1)$$

where  $[K]$ ,  $[N]$ ,  $[M]$ , and  $[A]$  are, respectively, the stiffness, incremental stiffness, mass, and aerodynamic matrices assembled for the whole finite element system. The vector  $\{q\}$  contains the nodal degrees of freedom for the whole panel system. In this section, only the system aerodynamic matrix is formulated.

1. PRINCIPLE OF VIRTUAL WORK

For a system of plate finite elements, the deflection and aerodynamic pressure may be written by separating the time and space variables as,

$$\begin{aligned} \bar{z}(x,y,t) &= z(x,y)e^{i\omega t} \\ \bar{p}(x,y,t) &= p(x,y)e^{i\omega t} \end{aligned} \quad (2)$$

where the coordinates are defined in Fig. 1.

The strain energy for the panel system is equal to the work produced by the aerodynamic pressure

$$U = \frac{1}{2} \iint z(x,y)p(x,y) \, dx dy \quad (3)$$

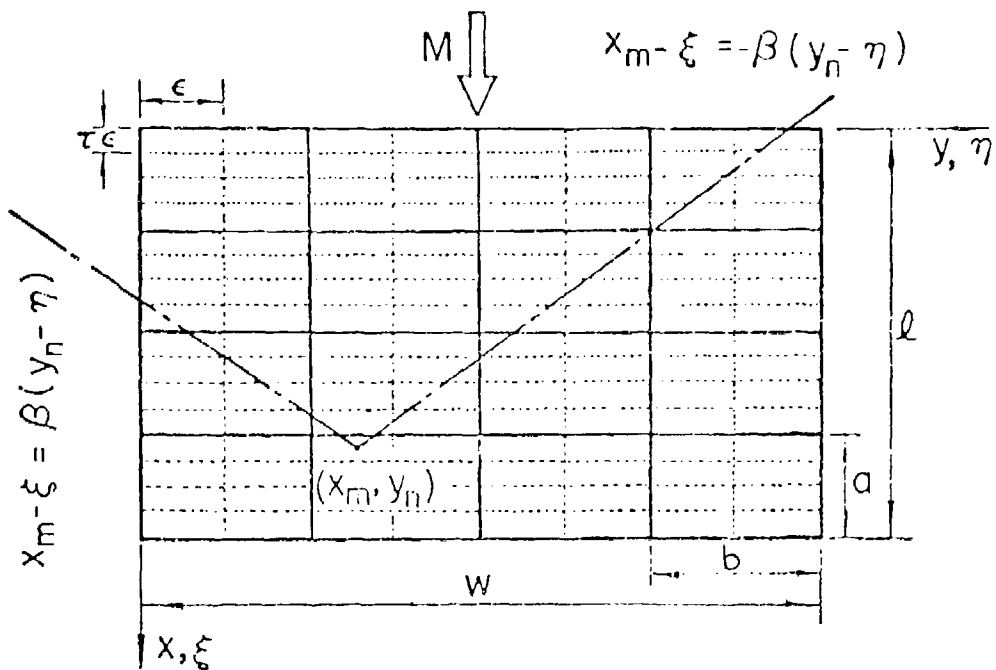


Figure 1. Panel divided into finite elements (solid lines) and boxes (dash lines) with coordinates, dimensions, and Mach core

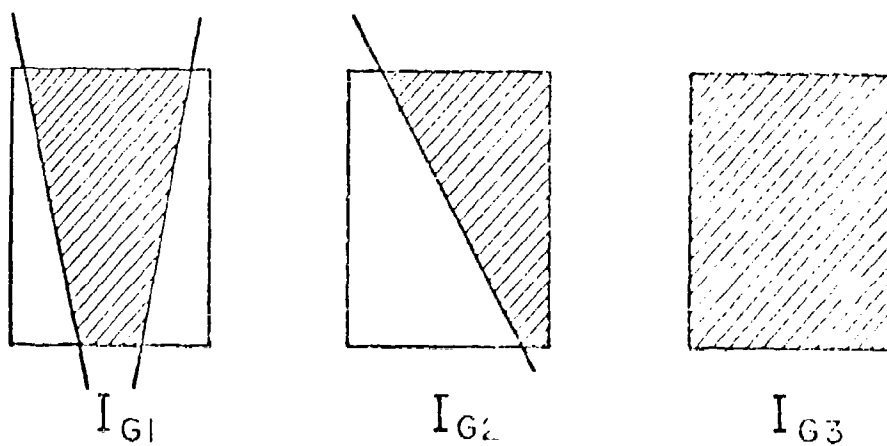


Figure 2. Three forms of integrals for computing the aerodynamic influence coefficients

The deflection function for the total finite element system may be assumed as

$$z(x,y) = \sum_{j=1}^N f_j(x,y)q_j = \{f\}^T\{q\} \quad (4)$$

where  $f_j(x,y)$  represents the assembled shape function corresponding to the nodal d.o.f. " $q_j$ " and  $N$  is the number of degrees of freedom for the entire panel system. Usually,  $q_j$  represents deflection, slopes, twist, and curvatures of the plate at the nodal point  $j$ .

Similarly, the aerodynamic pressure may be assumed as

$$p(x,y) = \sum_{j=1}^N P_j(x,y)q_j = \{P\}^T\{q\} \quad (5)$$

where  $P_j(x,y)$  is defined in Eq. (8) as the pressure function associated with the shape function  $f_j(x,y)$  and d.o.f. " $q_j$ ."

Substituting Eqs. (4) and (5) into (3), the strain energy expression becomes

$$U = \frac{1}{2} \{q\}^T[A]\{q\} \quad (6)$$

with

$$[A] = \iint \{f\}\{P\}^T dx dy \quad (7)$$

Using the principle of virtual work, it can be interpreted that Eq. (7) yields the aerodynamic matrix.

## 2. AERODYNAMIC MATRIX AND AERODYNAMIC PRESSURE

The aerodynamic perturbation pressure is obtained from the linearized three-dimensional supersonic unsteady potential flow theory. When associated

with the d.o.f. "q<sub>j</sub>" and the shape function f<sub>j</sub>(x,y), the perturbation pressure may be expressed in terms of the velocity potential through the relation (see, for example, Ref. 12),

$$P_j(\bar{x}, \bar{y}) = -\frac{\rho V}{\ell} \left( \frac{\partial \phi_j}{\partial \bar{x}} + i \frac{\omega \ell}{V} \phi_j \right) \quad (8)$$

where  $\phi_j$  is the velocity potential associated with d.o.f. "q<sub>j</sub>".

The coefficient for the ith row and jth column of the aerodynamic matrix [A] is obtained by substituting Eq. (8) into Eq. (7).

$$A_{ij} = -\frac{\rho V}{\ell} \iint f_i(\bar{x}, \bar{y}) \left( \frac{\partial \phi_j}{\partial \bar{x}} + i \frac{\omega \ell}{V} \phi_j \right) d(\ell \bar{x}) d(w \bar{y}) \quad (9)$$

Performing integration by parts and assuming restrained trailing edge, Eq. (9) becomes

$$A_{ij} = \frac{\rho V}{\ell} \iint \phi_j \left( \frac{\partial f_i}{\partial \bar{x}} - i \frac{\omega \ell}{V} f_i \right) d(\ell \bar{x}) d(w \bar{y}) \quad (10)$$

where the quantity within the parentheses is the complex conjugate of the downwash ratio for unit d.o.f. "q<sub>i</sub>" and unit panel length. The coefficient A<sub>ij</sub> is evaluated numerically through the following simple summation

$$A_{ij} = \frac{\rho V}{\ell} \sum \phi_j \left( \frac{\partial f_i}{\partial \bar{x}} - i \frac{\omega \ell}{V} f_i \right) \cdot (\text{Box Area}) \quad (11)$$

where the summation is to be made for every box and the quantities related to  $\phi_j$  and  $f_i$  are evaluated numerically at the center of each box. The method for numerically evaluating the velocity potential at the center of each box is given as follows.

### 3. VELOCITY POTENTIAL AND AERODYNAMIC INFLUENCE COEFFICIENT

The method of Mach box as employed by Cunningham in Reference 9 is used here to derive the aerodynamic influence coefficients between each pair of boxes and the resulting velocity potentials at each box.

In this method, each finite element is divided into several equal-size boxes as shown in Fig. 1. The numbers of boxes in the stream and cross-stream directions are defined as  $B_X$  and  $B_{XS}$ , respectively. The width and length of each box are defined as  $\epsilon$  and  $\tau\epsilon$ , respectively, where  $\epsilon = w/B_{XS}$  and  $\tau = zB_{XS}/wB_X$ . The boxes are numbered in sequence from the origin with  $m$  (or  $\lambda$ ) and  $n$  (or  $\nu$ ) as the box number in the stream and the cross-stream directions, respectively. The numbers  $(m,n)$  and  $(\lambda,\nu)$  refer to the receiving and sending boxes, respectively.

The boxes are assumed as sufficiently small so that the downwash over any sending box is considered as uniformly distributed at any instant, and the resulting perturbation pressure at the center of each receiving box represents the average of the pressure distributed over the box.

The velocity potential at the center of a receiving box  $(m,n)$  due to a uniformly distributed but otherwise unspecified downwash  $w(\lambda,\nu)$  over the sending box  $(\lambda,\nu)$  can be expressed, for harmonic motion, as

$$\bar{\phi}(m,n) = \epsilon w(\lambda,\nu) \alpha_\phi(r,s) \quad (12)$$

where the relative locations in stream and cross-stream directions, respectively, between the two boxes are defined as  $r = m - \lambda$  and  $s = n - \nu$ . The aerodynamic influence coefficient from Reference 9 is,

$$\alpha_{\phi}(r,s) = \frac{1}{2\pi} \int_{u_1}^{u_2} e^{-i(\beta\bar{\omega}/r)u} \left\{ \cos^{-1} \frac{v_1}{u} - \cos^{-1} \frac{v_2}{u} + \int_{v_1}^{v_2} \frac{\cos\left[\frac{\beta\bar{\omega}}{2M}(u^2-v^2)^{1/2}\right] - 1}{(u^2-v^2)^{1/2}} dv \right\} du \quad (13)$$

where all the parameters are defined in the List of Symbols.

In Eq. (13), the surface integration limits  $u_1$ ,  $u_2$ ,  $v_1$ , and  $v_2$  result in only three different forms  $I_{G1}$ ,  $I_{G2}$ , and  $I_{G3}$  as shown in Fig. 2.

The first form is for any portion of a sending box ( $x, y$ ) cut by both sides of the Mach cone so that  $v_2 = -v_1 = u$  and  $s = 0$ .

$$I_{G1} = \frac{1}{2} \int_{u_1}^{u_2} e^{-i(\beta\bar{\omega}/r)u} J_0\left(\frac{\beta\bar{\omega}}{2M} u\right) du \quad (14)$$

where  $J_0$  is the Bessel function of the first kind of order zero.

The second form is for portions of a box cut by one side of the Mach cone so that the limits  $v_2 = u$  and  $v_1 = 2s - 1 \geq 1$ .

$$I_{G2} = \frac{1}{2\pi} \int_{u_1}^{u_2} e^{-i(\beta\bar{\omega}/r)u} \left\{ \cos^{-1} \frac{v_1}{u} + \int_{v_1}^u \frac{\cos\left[\frac{\beta\bar{\omega}}{2M}(u^2-v^2)^{1/2}\right] - 1}{(u^2-v^2)^{1/2}} dv \right\} du \quad (15)$$

The third form is for boxes that are completely within the Mach cone and also for portions of boxes ahead of the point where the Mach line cuts the side of the box.

$$I_{G3} = \frac{1}{2\pi} \int_{u_1}^{u_2} e^{-i(\beta\bar{\omega}/r)u} \left\{ \cos^{-1} \frac{v_1}{u} - \cos^{-1} \frac{v_2}{u} + \int_{v_1}^{v_2} \frac{\cos\left[\frac{\beta\bar{\omega}}{2M}(u^2-v^2)^{1/2}\right] - 1}{(u^2-v^2)^{1/2}} dv \right\} du \quad (16)$$

The complete  $\alpha_{\phi}(r,s)$  for any one sending box ( $x, y$ ) consists of  $I_{G1}$ ,  $I_{G2}$ , or  $I_{G3}$ , or a combination of  $I_{G1}$  and  $I_{G2}$ , or of  $I_{G1}$  and  $I_{G3}$ . The types of integrals and limits of integration for computing  $\alpha_{\phi}(r,s)$  for all possible relative locations of box ( $x, y$ ) and the Mach cone from ( $m, n$ ) are given in Reference 9.



The evaluation of the above three integrals is carried out through the method of Gaussian quadrature. In the subsequent numerical examples, three Gaussian points are used in both x and y directions for computing  $I_{G3}$ . Five Gaussian points in both x and y directions are used for computing  $I_{G1}$  and  $I_{G2}$ .

Once all possible values of the aerodynamic influence coefficient  $\alpha_\phi(r,s)$  are obtained for a certain shape function  $f_j(\bar{x},\bar{y})$ , the total velocity potential at the center of a receiving box (m,n) for the downwash associated with the same shape function is a weighted sum of the  $\bar{\phi}_j(m,n)$  defined in Eq. (12)

$$\phi_j(m,n) = V \epsilon \sum_{\lambda} \sum_{\nu} \frac{w_j(\lambda,\nu)}{V} \alpha_\phi(r,s) \quad (17)$$

The summation is extended over all the sending boxes. The downwash ratios  $w_j(\lambda,\nu)/V$  for a unit d.o.f. "q<sub>j</sub>" are the total time derivatives of the shape function  $f_j(\bar{x},\bar{y})e^{i\omega t}$

$$\frac{w_j}{V} = \frac{1}{\ell} \left( \frac{\partial f_j}{\partial \bar{x}} + i \frac{\omega \ell}{V} f_j \right) \quad (18)$$

Once the velocity potentials are obtained for each box for each shape function, they can readily be substituted into Eq. (11) for computing the aerodynamic matrix for the entire panel system.

### SECTION III

#### FORMULATION FOR FLUTTER DETERMINANT IN TERMS OF FINITE ELEMENT SHAPE FUNCTIONS

In the present finite element flutter formulation, the parameters are so grouped and nondimensionalized that the solution is general enough to include every parameter. Assuming harmonic motion with natural frequency  $\omega$ , the equations of motion (1) are rewritten in an element form as

$$\left\{ \Omega [c_1[k] + Fc_2[n]] - [c_3[m] - c_4[A]] \right\} \{q\} = \{0\} \quad (19)$$

where  $\Omega = \omega_1^2/\omega^2(1 + ig)$  is the flutter eigenvalue parameter, and

$$\begin{aligned} c_1 &= \frac{\mu(\ell/a)^5 D}{\omega_1^2 \sigma h \ell^4} \quad ; \quad c_2 = \mu(\ell/a)^3 \quad ; \\ c_3 &= \mu(\ell/a) \quad ; \quad c_4 = \left(\frac{\ell}{a}\right)^3 \left(\frac{\epsilon}{\ell}\right) \left(\frac{1}{k_\ell}\right)^2 \left(\frac{\tau \epsilon^2}{ab}\right) \end{aligned} \quad (20)$$

The element matrix terms are obtained as

$$\begin{aligned} k_{ij} &= \int_0^1 \int_0^1 \left[ \frac{\partial^2 f_i}{\partial \bar{x}^2} \frac{\partial^2 f_j}{\partial \bar{x}^2} + \left(\frac{a}{b}\right)^4 \frac{\partial^2 f_i}{\partial \bar{y}^2} \frac{\partial^2 f_j}{\partial \bar{y}^2} + \nu \left(\frac{a}{b}\right)^2 \frac{\partial^2 f_i}{\partial \bar{x}^2} \frac{\partial^2 f_j}{\partial \bar{y}^2} \right. \\ &\quad \left. + \nu \left(\frac{a}{b}\right)^2 \frac{\partial^2 f_j}{\partial \bar{x}^2} \frac{\partial^2 f_i}{\partial \bar{y}^2} + 2(1 - \nu) \left(\frac{a}{b}\right)^2 \frac{\partial^2 f_i}{\partial \bar{x} \partial \bar{y}} \frac{\partial^2 f_j}{\partial \bar{x} \partial \bar{y}} \right] d\bar{x} d\bar{y} \end{aligned} \quad (21)$$

$$n_{ij} = \int_0^1 \int_0^1 \left[ \frac{\partial f_i}{\partial \bar{x}} \frac{\partial f_j}{\partial \bar{x}} + \frac{N_y}{N_x} \frac{\partial f_i}{\partial \bar{y}} \frac{\partial f_j}{\partial \bar{y}} + \frac{N_{xy}}{N_x} \frac{\partial f_i}{\partial \bar{x}} \frac{\partial f_j}{\partial \bar{y}} + \frac{N_{xy}}{N_x} \frac{\partial f_j}{\partial \bar{x}} \frac{\partial f_i}{\partial \bar{y}} \right] d\bar{x} d\bar{y} \quad (22)$$

$$m_{ij} = \int_0^1 \int_0^1 f_i f_j d\bar{x} d\bar{y} \quad (23)$$

$$A_{ij} = \sum \frac{\phi_j}{V\epsilon} \left( \frac{\partial f_i}{\partial \bar{x}} - i \frac{\omega a}{V} f_i \right) \quad (24)$$

The shape functions  $f_i(\bar{x}, \bar{y})$  are usually cubic or higher order functions of nondimensional coordinate variables  $\bar{x}$  and  $\bar{y}$ . Their differentiations with respect to  $\bar{x}$  and  $\bar{y}$  are performed analytically. The subscript "i" indicates the degree of freedom number with which the shape function is associated. Eqs. (19-24) are suitable for any plate finite element so long as it is a displacement model with assumed shape functions. According to the state-of-the-art of the finite element development, the stiffness matrix [k], mass matrix [m], and incremental stiffness matrix [n] have been formulated analytically and explicitly for almost every plate and shell finite element. Only the aerodynamic matrix [A] remains to be formulated and it is to be obtained by numerical integration here.

Eq. (19) constitutes an eigenvalue problem. The flutter solution is obtained by first assuming a value of reduced frequency  $k_\lambda$ , then varying the air-panel mass ratio  $1/\mu$  incrementally and solving for the corresponding eigenvalues  $\Omega$  or  $(\omega_1/\omega)^2(1 + ig)$ . When the structural damping coefficient  $g$  changes its value from negative to positive, the panel goes from the stable region to unstable region, and vice versa. The values of  $k_\lambda$  and  $1/\mu$  that correspond to zero  $g$  value define the flutter boundary and the corresponding mode shape defines the flutter mode. The complex eigenvalue problem is solved by using a subroutine in EISPACK provided by Argonne National Laboratory.

Before performing analysis for each class of problems, a convergence study by varying the meshes of Mach boxes and finite elements must be made in order to find the suitable meshes needed for obtaining converged results. Such meshes depend on the panel geometry, boundary conditions, flow speed, and flutter modes. However, due to the enormous computations needed for obtaining massive data in this study, not the finest meshes are used. Most of the present results are compared with those obtained by the modal method (Reference 9) and good results are obtained.

## SECTION IV

### RESULTS

The 16 d.o.f. conforming rectangular plate finite elements were employed to demonstrate the present formulation and procedure. The examples chosen were rectangular panels, stressed as well as unstressed, with clamped edges. For the unstressed panels, a sophisticated analytical solution by Cunningham (Reference 9) using the box method (400 boxes) and Galerkin's modal approach (6 to 16 modes) was available for comparison.

In all examples studied here, the flutter mode shapes were assumed as symmetrical about the center chord-line of the panel. Thus, only half of each panel was modeled by finite elements. In all cases, two elements in the cross stream direction were used for half of the panel. The number of elements in the stream direction varied from 4 to 10 dependent on the dominating flutter mode shapes. Each element was divided into 4 by 2 boxes in the stream and cross stream directions, respectively.

It is important to note that symmetry does not exist for the mesh of boxes unless the Mach cone apex is located at the center chord-line of the panel. The boxes on the other (disregarded) half of the panel can, however, still be accounted for since their deflection shapes are known by symmetry.

#### Case 1 Clamped Panels with Various Chord-span Ratios at $M = 1.3$

The rectangular panels with all edges clamped and chord-span ratios ( $l/w$ ) equal to 0, 1/4, 1/2, 1, 2, and 4 were studied for  $M = 1.3$ .

The resulting flutter boundaries are presented as plots of each dominating mode with the air-panel mass ratio  $1/\mu$  as the vertical coordinate and the stiffness parameter  $\omega_1^2 \ell/V$  as the horizontal coordinate. The values of reduced frequency  $k_y$  or  $\omega_1 \ell/V$  are marked along each curve. The results for the infinite panel with  $\ell/w = 0$  are in exact agreement with those obtained by Cunningham, therefore, they are not presented here.

Fig. 3 shows that for the wide panel with  $\ell/w = 1/4$ , the first mode flutter boundary crosses the second mode flutter boundary. The critical flutter boundaries are thus dominated by the first mode in the high mass ratio range and by the second mode in the low mass ratio range. A slight amount of structural damping was also included ( $g = 0.01$ ). The results agree well with those obtained by Cunningham (Reference 9).

The first flutter mode shape (real part) corresponding to point A ( $k_y = 0.635$ ) in Fig. 3 is shown in Fig. 4. It is seen that, due to the effect of the flow, the mode is not symmetrical about the cross stream centerline. The maximum deflection occurs at a point behind the center of the panel. The second flutter mode shape (real part) for the center chord-line of the panel corresponding to point B ( $k_y = 1.59$ ) in Fig. 3 is shown in Fig. 5. The effect of the flow that pushes down the front part of the panel is seen.

Fig. 6 shows that, as the panel width is reduced ( $\ell/w = 1/2$ ), the first mode boundary shifts to the left and the second mode boundary becomes the critical flutter boundary. Again, the results agree well with Cunningham's solution.

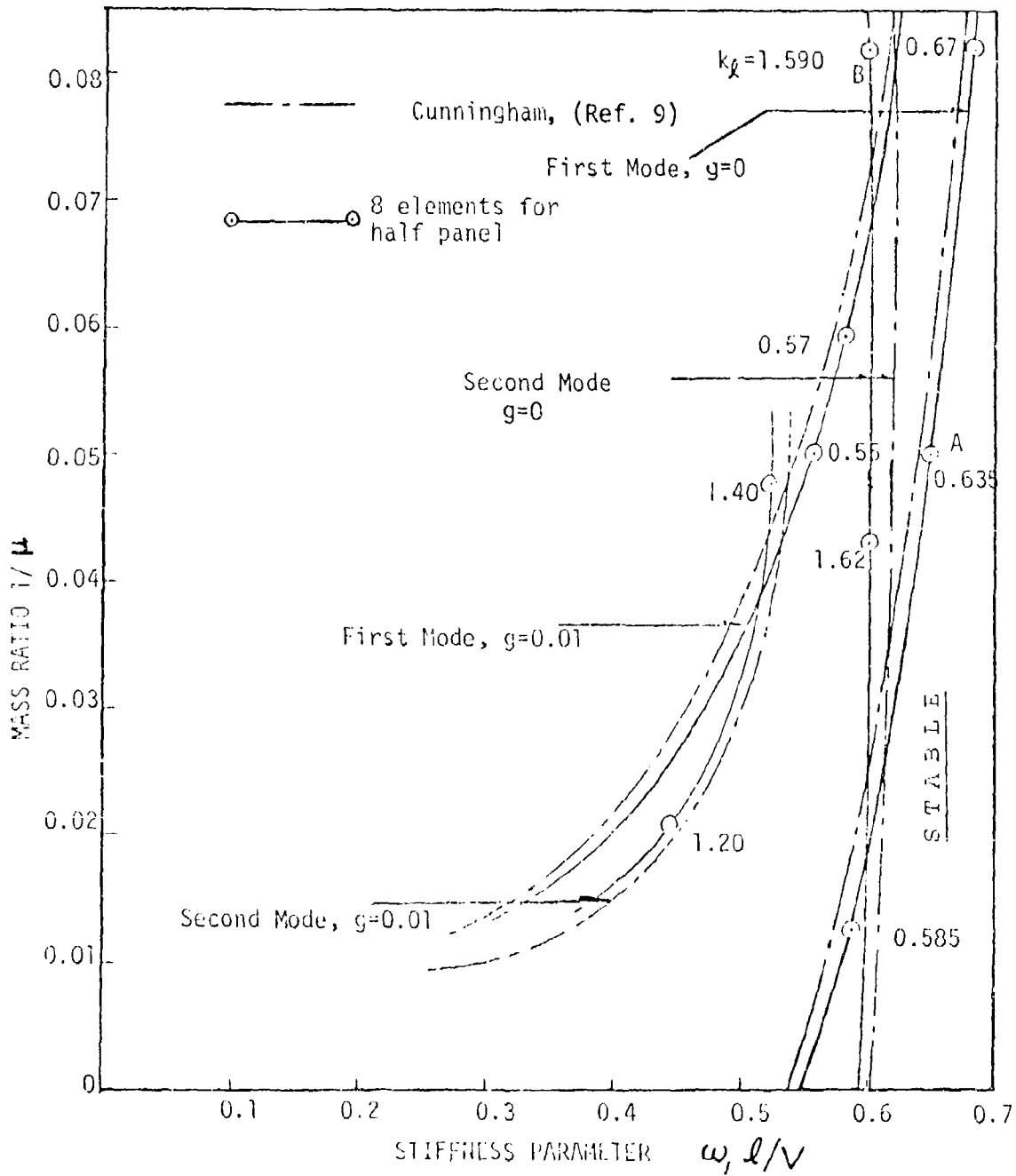


Figure 3 Flutter boundaries for clamped panel with  $l/w = 1/4$  and  $M = 1.3$

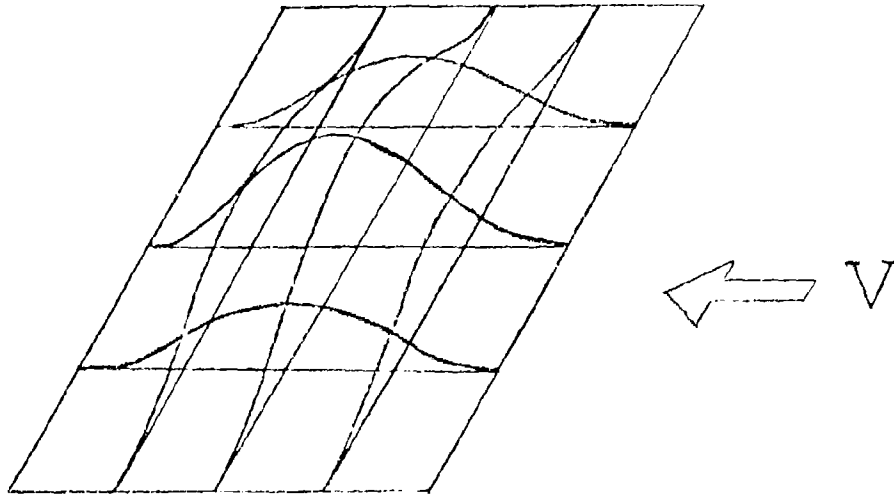


Figure 4. The first mode shape (real part) for panel corresponding to point A in Fig. 3

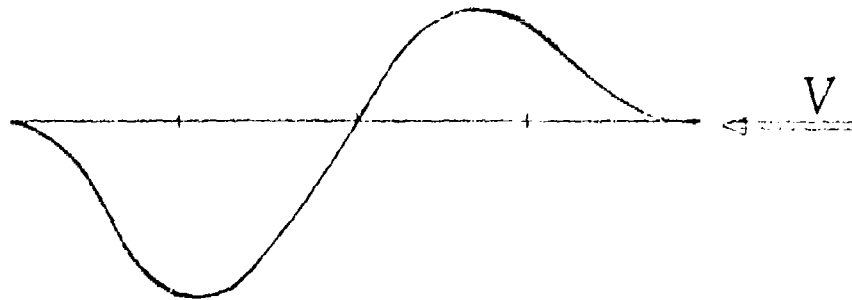


Figure 5 The second mode shape (real part) for the center line of panel corresponding to point B in Fig. 3

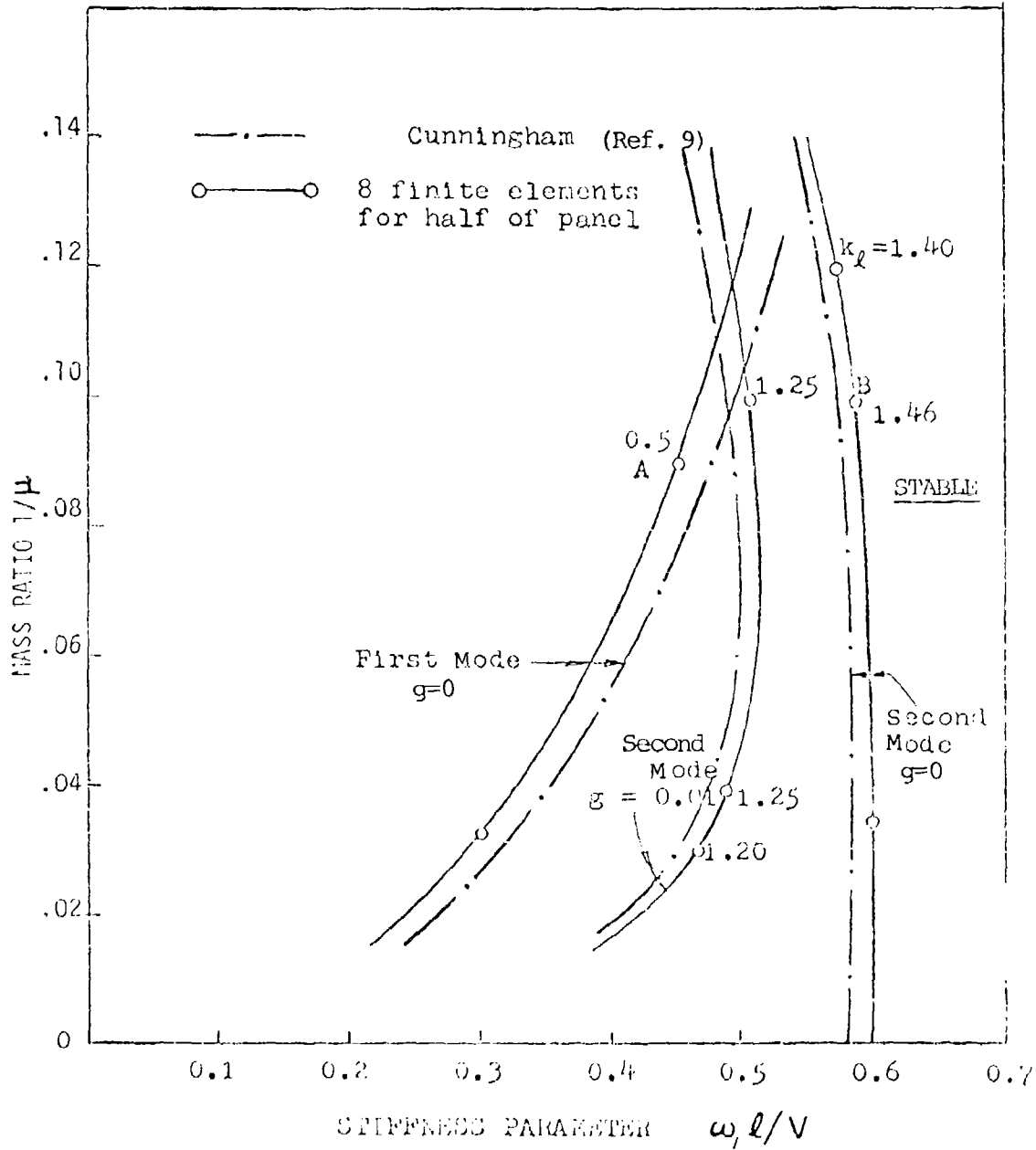


Figure 6 Flutter boundaries for clamped panel with  $l/w = 1/2$  and  $H = 1.3$



The first and second flutter mode shapes (real part) corresponding to points A and B in Fig. 6 are plotted in Figs. 7 and 8, respectively. They are quite similar to those shown in Figs. 4 and 5.

Fig. 9 shows that, as the panel becomes square, the third and fourth mode boundaries emerge and the third mode boundary becomes the critical flutter boundary. The results are in good agreement with Cunningham's solution. The results for the first mode boundary obtained by Houbolt using the piston theory are also shown in the figure.

The third and fourth flutter mode shapes (real part) corresponding to points A and B in Fig. 9 are shown in Figs. 10 and 11, respectively. The effect of the flow that tends to blow flat the front part of the panel is seen.

Fig. 12 shows that, for a long panel with  $\ell/w = 2$ , the fifth mode flutter boundary becomes dominant in the low mass ratio range and the first mode boundary dominates the high mass ratio range. It also shows that Houbolt's solution for first mode and this solution are very close. There are, however, some discrepancies between this solution and Cunningham's solution for the first mode boundary. This may be due to the fact that the stiffness coupling effect between assumed beam natural modes was uniformly neglected by Cunningham. Such coupling effect can become significant as the chord-span ratio increases. It should be noted that, due to the limited number of elements and boxes used, the present results are not the most accurate that this approach can produce.

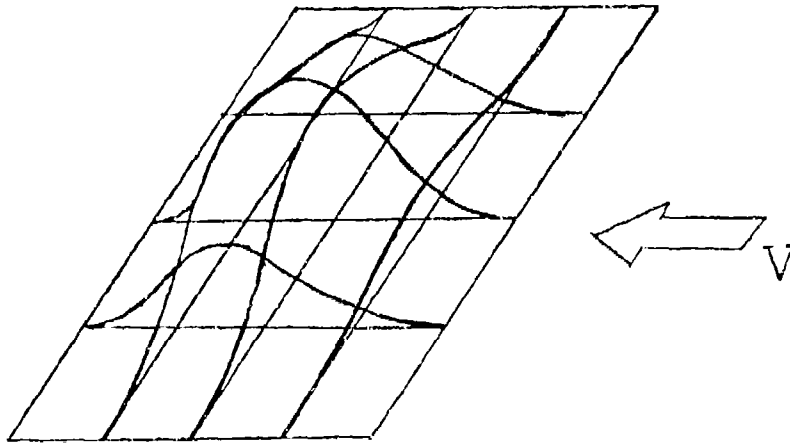


Figure 7 The first mode shape (real part) for panel corresponding to point A in Fig. 6

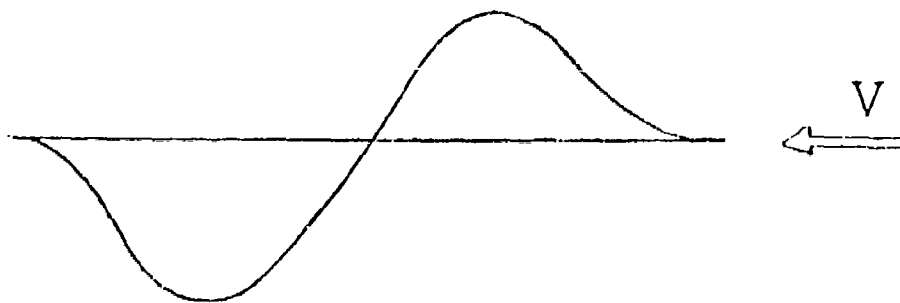


Figure 8 The second mode shape (real part) for the center line of panel corresponding to point B in Fig. 6

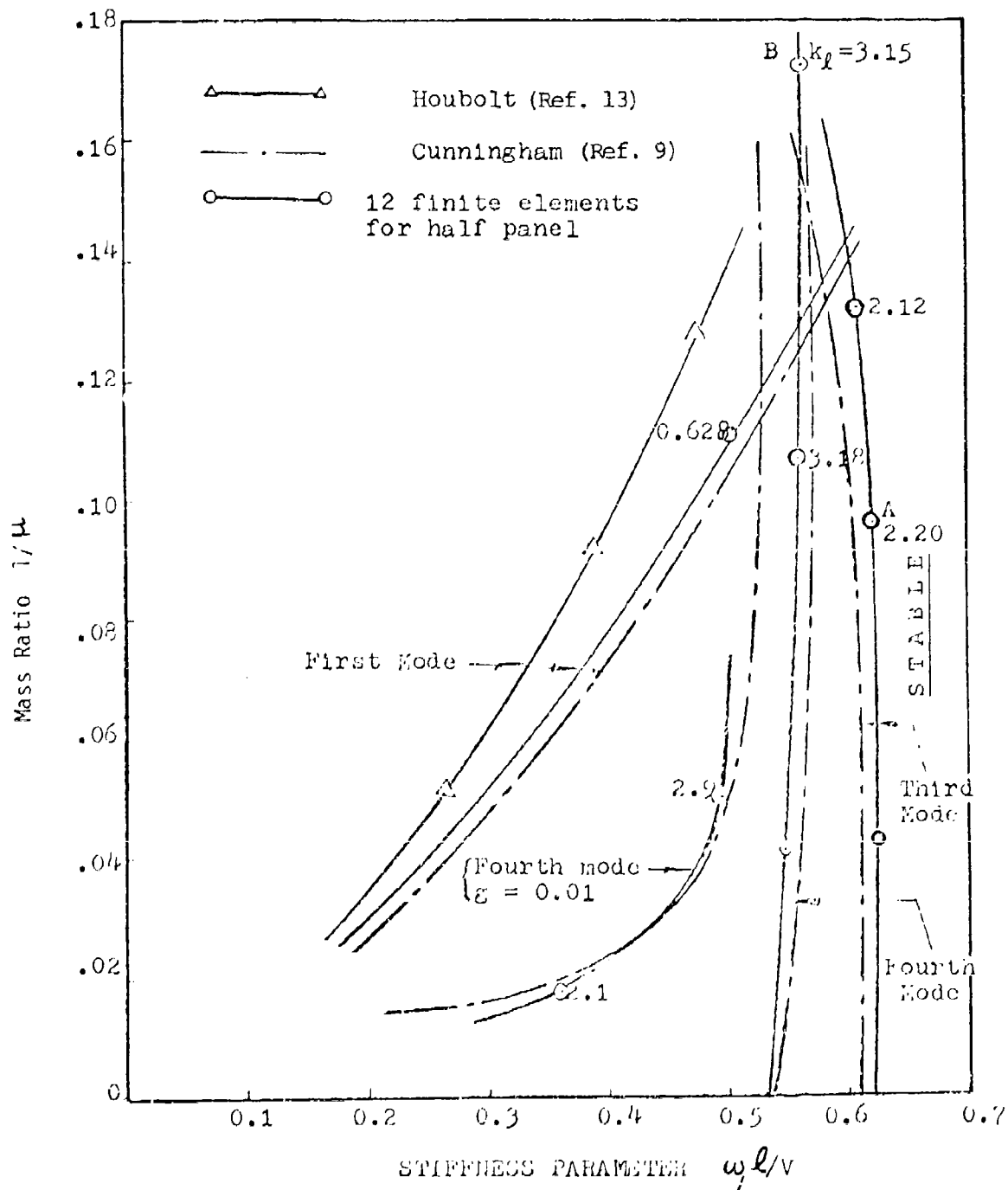


Figure 9 Flutter boundaries for clamped panel with  $l/w = 1$  and  $M = 1.3$

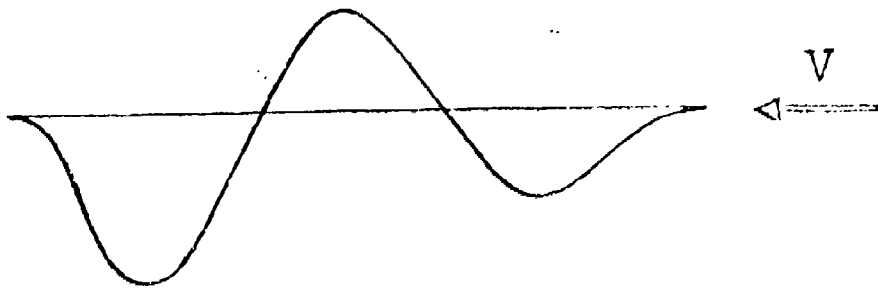


Figure 10 The third mode shape (real part) for the center line of panel corresponding to point A in Fig. 9

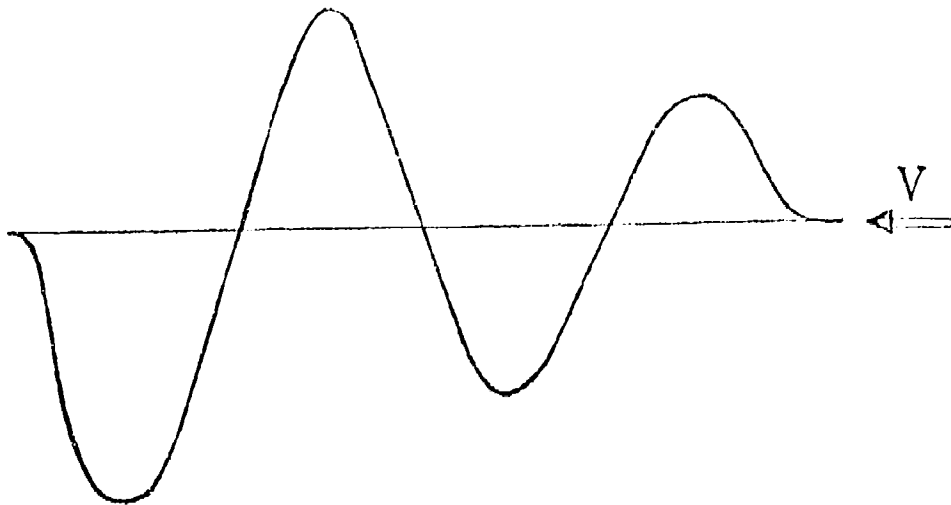


Figure 11 The fourth mode shape (real part) for the center line of panel corresponding to point B in Fig. 9

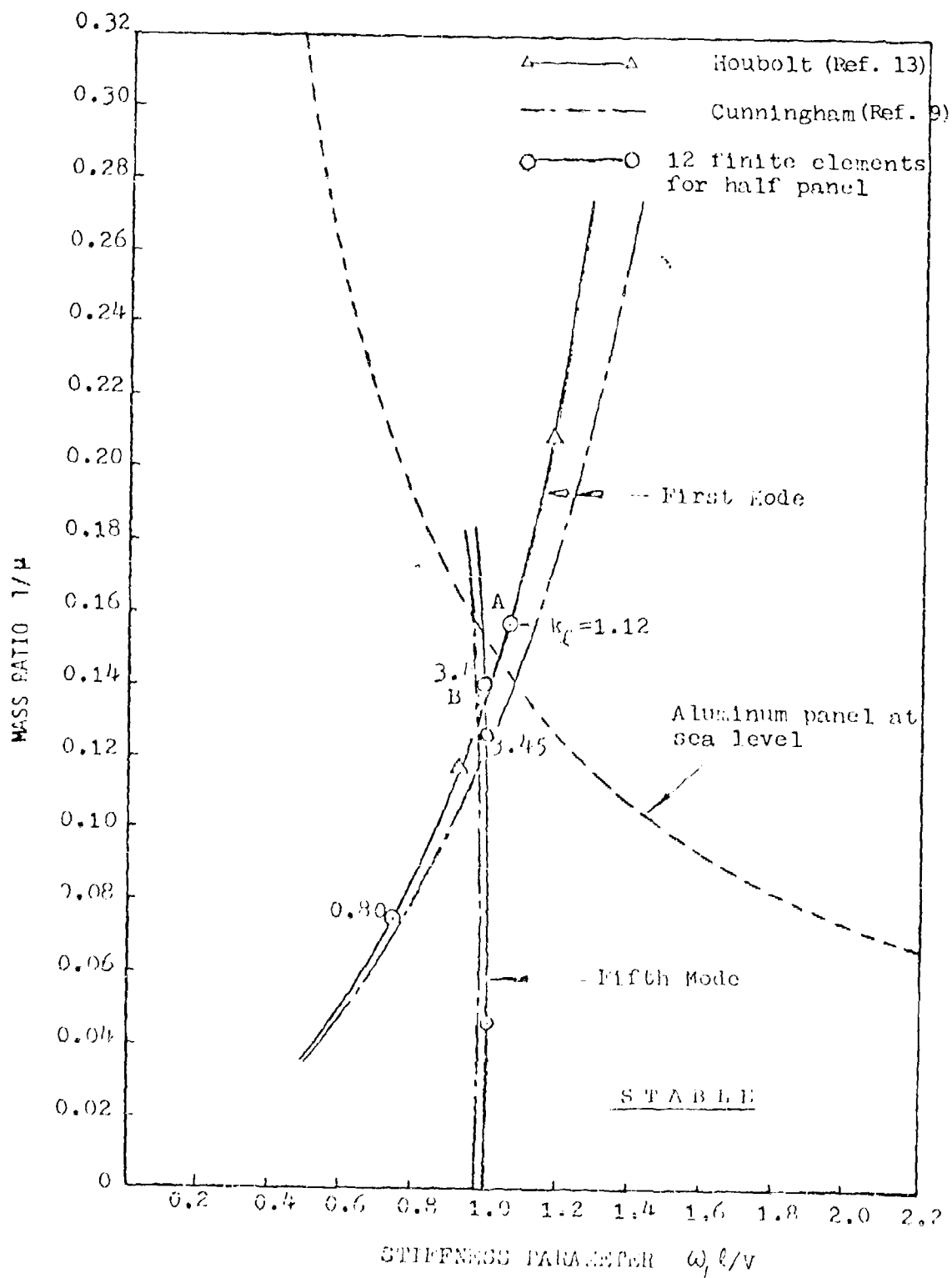


Figure 12 Flutter boundaries for clamped panel with  $\ell/w = 2$  and  $M = 1.3$

The first and third flutter mode shapes (real part) corresponding to points A and B in Fig. 12 are shown in Figs. 13 and 14, respectively. The difference between a symmetrical in vacuo first mode and the first flutter mode with front part blown flat is clearly shown in Fig. 13.

Fig. 15 shows that, for a very long panel with  $l/w = 4$ , the tenth mode flutter boundary dominates the lower mass ratio range while the first mode boundary dominates the upper mass ratio range. The discrepancy between the present solution and Cunningham's solution may be attributed to the same reasons as explained for Fig. 6. Houbolt's solution for first mode boundary is also shown.

The second and tenth flutter mode shapes (real part) corresponding to points A and B in Fig. 15 are plotted in Figs. 16 and 17, respectively.

#### Case 2 Clamped Panel with $l/w = 2$ at Various Mach Numbers

A clamped panel with  $l/w = 2$  and with one surface exposed to air stream with various Mach numbers was studied. One of the main purposes was to establish a curve for the thickness ratios required to prevent flutter of panel at various air speeds and at sea level.

The first mode flutter boundaries for panel with  $l/w = 2$  and  $M = 1.05, 1.1; 1.4, 1.5; 2.0, \text{ and } 3.0$  are shown in Figs. 18, 19, and 20, respectively. Corresponding to each curve, a dashed parabola is shown. Each parabola is plotted for the equation  $xy = C$  or  $(\rho \bar{x} / \sigma h) (\omega_1 \bar{x} / V) = C$ . The constant  $C$  is dependent upon

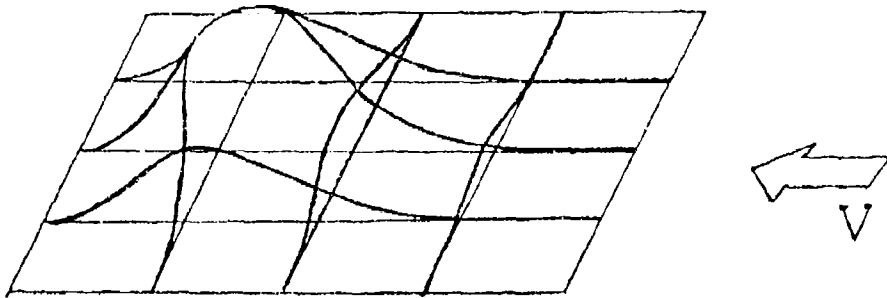


Figure 13 The first mode shape (real part) for panel corresponding to point A in Fig. 12.

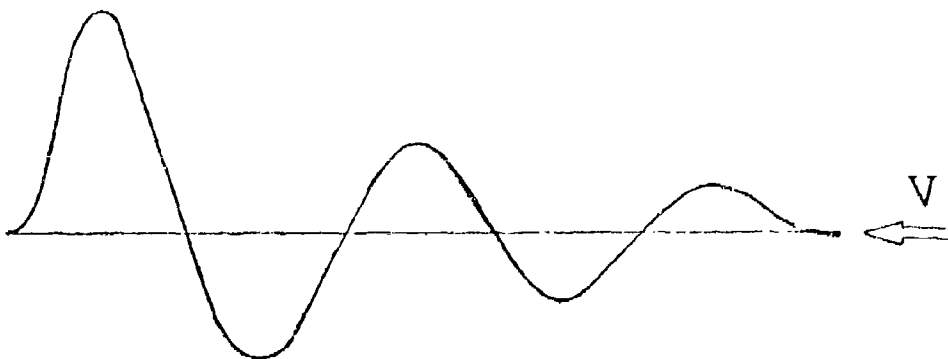


Figure 14 The fifth mode shape (real part) for the center line of panel corresponding to point B in Fig. 12.

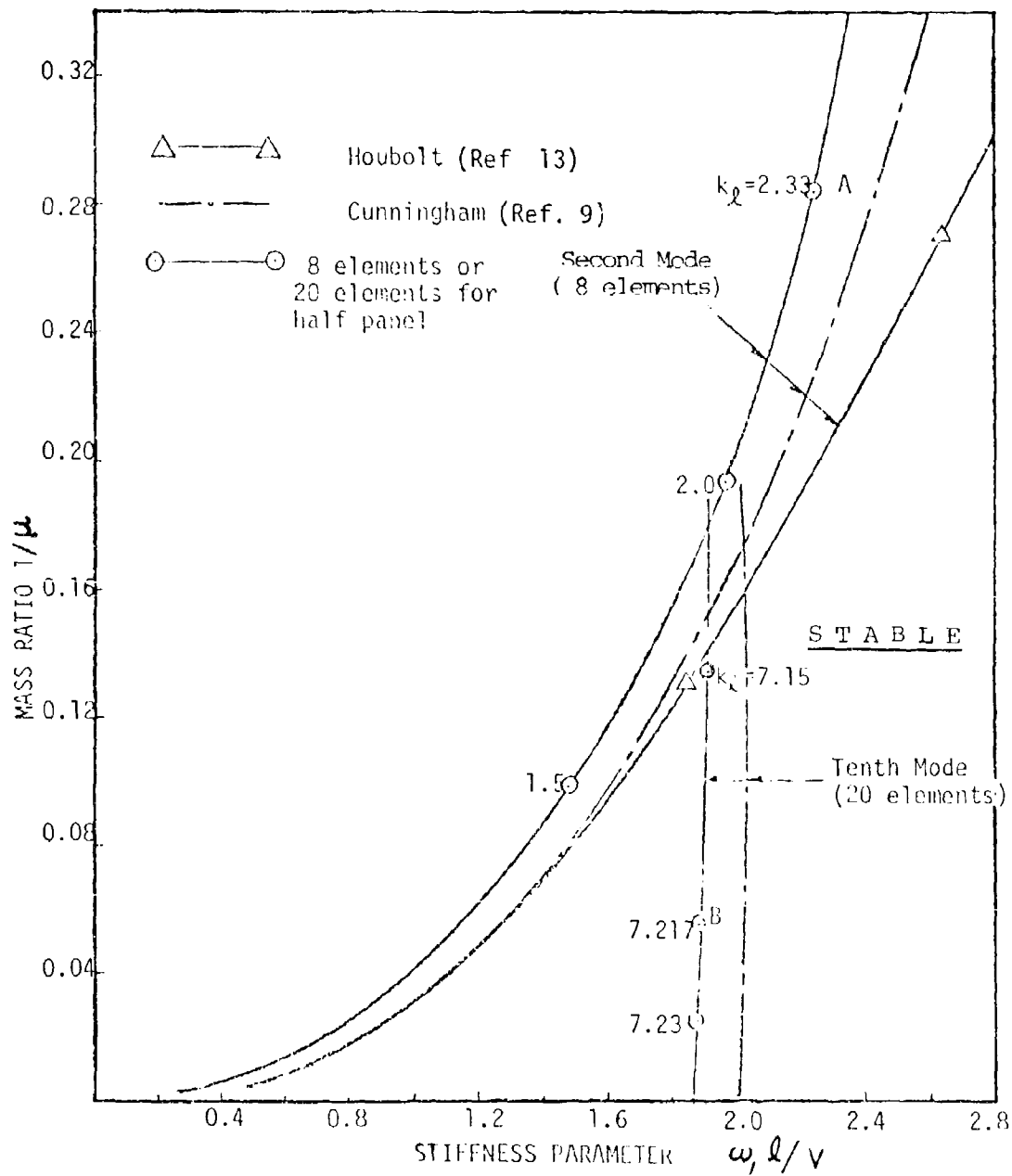


Figure 15 Flutter boundaries for clamped panel with  $l/w = 4$  and  $M = 1.3$



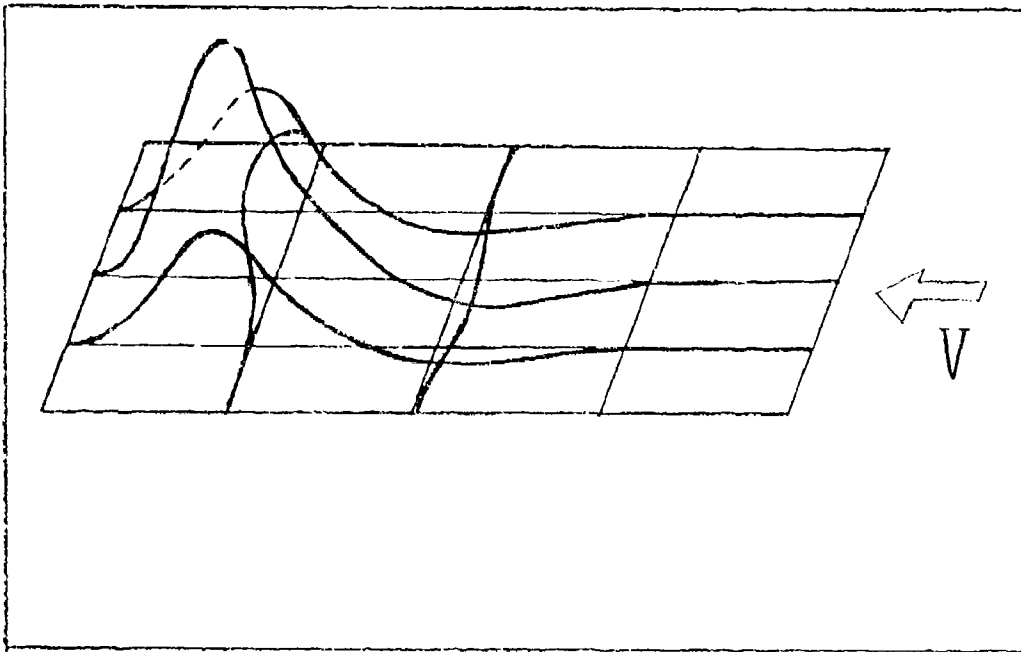


Figure 16 The second mode shape (real part) for panel corresponding to point A in Fig. 15.

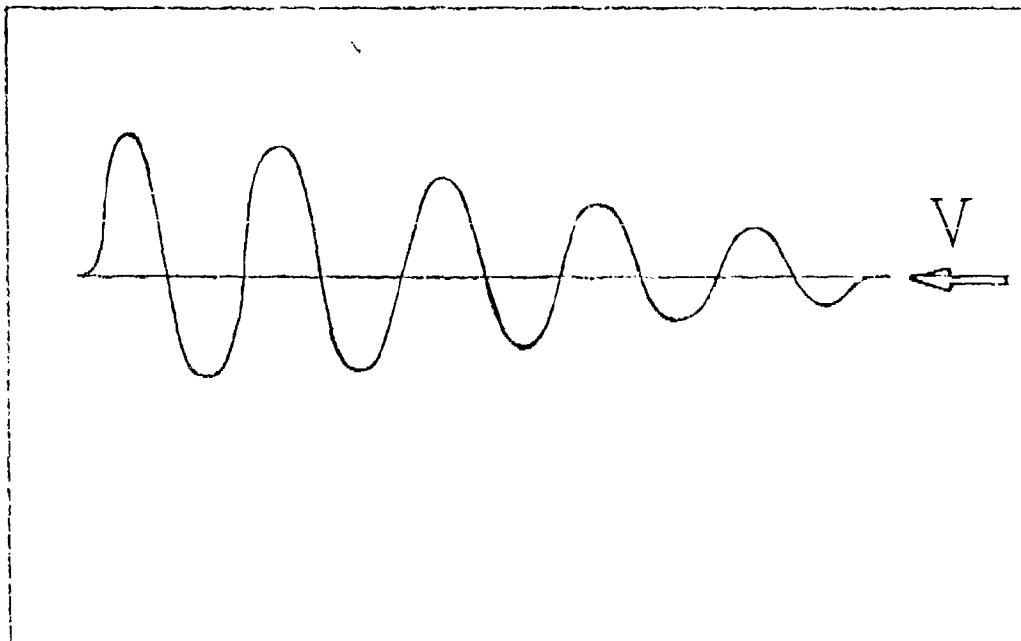


Figure 17 The tenth mode shape (real part) for the center line of panel corresponding to point B in Fig. 15.

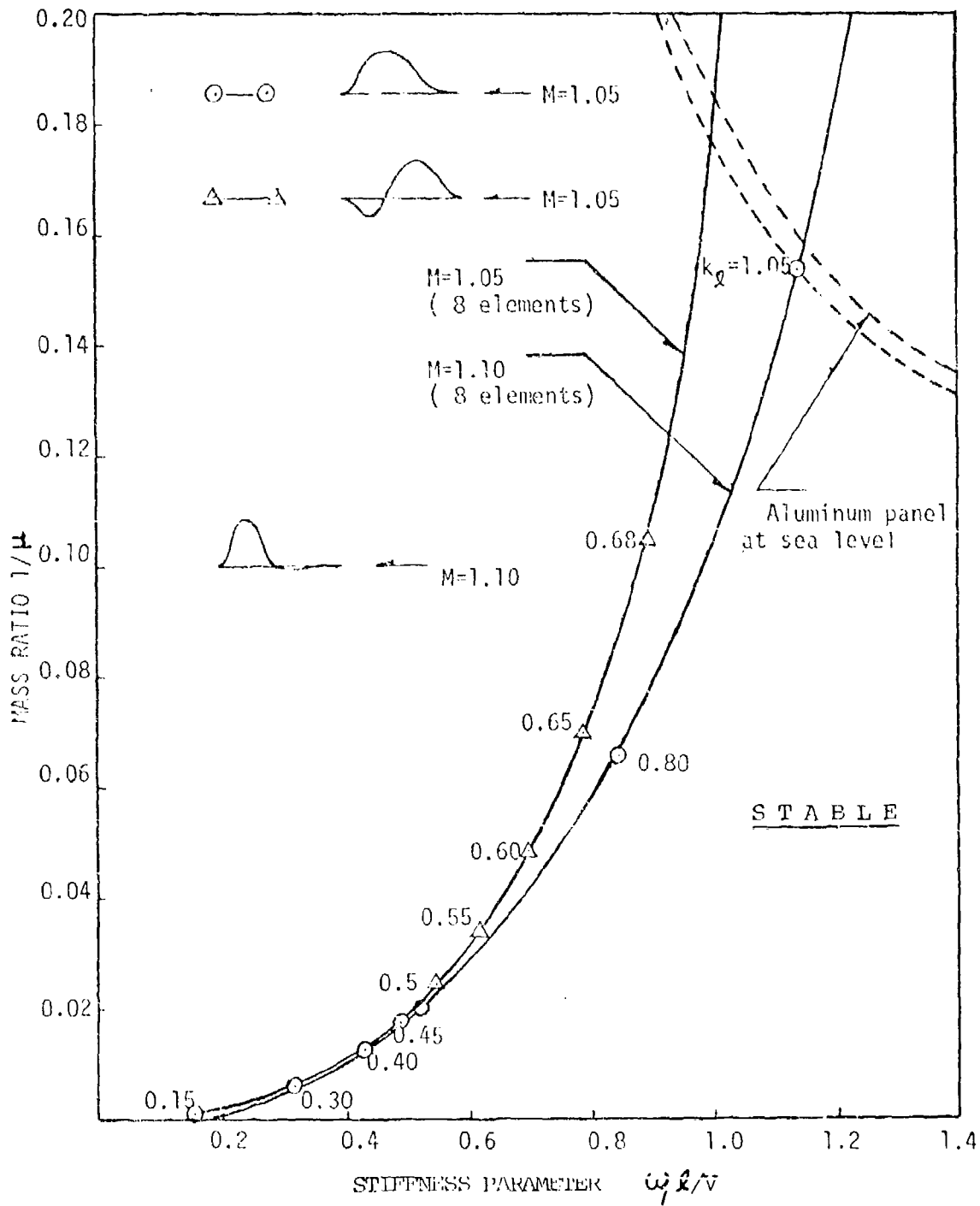


Figure 18 Flutter boundaries for clamped panel with  $l/w = 2$  and  $M = 1.05, 1.10$ .

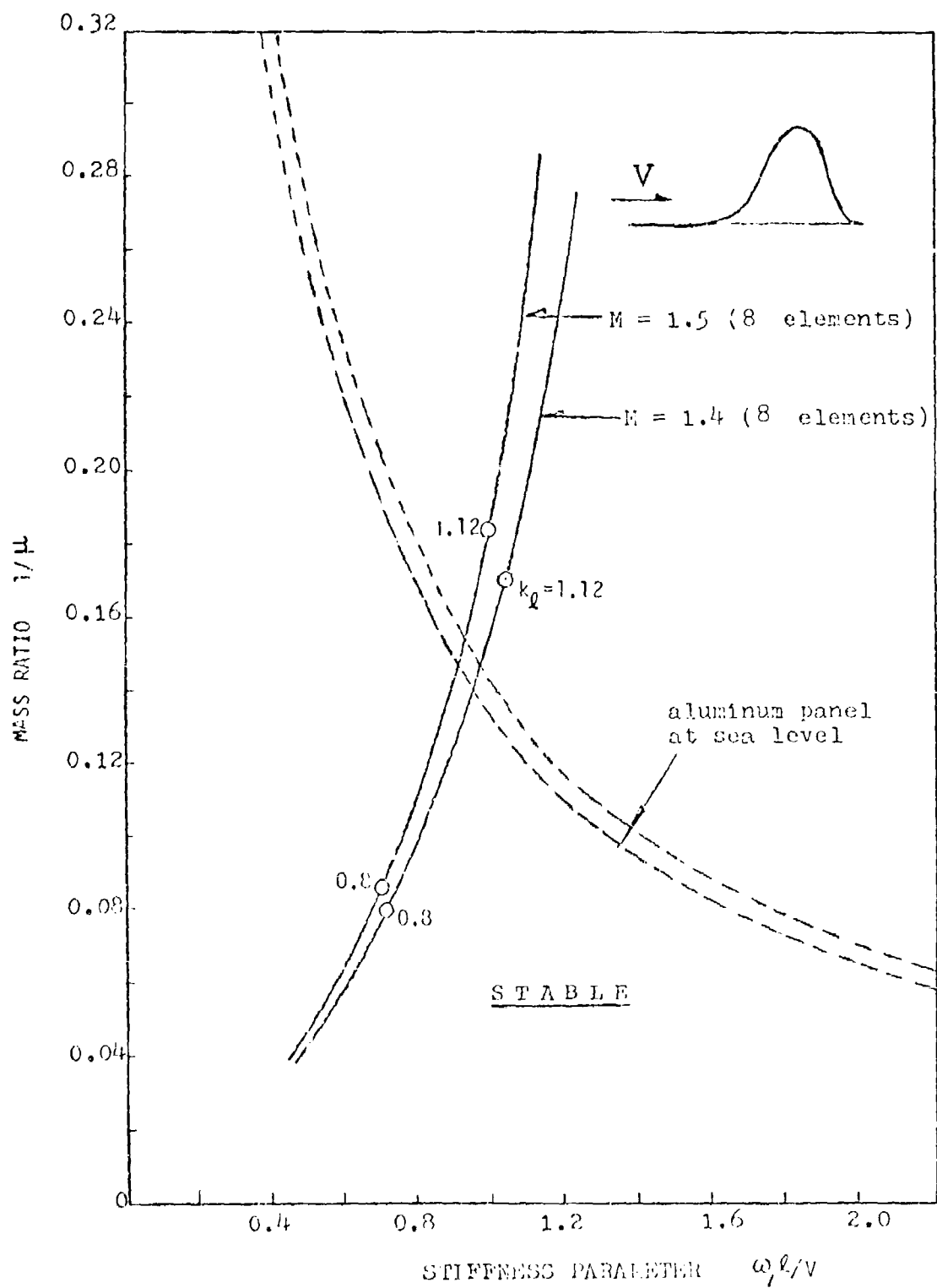


Figure 19 Flutter boundaries for clamped panel with  $\ell/w = 2$  and  $M = 1.40, 1.50$ .

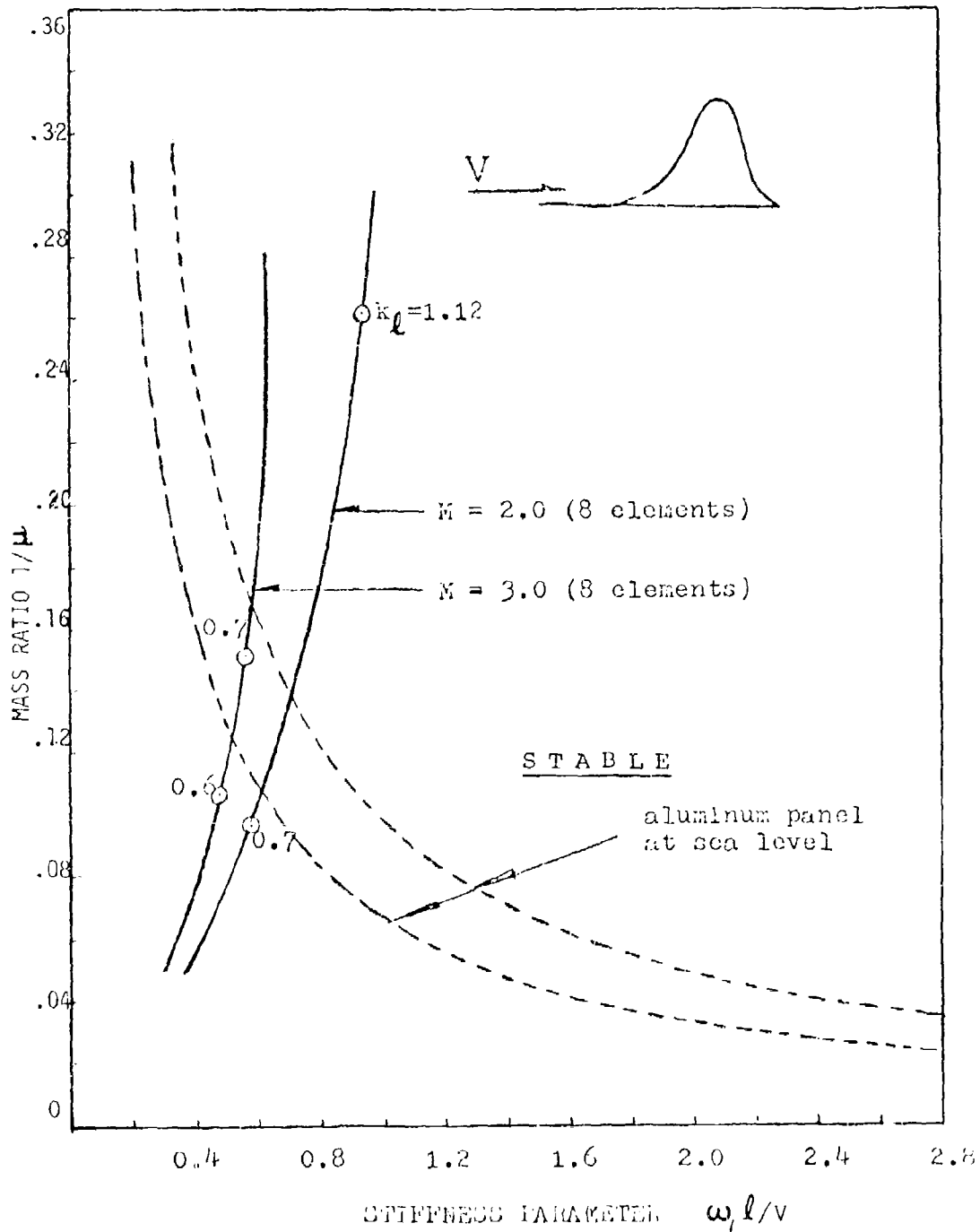


Figure 20 Flutter boundaries for clamped panel with  $l/w = 2$  and  $M = 2.0$  and  $3.0$ .

the densities of the aluminum and the air at sea level, the dimensions of the panel, the air speed, and the bending rigidity of the panel. The intersecting point between a pair of dashed and solid curves gives the thickness ratio  $h/l$  required to prevent flutter of the aluminum panel at sea level. For all Mach numbers considered here, the first mode flutter boundaries are critical for the dashed curves for the sea level altitude.

The results are shown in Fig. 21. The present results are slightly on the unconservative side as compared to the results of Cunningham.

### Case 3 Pinned-Edge Panels with Various Chord-Span Ratios at $M = 1.3$

The panels with simply-supported edges and various chord length-span width ratios were studied. The flow speed considered was  $M = 1.3$ . The dominating flutter boundaries for panels with  $l/w = 0.25, 0.5, 1.0,$  and  $2.0$  are shown in Figs. 22, 24, 26 and 28, respectively. They are all in good agreement with those found by Cunningham (Reference 9).

Fig. 22 shows that the first mode flutter boundary is the critical boundary for panels with  $l/w = 0.25$ . The mode shape (real part) is shown in Fig. 23.

Fig. 24 shows that the second mode flutter boundary is the critical boundary for panels with  $l/w = 0.5$ . The first and second flutter mode shapes (real part) are shown in Fig. 25.

Fig. 26 shows that the third mode flutter boundary is the critical boundary for panel with  $l/w = 1.0$ . The first mode boundary found by Hedgepeth (Reference 11) using the piston theory is also shown in the figure. The corresponding first and third flutter mode shapes (real part) are shown in Fig. 27.

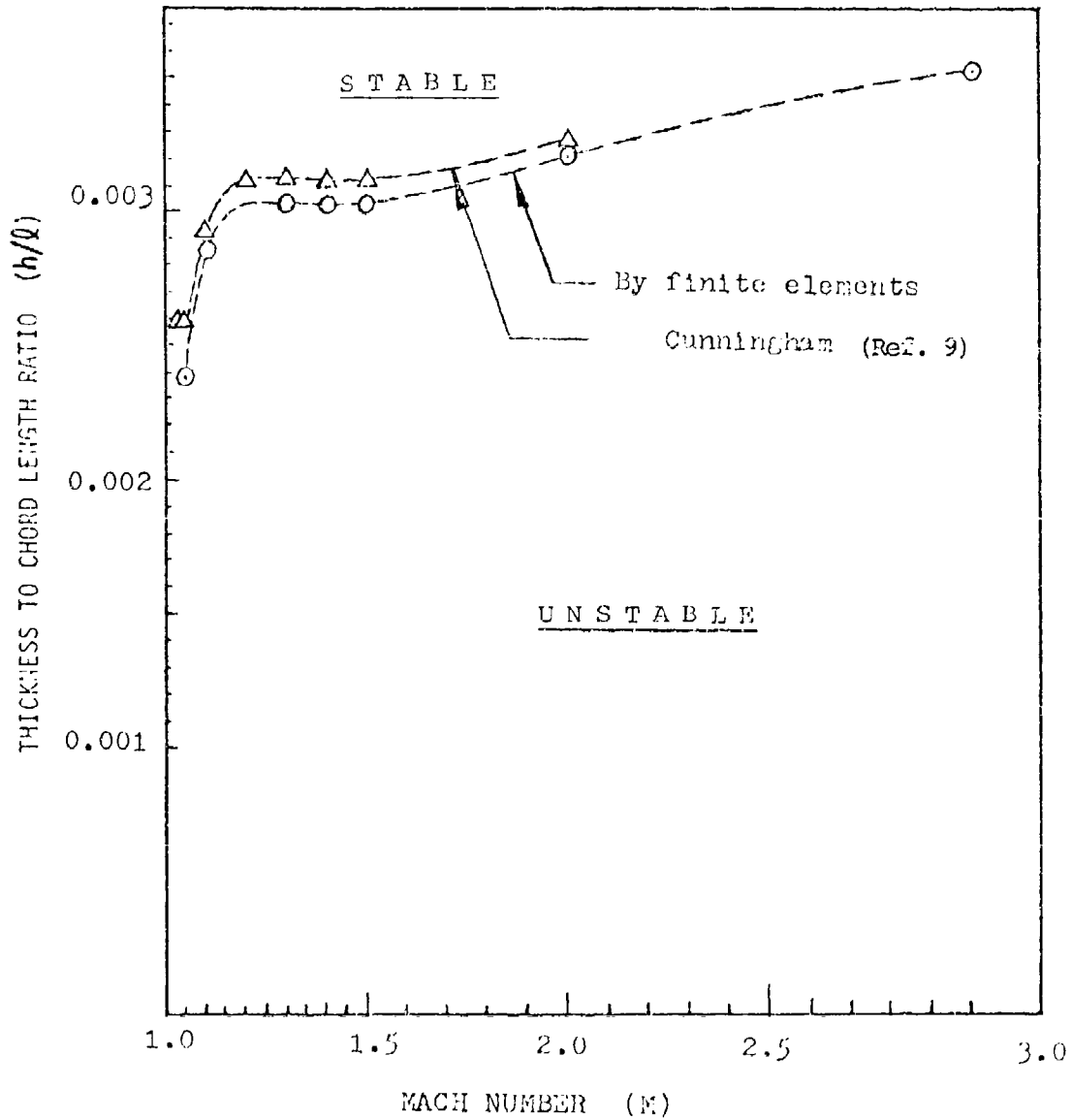


Figure 21 Thickness required to prevent flutter for clamped aluminum panel with  $q/w = 2$  at sea level.

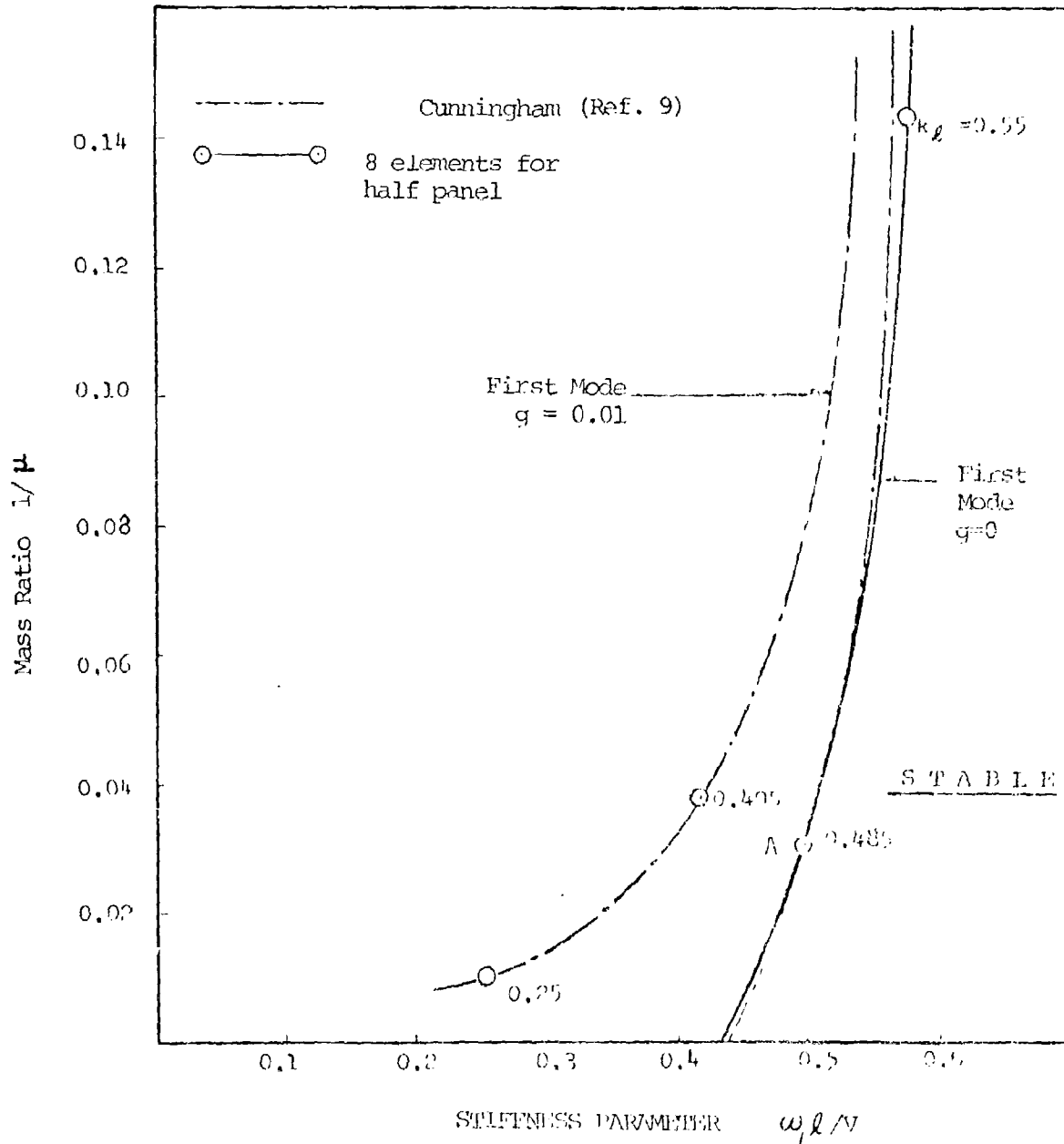


Figure 22 Flutter boundaries for pinned edge panel with  $l/w = 1/4$  and  $M = 1.3$ .

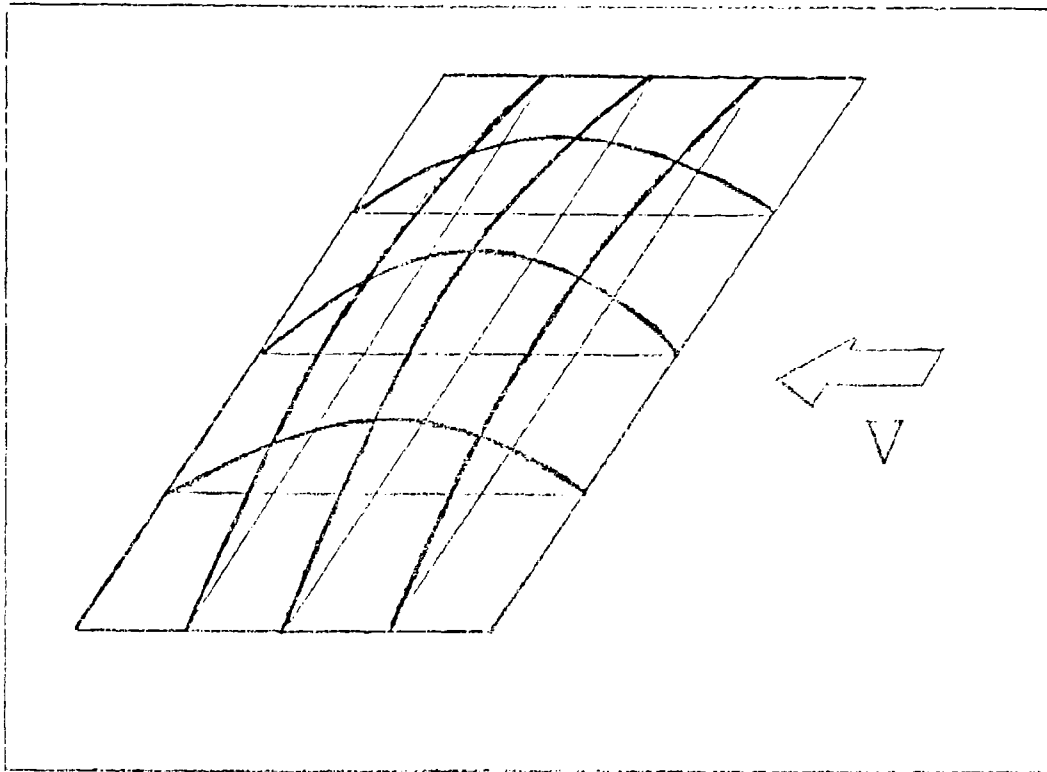


Figure 23 The First Mode Shape ( Real Part ) for Panel Corresponding  
to Point A in Fig. 22.



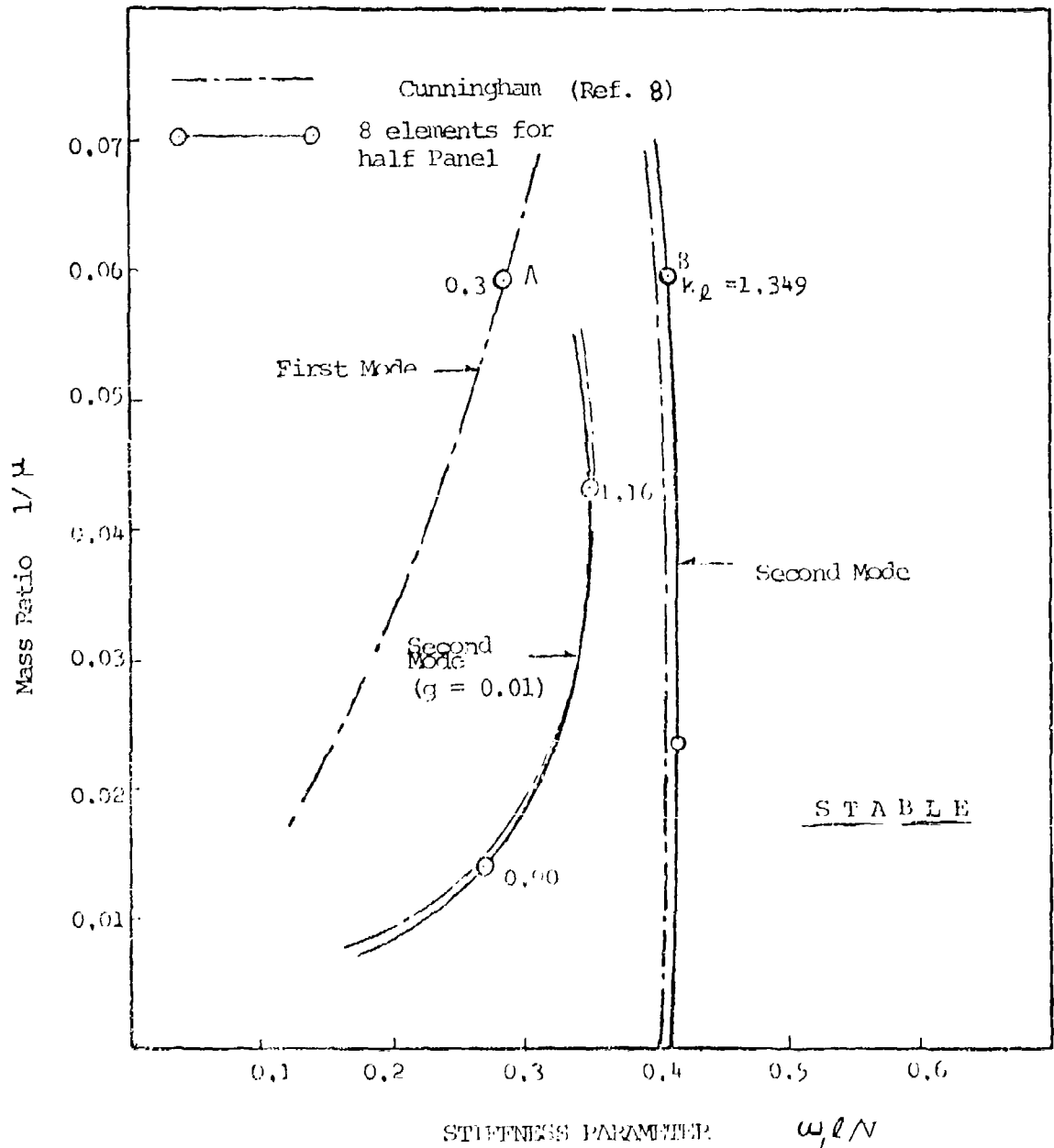


Figure 24 Flutter boundaries for pinned-edge panel with  $\ell/w = 1/2$  and  $M = 1.3$ .

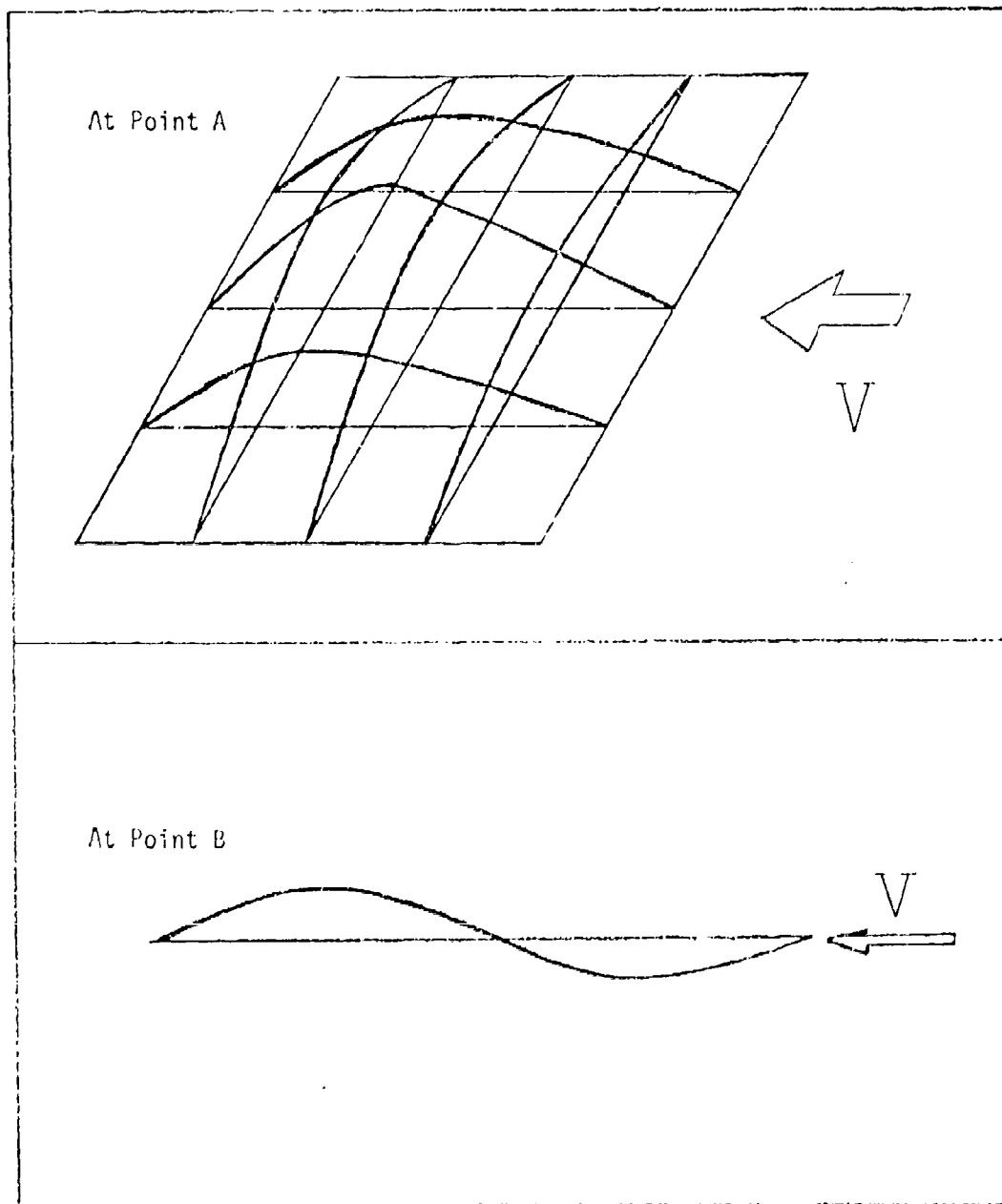


Figure 25 The First Mode Shape ( Real Part ) for Panel Corresponding to Point A in Fig. 24 and the Second Mode Shape ( Real Part ) for the Center Line of Panel Corresponding to Point B in Fig. 24.

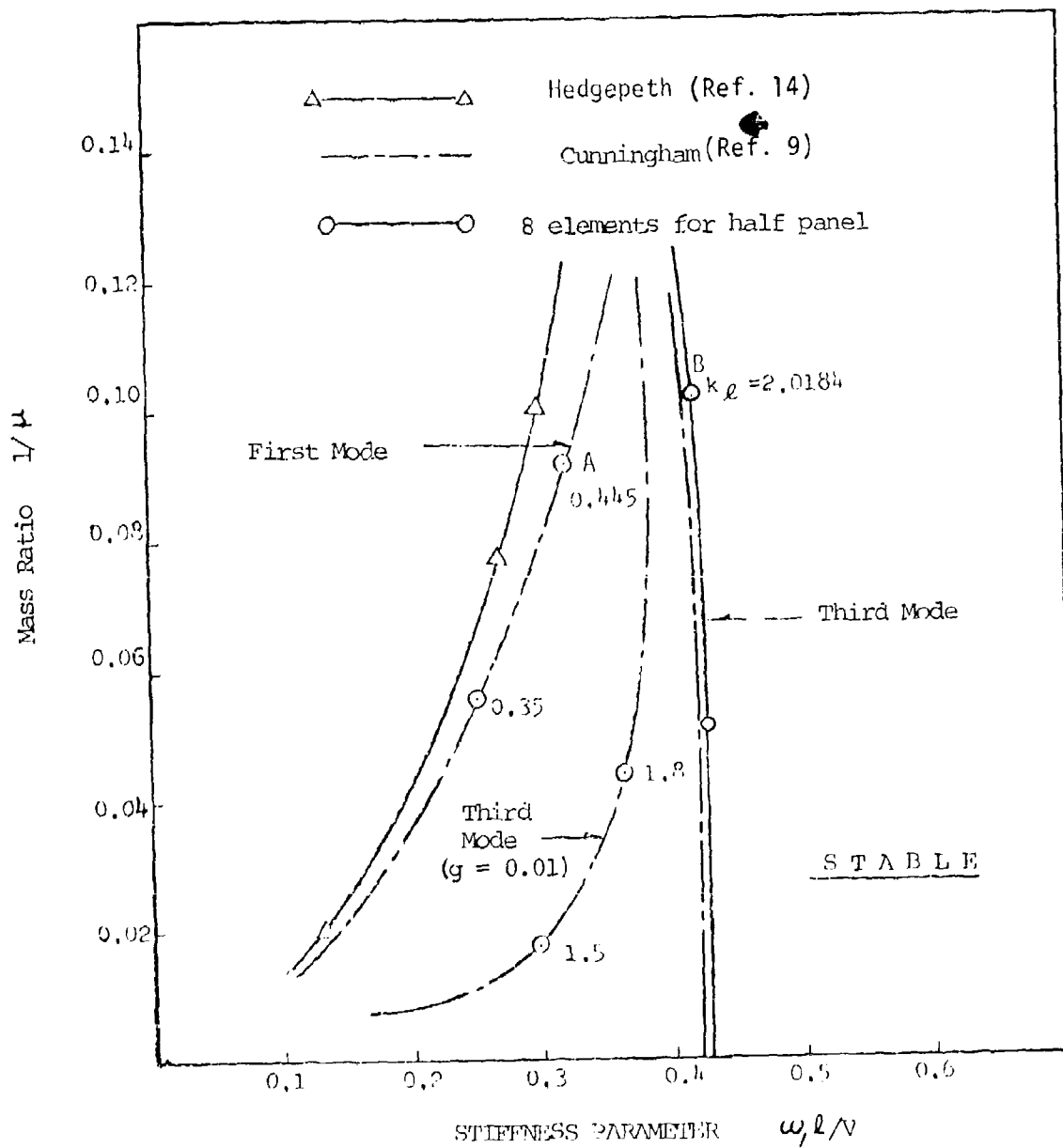


Figure 26 Flutter boundaries for pinned-edge panel with  $l/w = 1$  and  $M = 1.3$ .

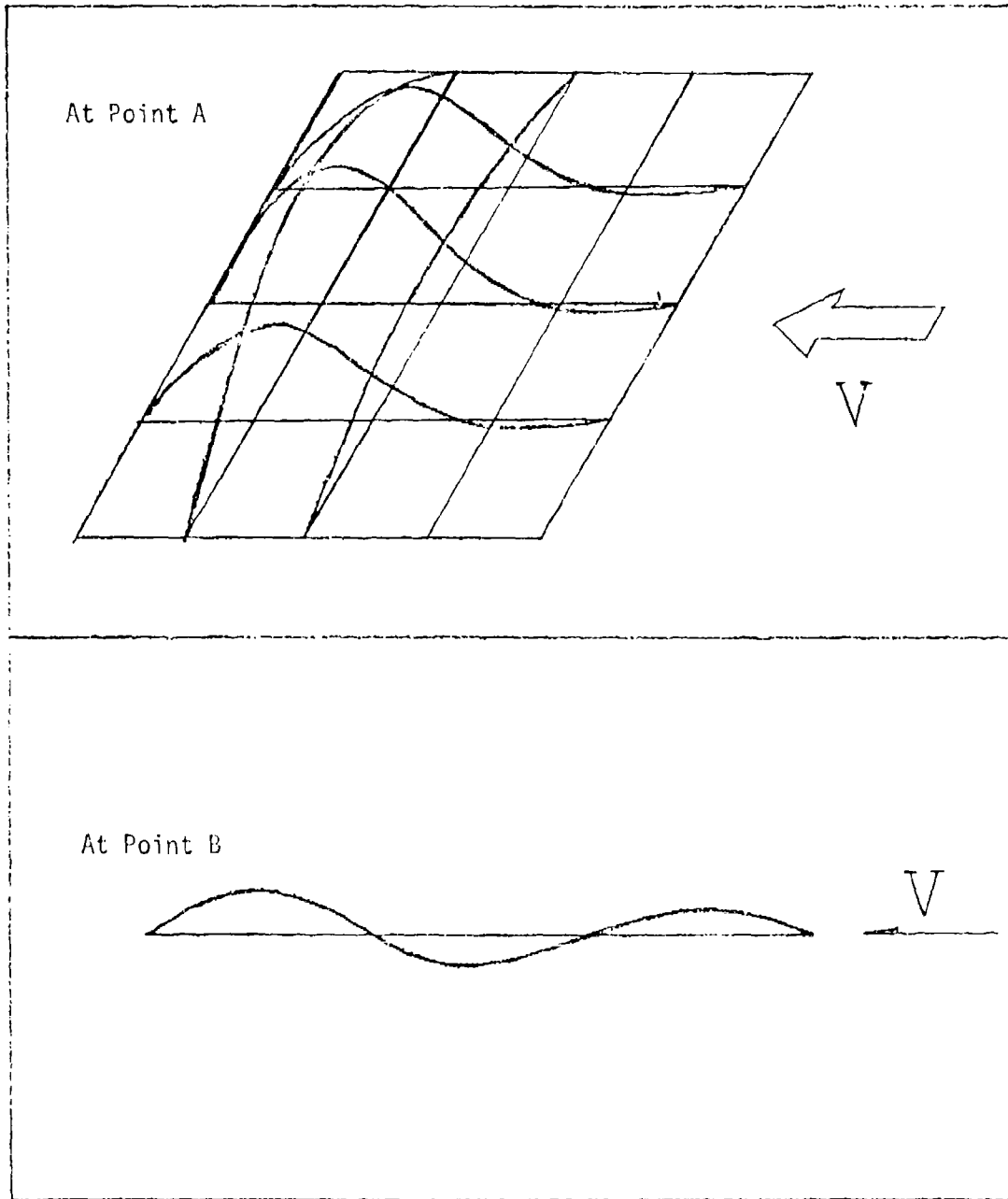


Figure 27 The First Mode Shape ( Real Part ) for Panel Corresponding to Point A in Fig. 26 and the Third Mode Shape ( Real Part ) for the Center Line of Panel Corresponding to Point B in Fig. 26.

Fig. 28 shows that the fifth mode flutter boundary is the critical boundary for panels with  $l/w = 2.0$ . The results by Hedgepeth and Cunningham are seen to be in good agreement with the present results. The corresponding first and fifth flutter mode shapes (real part) are shown in Fig. 29.

#### Case 4 Clamped Square Panels with Various Tension Parameters and Mach Numbers

One of the advantages of the finite element method is that the effect of in-plane forces can be included in a direct and accurate fashion. To demonstrate this, a square clamped panel was chosen and four different tension parameters  $F = 0.01, 0.1, 0.5,$  and  $1$  were considered. The flutter boundaries were obtained for various Mach numbers.

Fig. 30 shows the dominating first mode flutter boundaries and the hyperbola for the square, aluminum panel at 25,000 feet above sea level and at  $M = 1.1$ . Four values of tension parameters were included.

The mode shapes (real part) corresponding to points A ( $F = 0.01$ ) and point B ( $F = 0.1$ ) of the flutter boundaries in Fig. 30 are plotted in Figs. 31 and 32. The mode shapes for the case  $F = 0.5$  and  $1.0$  are similar to those shown in Figs. 31 and 32. They are thus not shown here.

Fig. 33 shows the first and the third mode flutter boundaries for  $M = 1.2$  and various tension parameters. For aluminum panels at 25,000 feet above sea level (dashed parabola), the third mode boundaries are the critical flutter boundaries. The first flutter mode shapes (real part) corresponding to points A and B in Fig. 33 are presented in Figs. 34 and 35, respectively.

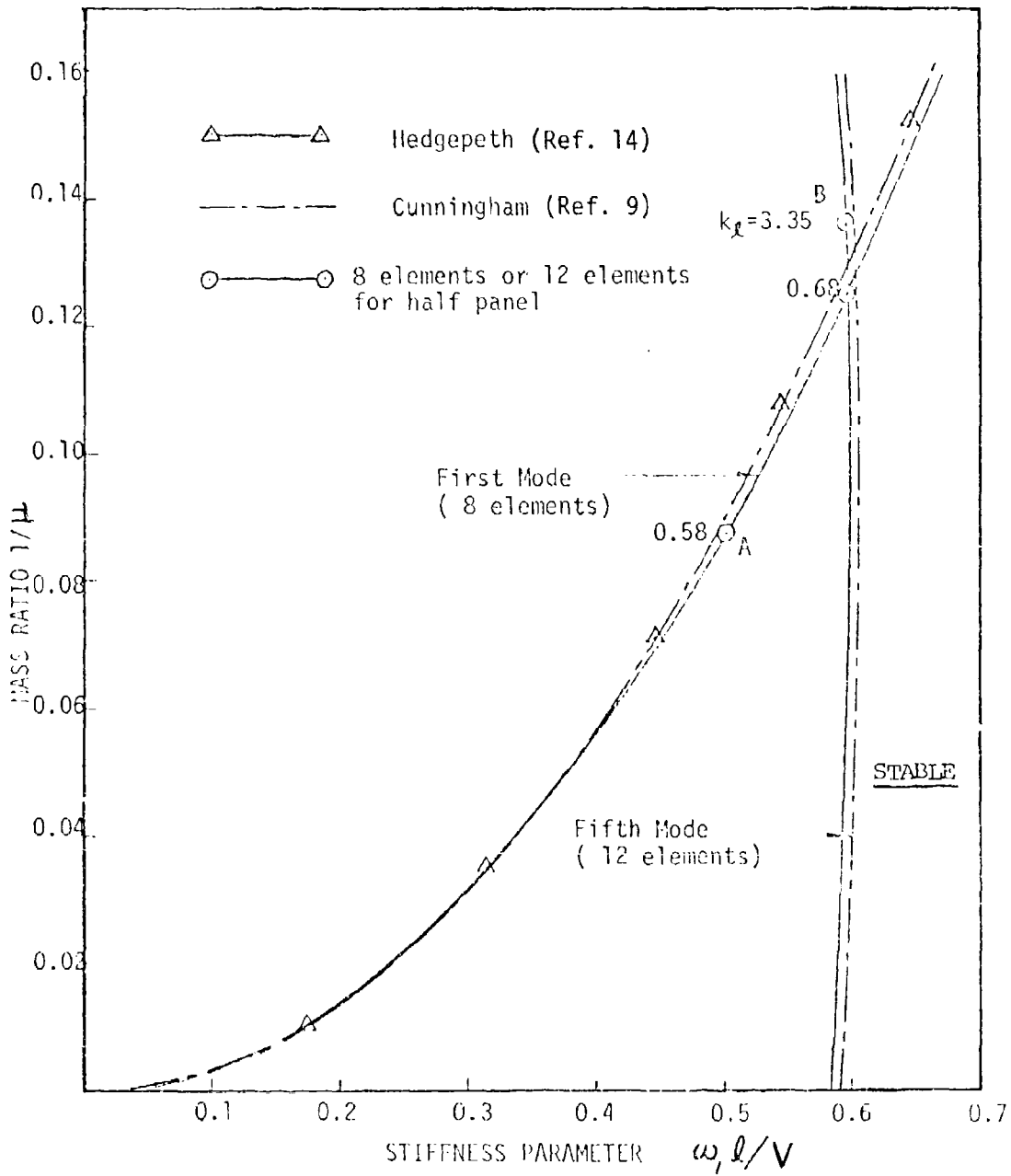


Figure 28 Flutter boundaries for pinned-edge panel with  $l/w = 2$  and  $M = 1.3$ .

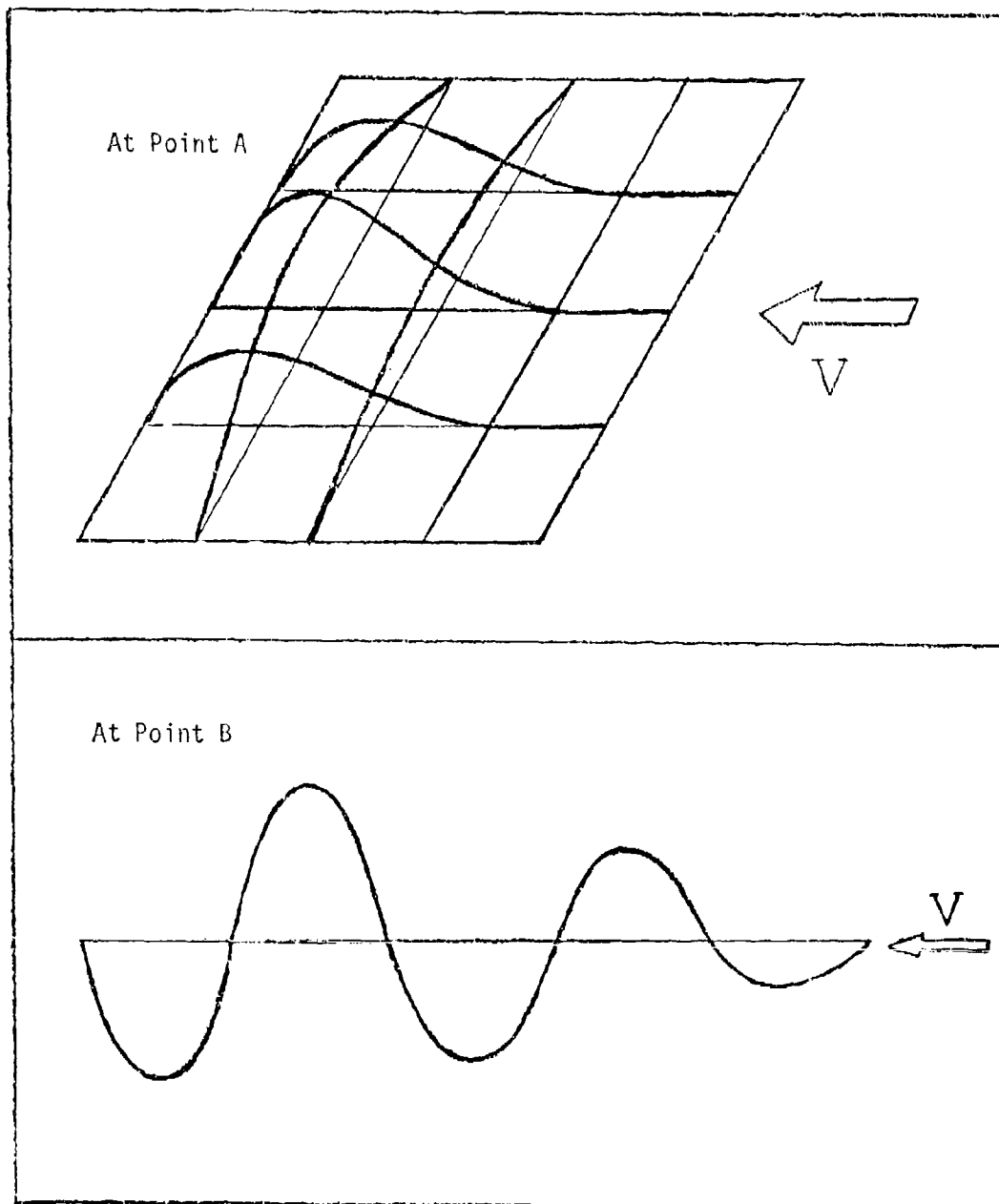


Figure 29 The First Mode Shape ( Real Part ) for Panel Corresponding to Point A in Fig. 28 and the Fifth Mode Shape ( Real Part ) for the Center Line of Panel Corresponding to Point B in Fig. 28.

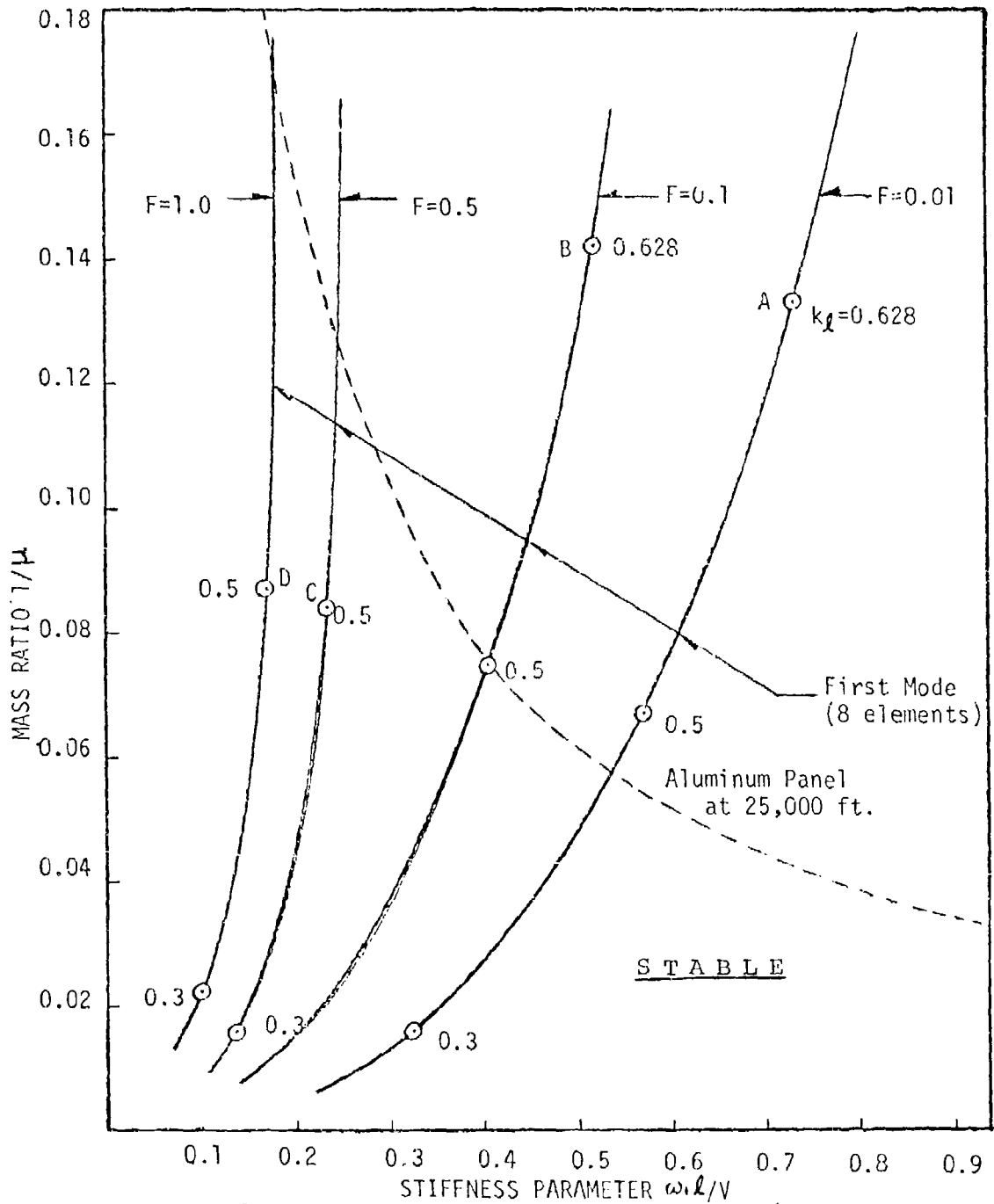


Figure 30. Flutter boundaries for clamped panels of  $l/w = 1.0$  with  $M = 1.1$  and various tension parameters  $F$ .



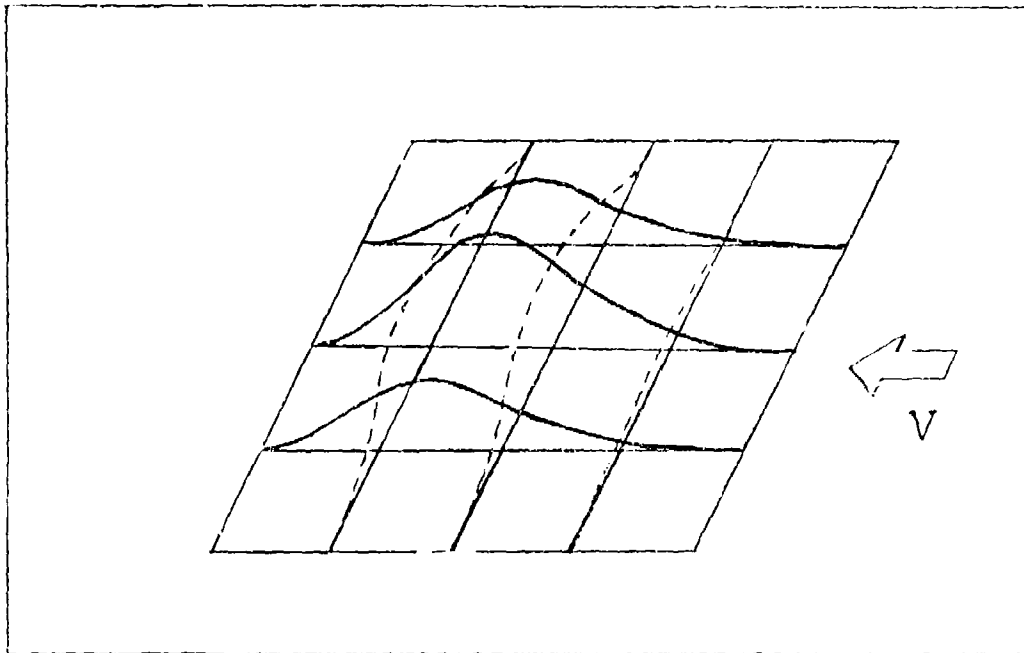


Figure 31 The First Mode Shape (Real Part) for Panel Corresponding to Point A in Fig. 30.

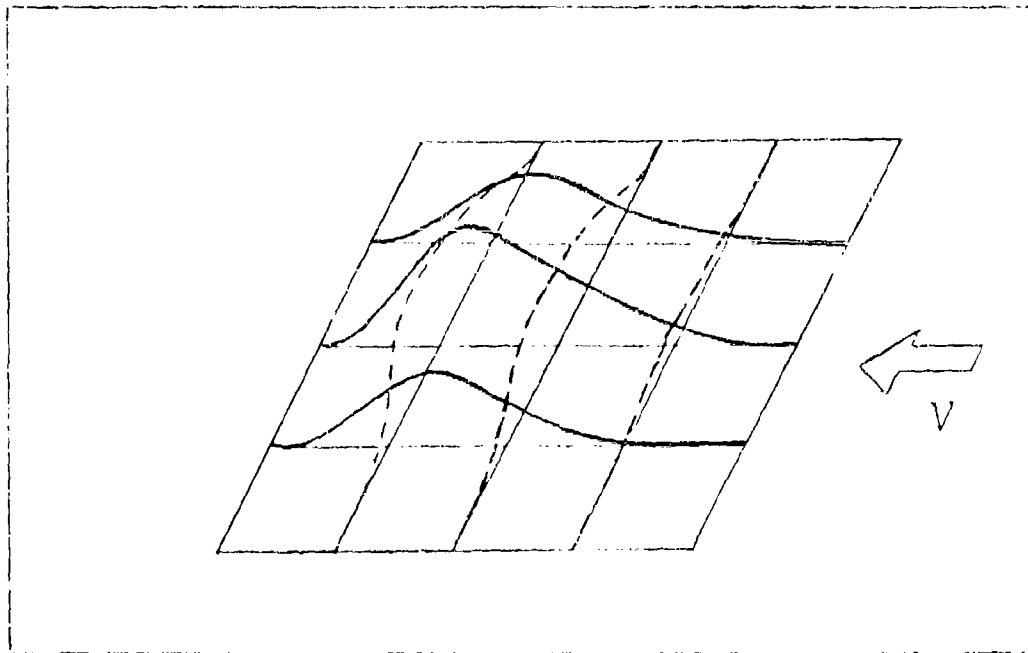


Figure 32 The First Mode Shape (Real Part) for Panel Corresponding to Point B in Fig. 30.

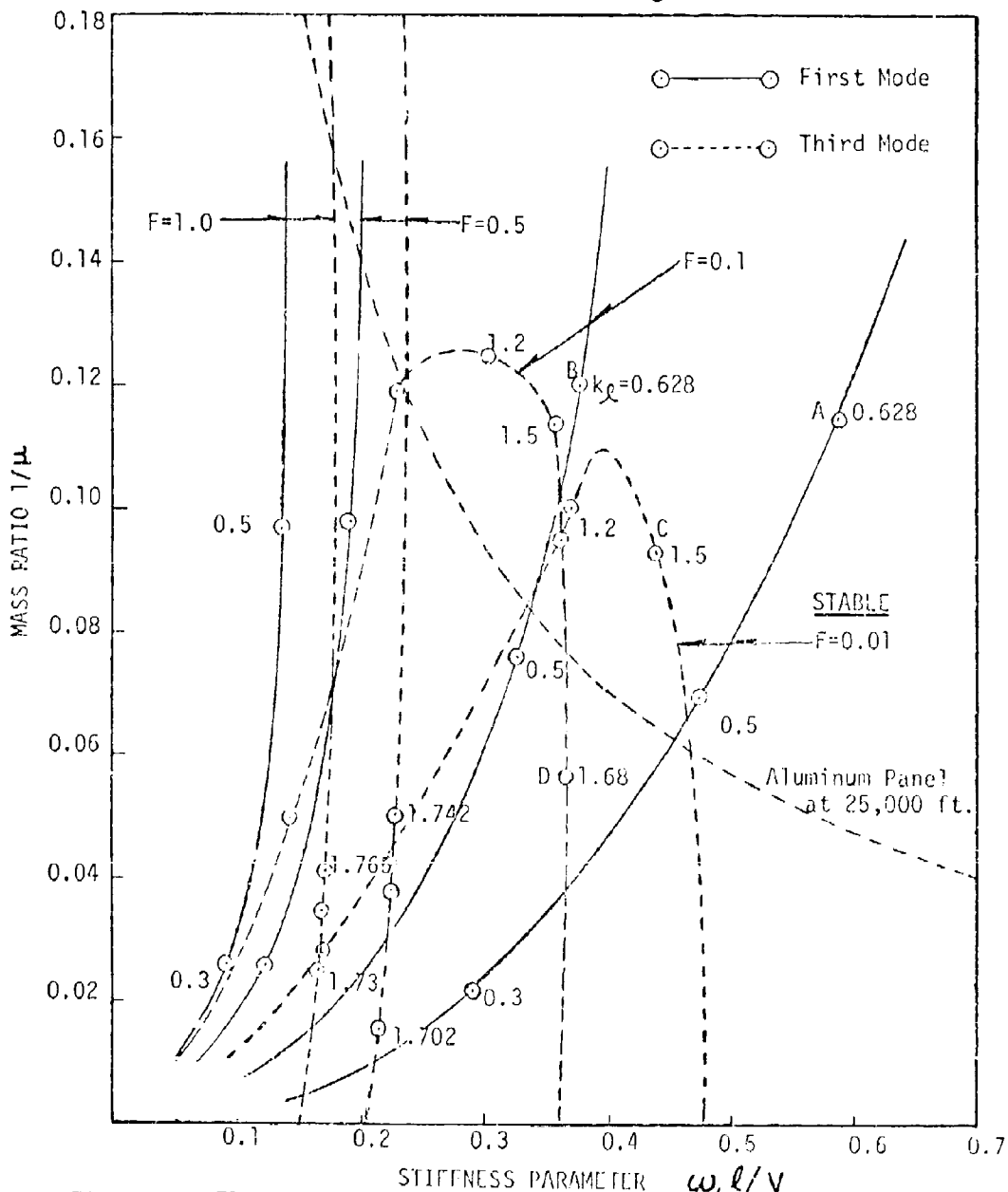


Figure 33 Flutter boundaries for clamped panels of  $l/w=1.0$  with  $M=1.2$  and various tension parameters  $F$

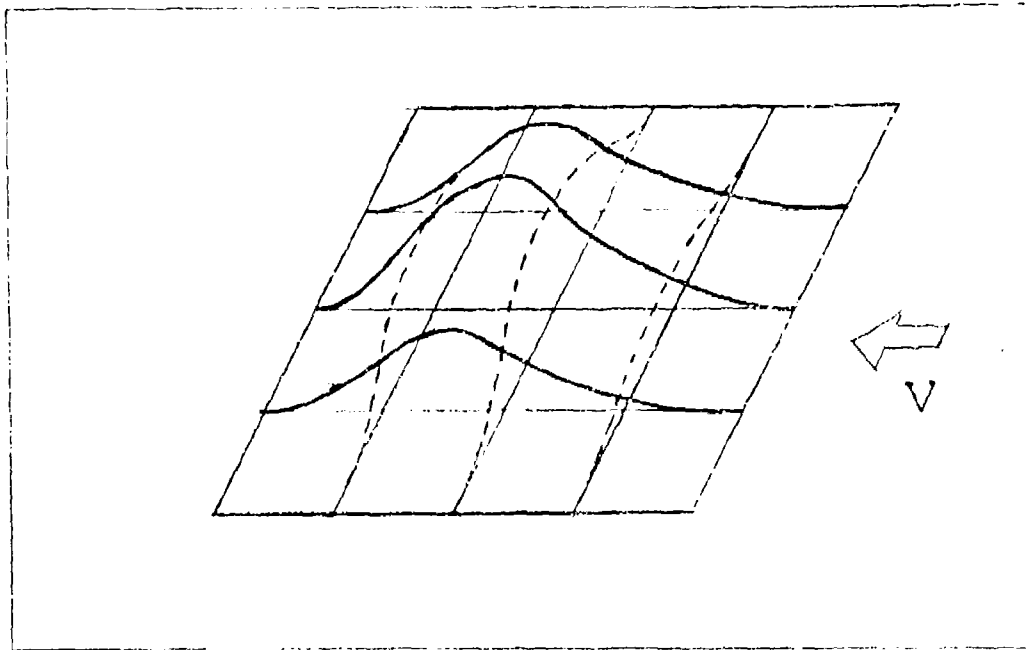


Figure 34 The First Mode Shape (Real Part) for Panel Corresponding to Point A in Fig. 33.

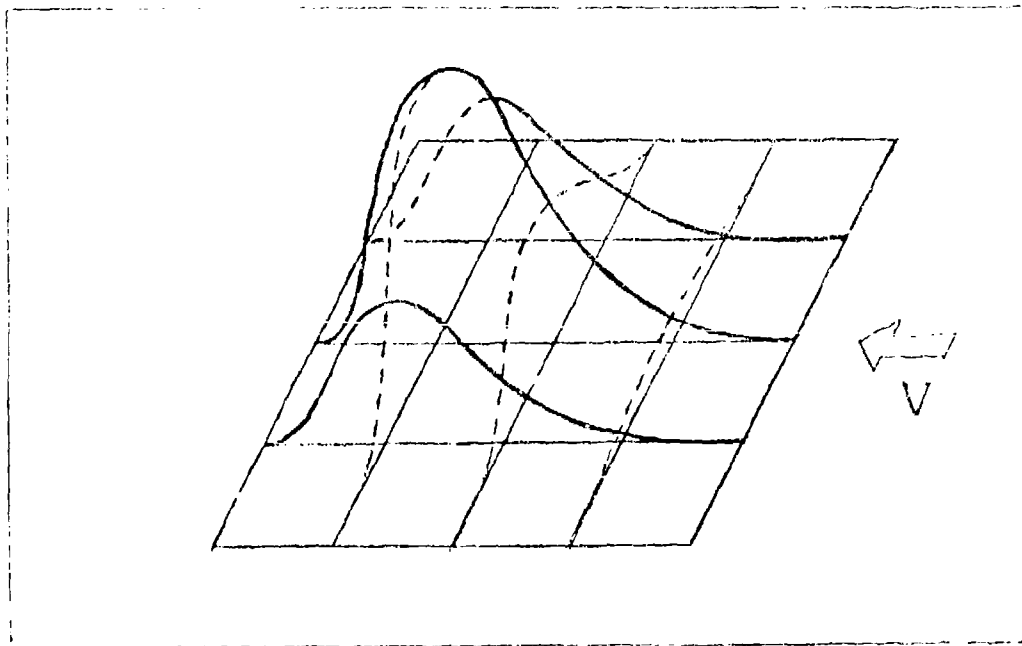


Figure 35 The First Mode Shape (Real Part) for Panel Corresponding to Point B in Fig. 33.

The third flutter mode shapes (real part) for the center chord lines corresponding to points C, D, E, and F are shown in Fig. 36.

Fig. 37 shows the first mode flutter boundaries for  $M = 1.3$  and the third mode flutter boundaries for  $M = 1.3, 1.32, 1.35$  for various values of tension. The flutter boundaries are dominated by the third mode. Since the flutter mode shapes are similar to those shown in the previous figures, they are not presented here.

Fig. 38 shows the flutter boundaries for  $M = 1.4, 1.45, 1.48$  and various tension parameters. The third mode flutter boundaries shift to the right as the Mach number increases. It is interesting to see that the top portions of the third mode flutter boundaries begin to bend down to the left as the Mach number increases.

Fig. 39 shows that for  $M = 1.5$  and various values of tension, the third mode flutter boundaries continue to bend down rapidly with a slight increase in Mach number.

Figs. 40 and 41 show that for  $M = 1.52$  and  $1.54$  and various values of tension, the third mode flutter boundaries bend down substantially to be small loops. They only dominate the lower range of the mass ratio.

Fig. 42 shows that for  $M = 1.6$ , all the third mode flutter boundaries disappear and the first mode flutter boundaries once again become the critical boundaries. Such a phenomenon is also the case for  $M = 2.0$  as shown in Fig. 43.

Also shown in Figs. 37-43 are the dashed parabolae for an aluminum panel at 25,000 feet above sea level.

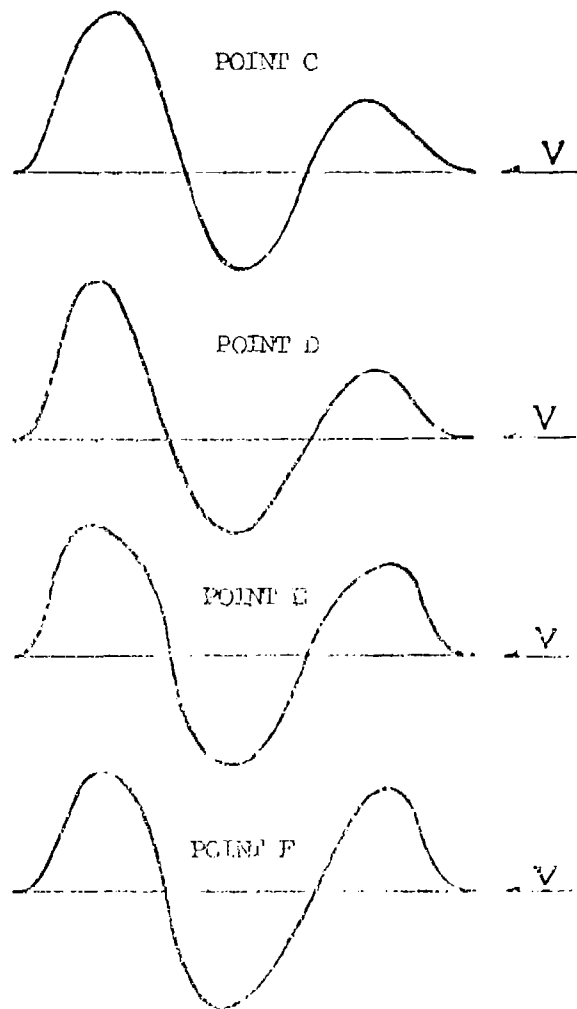


Figure 36 The Third Mode Shape (Real Part) for the Center Line of Panel with various tension parameter Corresponding to Point C, D, E, and F respectively in Fig. 33.

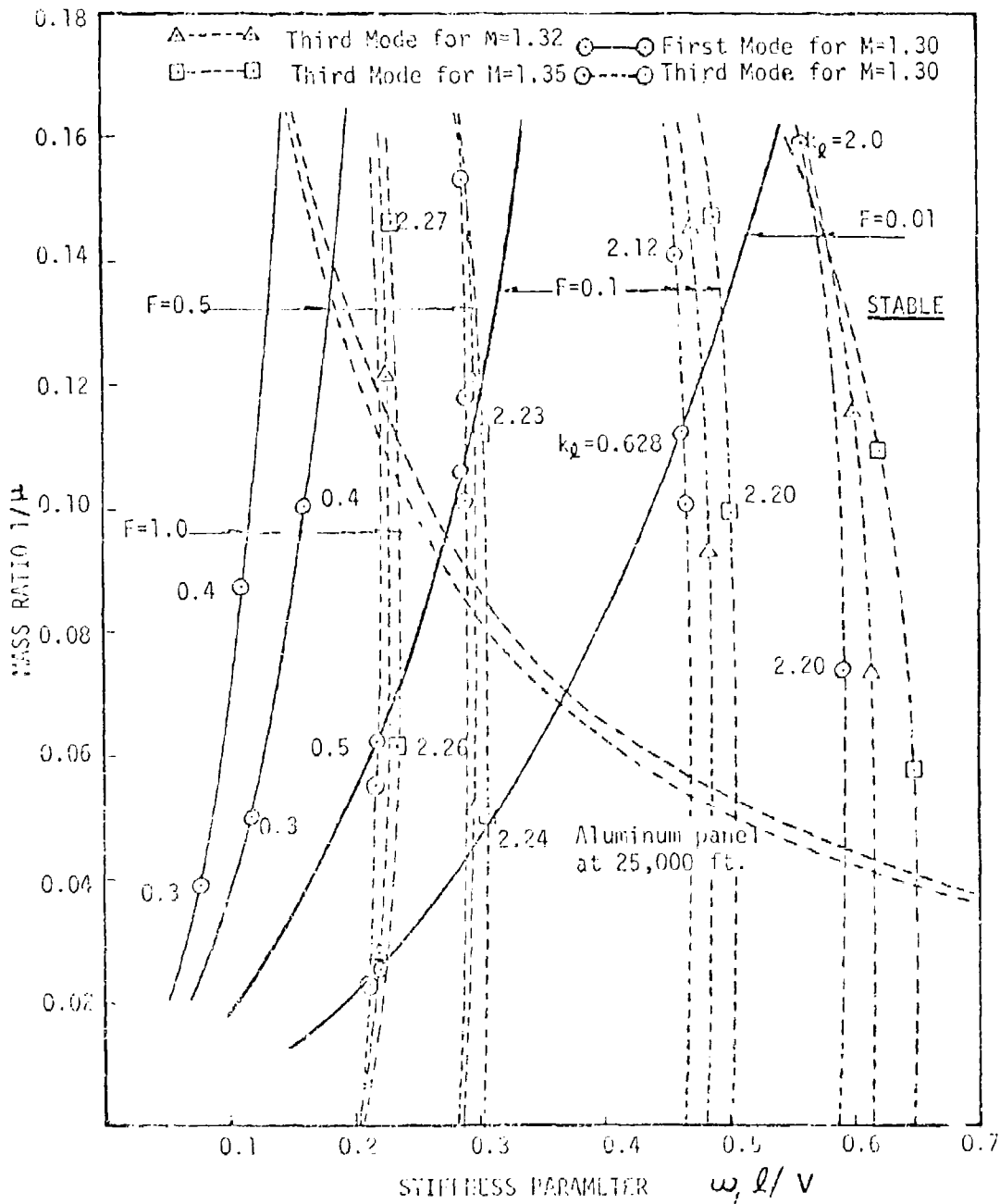


Figure 37 Flutter boundaries for clamped panels of  $l/w=1.0$  with  $M=1.3$ ,  $M=1.32$ ,  $M=1.35$  and various values of tension parameters  $F$ .

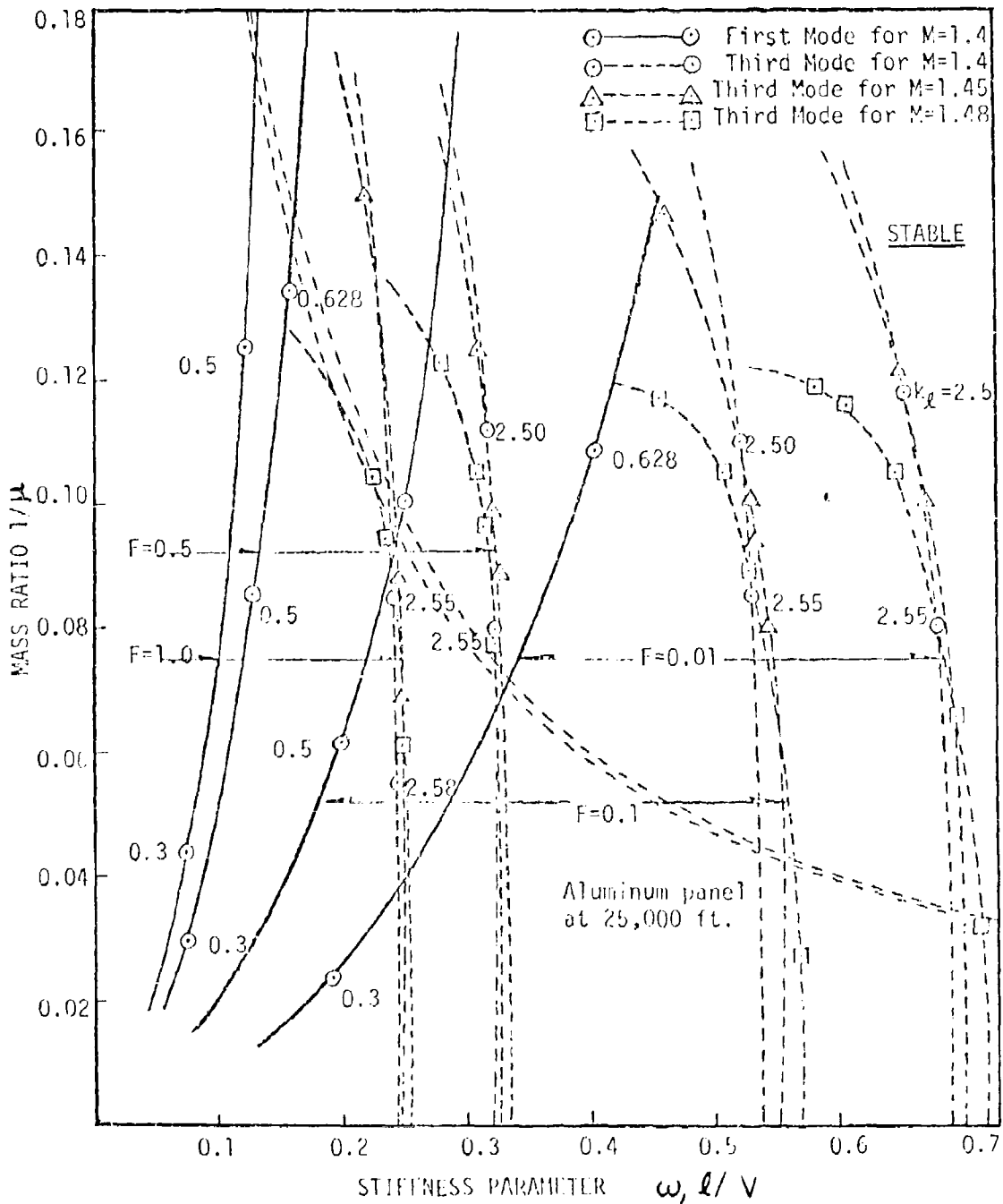


Figure 38 Flutter boundaries for clamped panels with  $l/w=1.0$  with  $M=1.4, M=1.45, M=1.48$  and various values of tension parameters  $F$ .

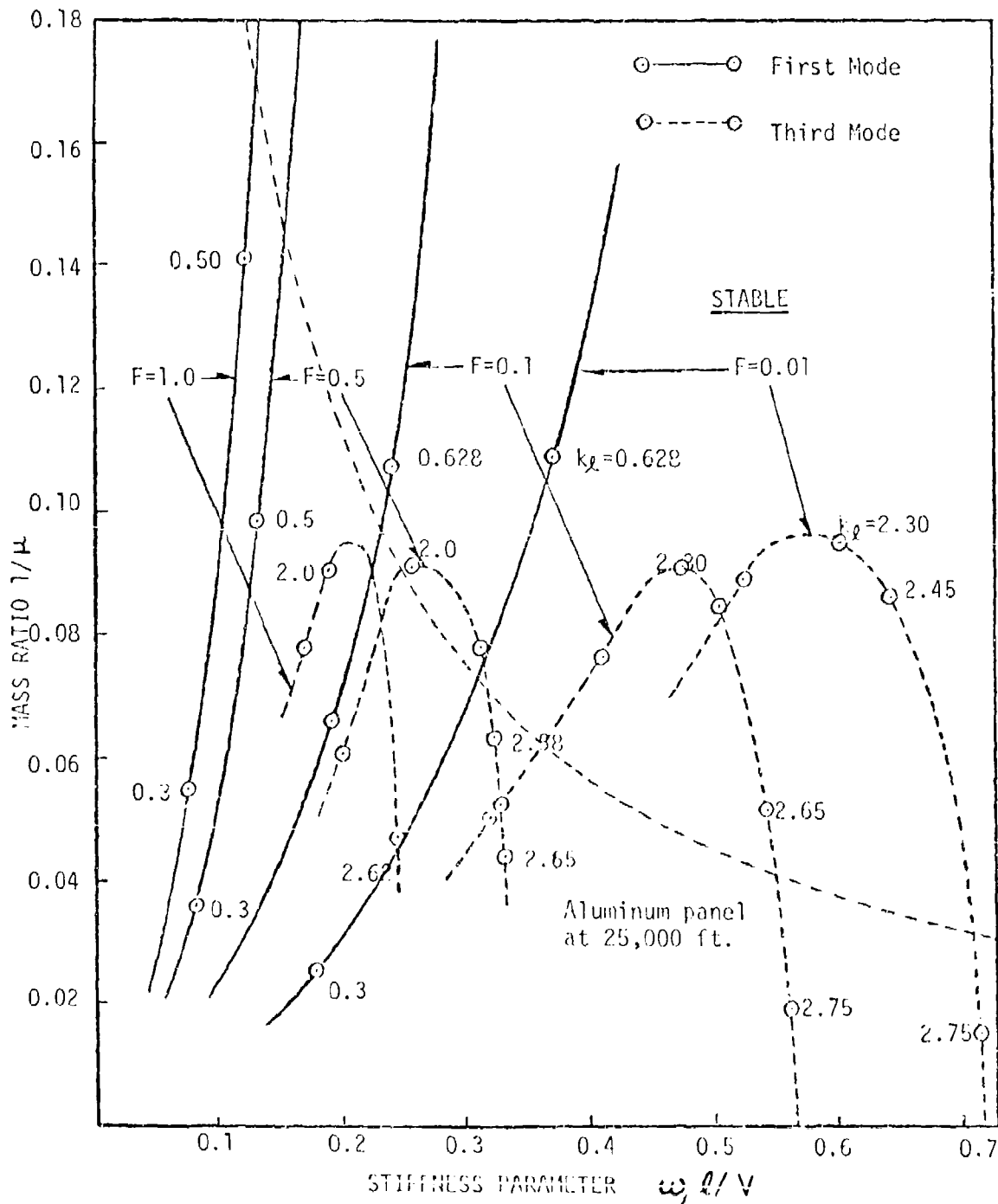


Figure 39 Flutter boundaries for clamped panels of  $l/w$  1.0 with  $M=1.5$  and various values of tension parameters  $F$ .



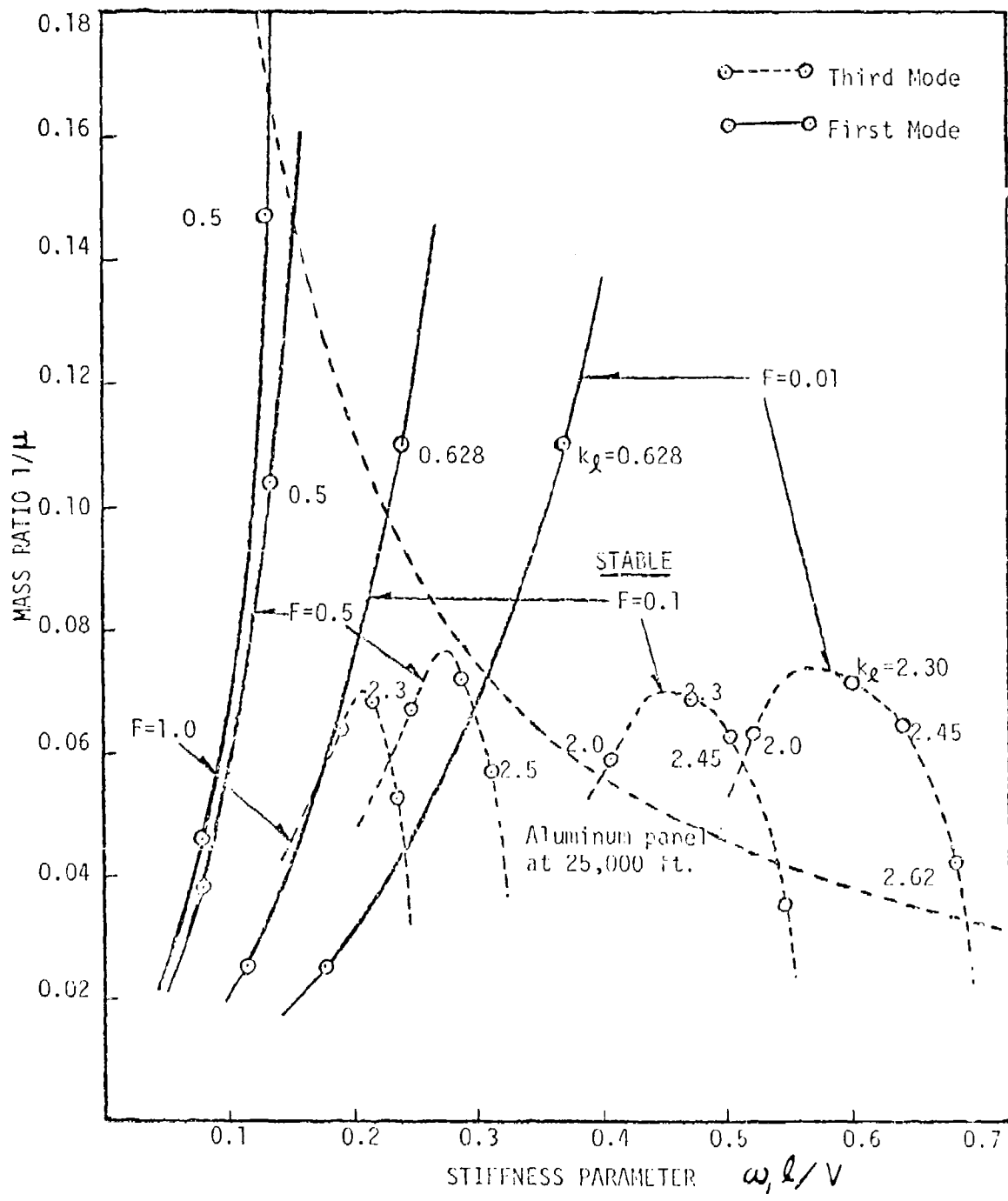


Figure 40. Flutter boundaries for clamped panels of  $l/w=1.0$  with  $M=1.52$  and various values of tension parameters  $F$ .

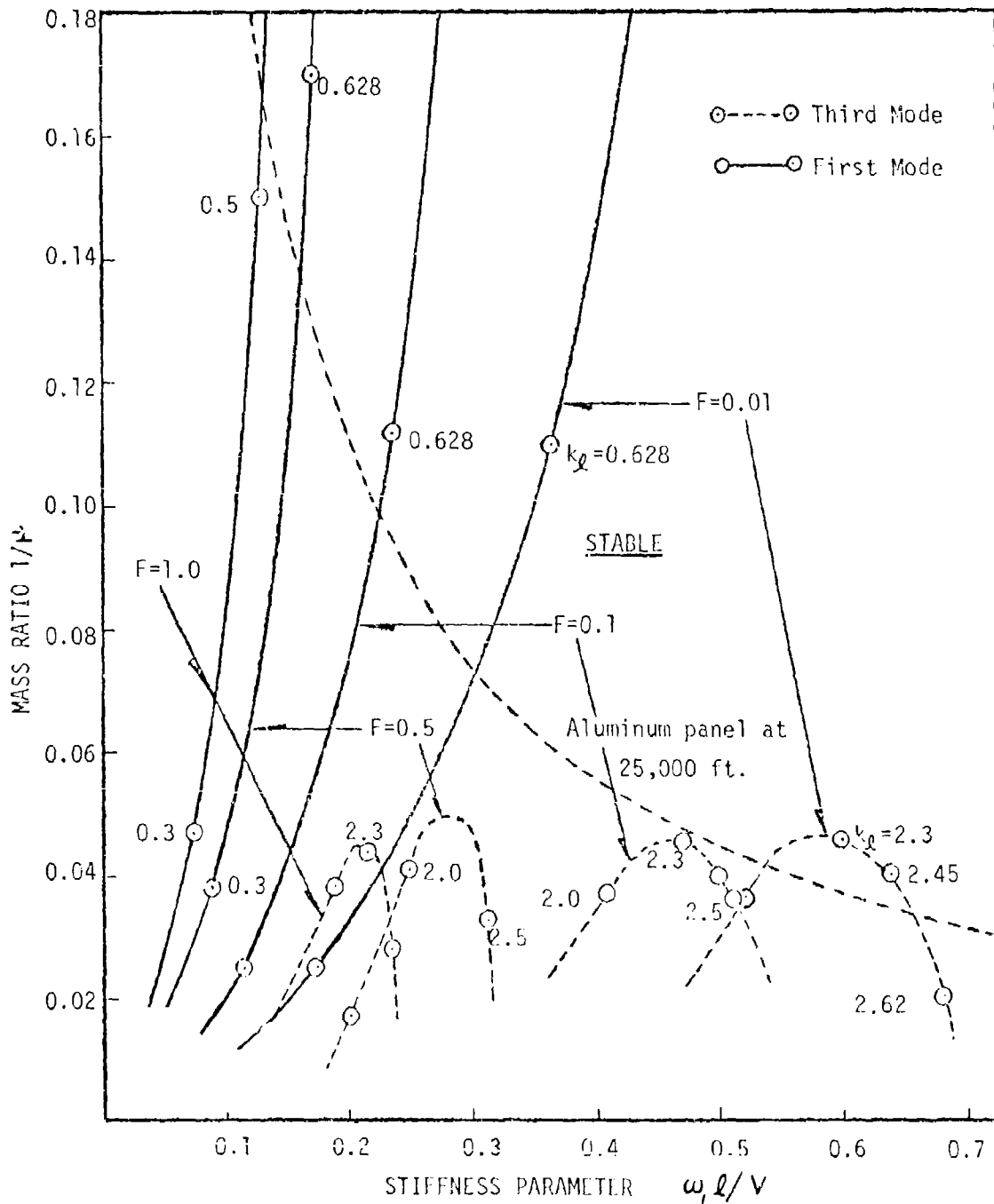


Figure 41 Flutter boundaries for clamped panels of  $l/w=1.0$  with  $M=1.54$  and various values of tension parameters  $F$ .

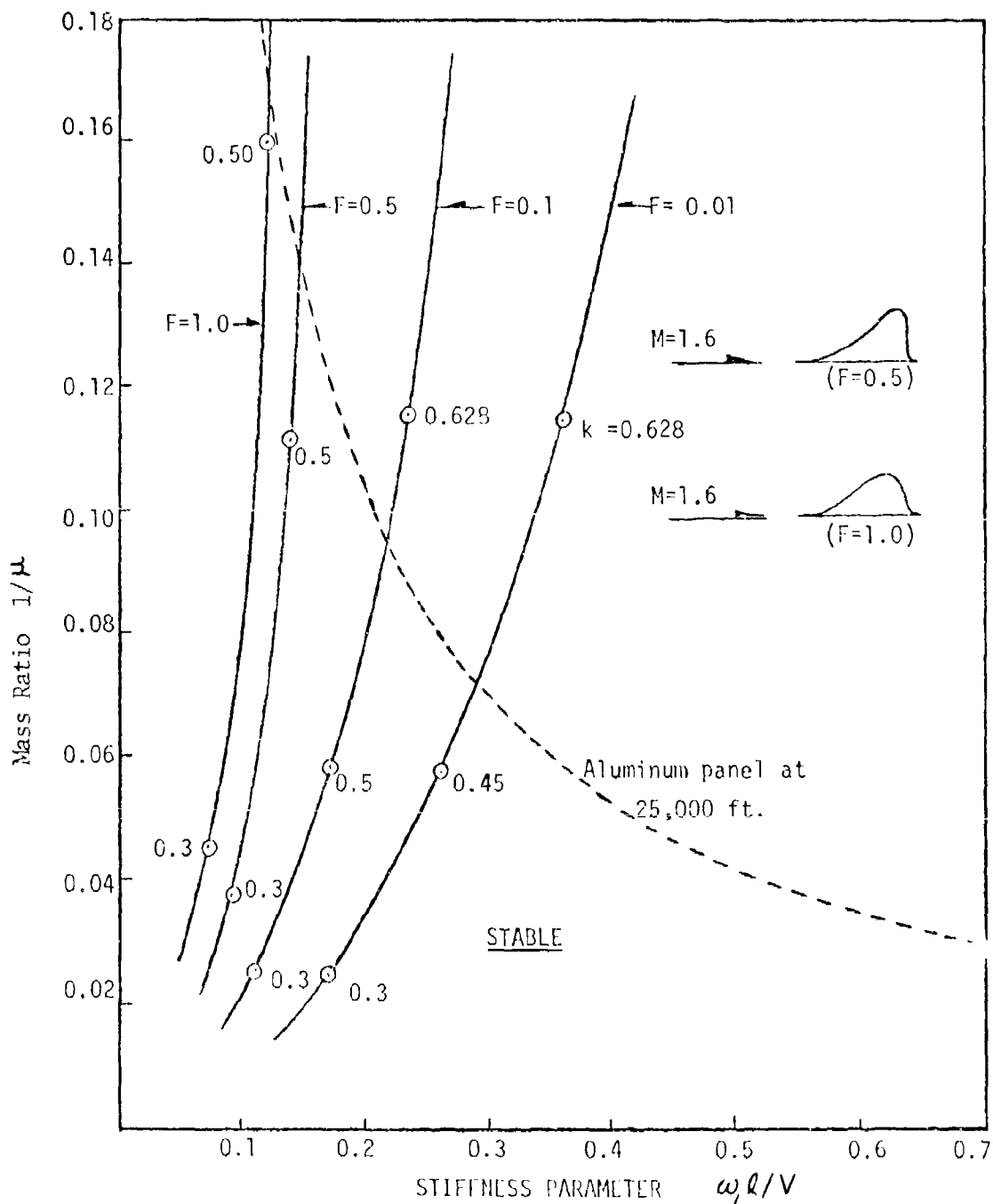


Figure 42 Flutter boundaries for clamped panels of  $l/w=1.0$  with  $M=1.6$  and various values of tension parameters  $F$ .

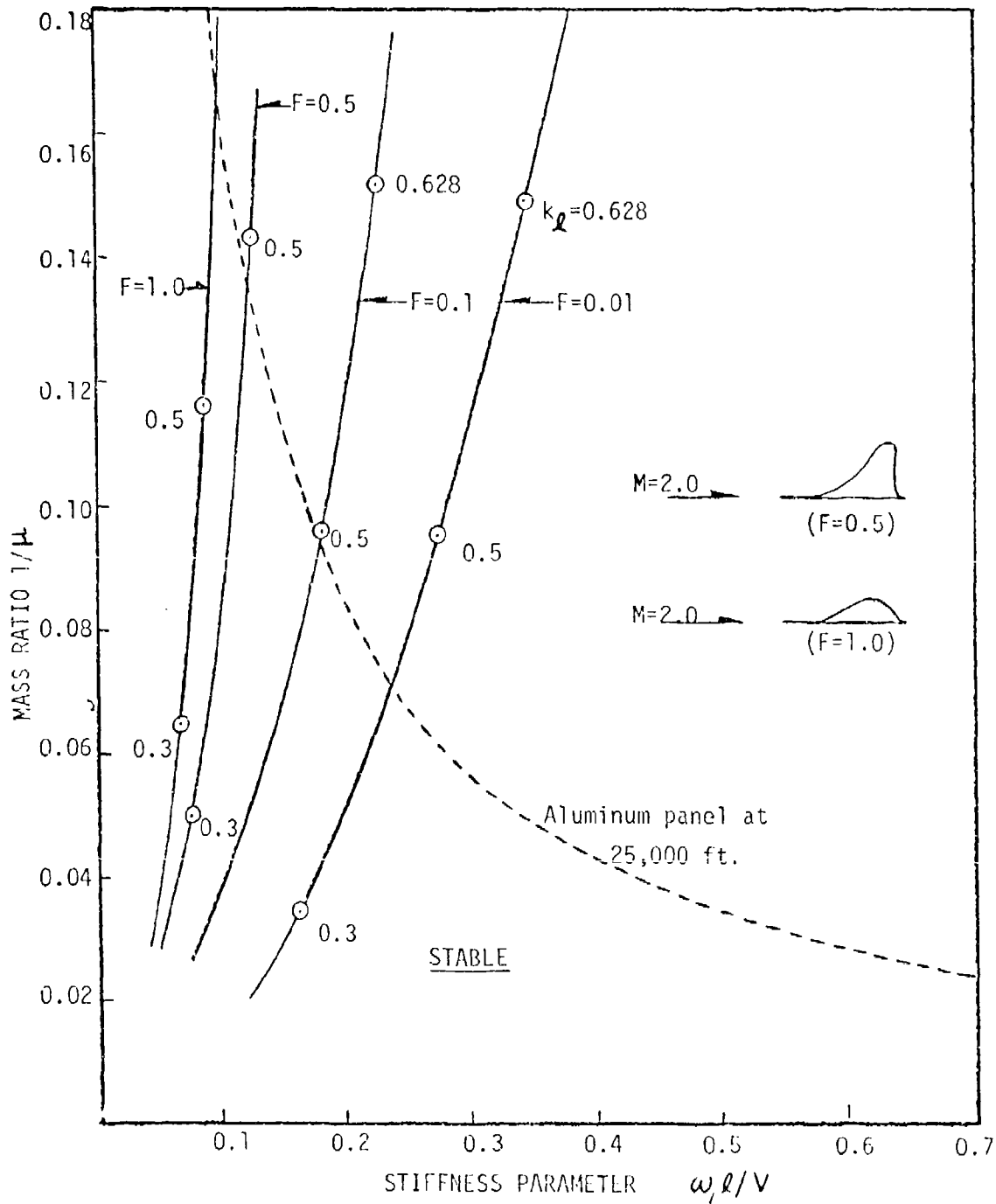


Figure 43 Flutter boundaries for clamped panel of  $\ell/w=1.0$  with  $M=2.0$  and various values of tension parameters  $F$ .

By collecting all the intersecting points between the dashed parabolas and the critical flutter boundaries in Figs. 30, 33, and 37-43, the results for thickness ratios required to prevent flutter of the panel are shown in Fig. 44 for various values of Mach numbers and tension.

In Fig. 44, the critical flutter boundaries were dominated by the third mode in the Mach region between approximately 1.2 and 1.5. For other lower and higher Mach regions, the first mode flutter boundaries dominate. The sharp drops in the curves are due to the abrupt changes in critical flutter modes.

The beneficial effect of introducing in-plane tensions to reduce the required panel thickness to avoid flutter is clearly demonstrated. Fig. 44 should be of value to panel flutter analysts and designers.

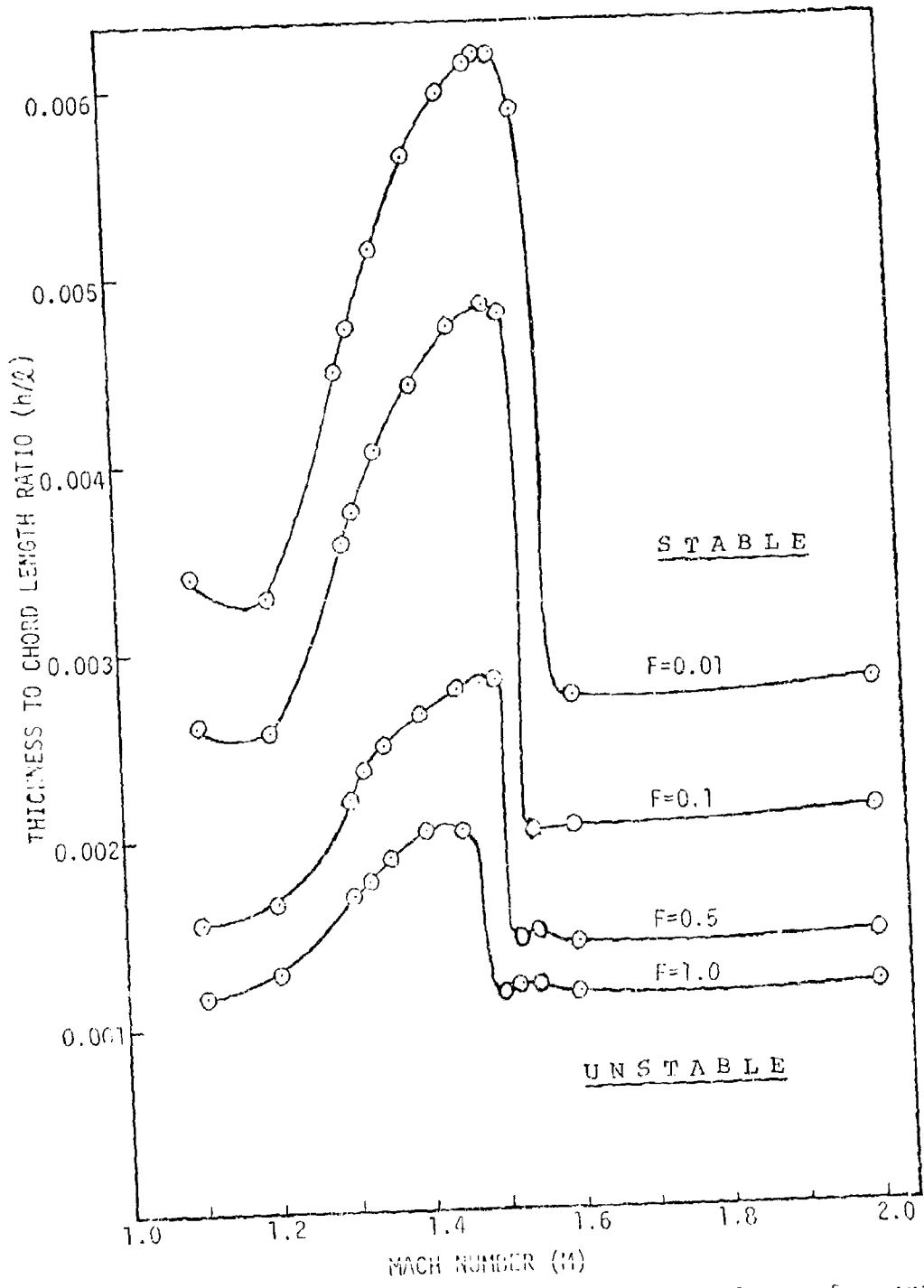


Figure 44 Thickness ratio required to prevent flutter for various values of tension parameter  $F$  for a square clamped aluminum panel at 25,000 ft. above sea level

SECTION V  
CONCLUDING REMARKS

A basic finite element procedure for panel flutter analysis has been developed and performed with examples. The following concluding remarks may be made.

(1) The three-dimensional supersonic unsteady potential flow theory was employed. This theory allows the treatment of panels with finite aspect ratio. It is particularly advantageous at low supersonic range ( $1 < M < \sqrt{2}$ ) for panels with chord-span ratio less than one, when the piston theory does not give satisfactory results.

(2) The finite element method offers a set of elegant and straightforward eigenvalue equations. It can be used directly to solve for flutter frequencies and mode shapes without requiring the natural vibration frequencies and mode shapes before the eigensolution, and also without requiring the computation of mode shapes after the eigensolution.

(3) If the modal method is used in panel flutter analysis, one could use the natural frequencies and modes found by the finite element method. Such procedure is, however, basically different from the present finite element method.

(4) The formulations here (Eqs. 19-24) are general. They are readily applicable to any plate finite element displacement model whose shape functions are known.

(5) The present results agree well with Galerkin's modal solution by Cunningham.

(6) The critical flutter boundaries for a square clamped panel change modes abruptly as the Mach number is varied.

(7) Fig. 44 clearly demonstrates the beneficial effect of in-plane tensions.

(8) The present development may provide a basic finite element procedure for panel flutter analysis. The present results may provide useful data to the flutter analysts and designers.

(9) A logical next step appears to be the development of a method using triangular plate finite elements combined with triangular Mach boxes. Such development will be of great value to the flutter predictions of wing panels with arbitrary configurations. It is suggested that the triangular element developed by Bell (Reference 15) be used.



## REFERENCES

1. Dowell, E.H., Aeroelasticity of Plates and Shells, Noordhoff International Publishing, Leyden, The Netherlands, 1975.
2. Garrick, I.E., Aerodynamic Flutter, AIAA Selected Reprint Series, Vol. V, March 1969.
3. Olson, M.D., "Finite Elements Applied to Panel Flutter," AIAA Journal, Vol. 5, December 1967, pp. 2267-2270.
4. Olson, M.D., "Some Flutter Solutions Using Finite Elements," AIAA Journal, Vol. 8, April 1970, pp. 747-752.
5. Appa, K. and Somashekar, B.R., "Application of Matrix Displacement Methods in the Study of Panel Flutter," AIAA Journal, Vol. 7, January 1969, pp. 50-53.
6. Appa, K., Somashekar, B.R., and Shah, C.G., "Discrete Element Approach to Flutter of Skew Panels with Inplane Forces under Yawed Supersonic Flow," AIAA Journal, Vol. 8, November 1970, pp. 2017-2022.
7. Sander, G., Bon, C., and Ceradin, M., "Finite Element Analysis of Supersonic Panel Flutter," International Journal for Numerical Methods in Engineering, Vol. 7, 1973, pp. 379-394.
8. Yang, T.Y., "Flutter of Flat Finite Element Panels in a Supersonic Potential Flow," AIAA Journal, Vol. 13, November 1975, pp. 1502-1507.
9. Cunningham, H.J., "Flutter Analysis of Flat Rectangular Panels Based on Three-Dimensional Supersonic Unsteady Potential Flow," NASA-TR R-256, 1967.
10. Dowell, E.H. and Voss, H.M., "Theoretical and Experimental Panel Flutter Studies in the Mach Number Range 1.0 to 5.0," AIAA Journal, Vol. 3, December 1965, pp. 2292-2304.
11. Bogner, F.K., Fox, R.L., and Schmit, L.A., "The Generation of Interelement - Compatible Stiffness and Mass Matrices by the Use of Interpolation Formulas," Proceedings of the Conference on Matrix Methods in Structural Mechanics, Air Force Flight Dynamics Laboratory, TR-66-80, 1966, pp. 397-443.
12. Watkins, E.E., "Three Dimensional Supersonic Theory," AGARD Manual on Aeroelasticity, November 1960, Part II, Chapter 5.

13. Houbolt, J.C., "A Study of Several Aerothermoelastic Problems of Aircraft Structures in High Speed Flight," Doctor of T.S. Thesis, The Swiss Federal Institute of Technology, Leeman, Zürich, 1958.
14. Hedgepeth, J.M., "Flutter of Rectangular Simply-Supported Panels at High Supersonic Speeds," Journal of Aeronautical Sciences, Vol. 24, No. 8, August 1957, pp. 563-573, 586.
15. Bell, K., "A Refined Triangular Plate Bending Finite Element," International Journal for Numerical Methods in Engineering, Vol. 1, 1969, pp. 101-122.

APPENDIX  
THE COMPUTER PROGRAM

The description and listing of the computer program are provided in this appendix. The flow chart is given on pages 69 and 70. The procedure for input is given on pages 62, 67, and 68. The use of the program is demonstrated by considering an example of a square clamped panel with  $k_g = 0.5$ ,  $M = 1.2$ , and  $F = 0.1$ . Both input and output data are provided.

The stiffness, mass, and incremental stiffness matrices are based on the known explicit coefficients. These coefficients are read in as input data given on pages 63-66. The program uses the subroutine EISPACK for solving the general complex eigenvalue equations.

## INPUT DATA

### 1. Control Card (2F5.2, 7I3, 4F7.4)

Columns	1-5	Panel chordwise length (XL)
	6-10	Panel spanwise width (YL)
	11-13	Number of elements in chordwise direction (NX)
	14-16	Half number of elements in spanwise direction (NY)
	17-19	Number of boxes in streamwise (or chordwise) direction for one element (IBX)
	20-22	Number of boxes in cross-streamwise (or spanwise) direction for one element (IBY)
	23-25	Total number of degrees of freedom for the panel (NXD)
	26-28	Number of nodes in streamwise direction (NDX)
	29-31	Number of nodes in cross-streamwise direction (NDY)
	32-38	Structural damping coefficient (SG)
	39-45	Mach number (MACH)
	46-52	Starting value for the mass ratio range (MUO)
	53-59	Increment for the values of mass ratios (XINCR)

### 2. Element matrix cards (8I4, 2I2, 2I4, 2I6)

Read in the data given on pages 63-66.

TABLE I DATA INFORMATION FOR QQ(I,J), QM(I,J) and QN(I,J)

QK(I,J)-ELEMENT STIFFNESS MATRIX  
 QM(I,J)-ELEMENT MASS MATRIX  
 QN(I,J)-ELEMENT INCREMENTAL STIFFNESS MATRIX

MATRIX LOCATION	CARD NUMBER	JS(1) 1-4	JS(2) 5-8	JS(3) 9-12	JS(4) 13-15	JS(5) 17-20	JS(6) 21-24	JS(7) 25-28	JS(8) 29-32	INDEX 12,14	QK(I,J) DATA JM(1) 37-40	QM(I,J) DATA JM(2) 41-44	QN(I,J) DATA JM(3) 45-50
(1,1)	1	156	25	156	35	72	25	-6	1	-0	169	1	78
(1,2)	2	175	25	175	35	72	25	-6	1	-0	143	6	13
(1,3)	3	533	25	533	35	72	25	-6	1	-0	143	3	26
(1,4)	4	22	78	22	35	6	35	6	5	1	143	6	33
(1,5)	5	11	35	11	35	6	35	6	5	1	121	3	11
(1,6)	6	4	35	4	35	6	35	6	5	1	13	3	2100
(1,7)	7	11	35	11	35	6	35	6	5	1	121	3	11
(1,8)	8	2	35	2	35	6	35	6	5	1	11	13	11
(1,9)	9	4	35	4	35	6	35	6	5	1	11	13	11
(1,10)	10	4	35	4	35	6	35	6	5	1	11	13	11
(1,11)	11	4	35	4	35	6	35	6	5	1	117	2	27
(1,12)	12	13	35	13	35	6	35	6	5	1	93	4	9
(1,13)	13	10	35	10	35	6	35	6	5	1	159	12	29
(1,14)	14	10	35	10	35	6	35	6	5	1	143	7	13
(1,15)	15	15	35	15	35	6	35	6	5	1	169	7	13
(1,16)	16	15	35	15	35	6	35	6	5	1	133	4	9
(1,17)	17	10	35	10	35	6	35	6	5	1	9	2	9
(1,18)	18	10	35	10	35	6	35	6	5	1	143	2	9
(1,19)	19	10	35	10	35	6	35	6	5	1	13	2	13
(1,20)	20	10	35	10	35	6	35	6	5	1	13	2	13
(1,21)	21	15	35	15	35	6	35	6	5	1	143	2	13
(1,22)	22	15	35	15	35	6	35	6	5	1	13	2	13
(1,23)	23	15	35	15	35	6	35	6	5	1	169	2	13
(1,24)	24	15	35	15	35	6	35	6	5	1	-169	2	-13
(1,25)	25	15	35	15	35	6	35	6	5	1	-143	2	-13
(1,26)	26	15	35	15	35	6	35	6	5	1	-143	2	-13
(1,27)	27	15	35	15	35	6	35	6	5	1	-143	2	-13
(1,28)	28	15	35	15	35	6	35	6	5	1	-143	2	-13
(1,29)	29	15	35	15	35	6	35	6	5	1	-143	2	-13
(1,30)	30	15	35	15	35	6	35	6	5	1	-143	2	-13
(1,31)	31	15	35	15	35	6	35	6	5	1	-143	2	-13
(1,32)	32	15	35	15	35	6	35	6	5	1	-143	2	-13
(1,33)	33	15	35	15	35	6	35	6	5	1	-143	2	-13
(1,34)	34	15	35	15	35	6	35	6	5	1	-143	2	-13
(1,35)	35	15	35	15	35	6	35	6	5	1	-143	2	-13

TABLE I DATA INFORMATION FOR QQ(I,J), QM(I,J) and QN(I,J), continued ...

(8, 8)	36	4	105	4	105	225	0	1	2	2	1	9	1	150	2
(9, 1)	37	54	35	105	72	35	0	1	1	1	1	9	1	150	2
(9, 2)	38	54	35	35	36	35	0	1	1	1	1	9	1	150	2
(9, 3)	39	54	35	35	36	35	0	1	1	1	1	9	1	150	2
(9, 4)	40	54	35	35	36	35	0	1	1	1	1	9	1	150	2
(9, 5)	41	54	35	35	36	35	0	1	1	1	1	9	1	150	2
(9, 6)	42	54	35	35	36	35	0	1	1	1	1	9	1	150	2
(9, 7)	43	54	35	35	36	35	0	1	1	1	1	9	1	150	2
(9, 8)	44	54	35	35	36	35	0	1	1	1	1	9	1	150	2
(9, 9)	45	54	35	35	36	35	0	1	1	1	1	9	1	150	2
(10, 1)	46	54	35	35	36	35	0	1	1	1	1	9	1	150	2
(10, 2)	47	54	35	35	36	35	0	1	1	1	1	9	1	150	2
(10, 3)	48	54	35	35	36	35	0	1	1	1	1	9	1	150	2
(10, 4)	49	54	35	35	36	35	0	1	1	1	1	9	1	150	2
(10, 5)	50	54	35	35	36	35	0	1	1	1	1	9	1	150	2
(10, 6)	51	54	35	35	36	35	0	1	1	1	1	9	1	150	2
(10, 7)	52	54	35	35	36	35	0	1	1	1	1	9	1	150	2
(10, 8)	53	54	35	35	36	35	0	1	1	1	1	9	1	150	2
(10, 9)	54	54	35	35	36	35	0	1	1	1	1	9	1	150	2
(10, 10)	55	54	35	35	36	35	0	1	1	1	1	9	1	150	2
(11, 1)	56	54	35	35	36	35	0	1	1	1	1	9	1	150	2
(11, 2)	57	54	35	35	36	35	0	1	1	1	1	9	1	150	2
(11, 3)	58	54	35	35	36	35	0	1	1	1	1	9	1	150	2
(11, 4)	59	54	35	35	36	35	0	1	1	1	1	9	1	150	2
(11, 5)	60	54	35	35	36	35	0	1	1	1	1	9	1	150	2
(11, 6)	61	54	35	35	36	35	0	1	1	1	1	9	1	150	2
(11, 7)	62	54	35	35	36	35	0	1	1	1	1	9	1	150	2
(11, 8)	63	54	35	35	36	35	0	1	1	1	1	9	1	150	2
(11, 9)	64	54	35	35	36	35	0	1	1	1	1	9	1	150	2
(11, 10)	65	54	35	35	36	35	0	1	1	1	1	9	1	150	2
(12, 1)	66	54	35	35	36	35	0	1	1	1	1	9	1	150	2
(12, 2)	67	54	35	35	36	35	0	1	1	1	1	9	1	150	2
(12, 3)	68	54	35	35	36	35	0	1	1	1	1	9	1	150	2
(12, 4)	69	54	35	35	36	35	0	1	1	1	1	9	1	150	2
(12, 5)	70	54	35	35	36	35	0	1	1	1	1	9	1	150	2
(12, 6)	71	54	35	35	36	35	0	1	1	1	1	9	1	150	2
(12, 7)	72	54	35	35	36	35	0	1	1	1	1	9	1	150	2
(12, 8)	73	54	35	35	36	35	0	1	1	1	1	9	1	150	2
(12, 9)	74	54	35	35	36	35	0	1	1	1	1	9	1	150	2
(12, 10)	75	54	35	35	36	35	0	1	1	1	1	9	1	150	2
(13, 1)	76	54	35	35	36	35	0	1	1	1	1	9	1	150	2
(13, 2)	77	54	35	35	36	35	0	1	1	1	1	9	1	150	2
(13, 3)	78	54	35	35	36	35	0	1	1	1	1	9	1	150	2
(13, 4)	79	54	35	35	36	35	0	1	1	1	1	9	1	150	2
(13, 5)	80	54	35	35	36	35	0	1	1	1	1	9	1	150	2
(13, 6)	81	54	35	35	36	35	0	1	1	1	1	9	1	150	2
(13, 7)	82	54	35	35	36	35	0	1	1	1	1	9	1	150	2
(13, 8)	83	54	35	35	36	35	0	1	1	1	1	9	1	150	2
(13, 9)	84	54	35	35	36	35	0	1	1	1	1	9	1	150	2
(13, 10)	85	54	35	35	36	35	0	1	1	1	1	9	1	150	2

TABLE I DATA INFORMATION FOR QQ(I,J), QM(I,J) and QH(I,J), continued ...

(13, 3)	81	-22	95	27	95	-6	25	-6	5	-0	1	93	4	-93	525
(13, 4)	82	-11	35	13	70	-1	25	-1	10	-0	1	143	72	-21	2100
(13, 5)	83	-24	35	-24	35	-72	25	-72	10	-0	-0	81	8	-27	175
(13, 6)	84	-27	35	-13	35	-6	25	-6	1	-0	1	96	8	-9	700
(13, 7)	85	13	70	13	70	-6	25	-6	1	-0	1	-66	14	13	200
(13, 8)	86	54	35	-1	35	-72	25	-72	1	-0	-0	117	2	12	175
(13, 9)	87	-27	35	22	35	-6	25	-6	5	-0	-0	-66	4	-9	700
(13, 10)	88	-13	35	79	35	-6	25	-6	1	-0	1	-166	12	-13	200
(13, 11)	89	13	70	-11	70	-1	25	-1	10	-0	-0	123	12	-13	400
(13, 12)	90	156	35	156	35	-72	25	-72	1	-0	-0	166	1	-13	200
(13, 13)	91	78	35	-13	35	-6	25	-6	1	-0	-0	166	1	-13	200
(14, 1)	92	26	35	-13	35	-2	25	-2	1	-0	-0	-169	12	-13	500
(14, 2)	93	11	35	-13	70	-1	25	-1	10	-0	-0	-1	4	-13	1000
(14, 3)	94	11	105	-13	70	-1	25	-1	30	-0	-0	-11	24	-11	600
(14, 4)	95	27	35	13	35	-6	25	-6	1	-0	1	-66	8	-9	700
(14, 5)	96	-9	35	13	35	-6	25	-6	1	-0	-0	-66	8	-9	700
(14, 6)	97	-13	70	-13	70	-1	25	-1	1	-0	-0	169	8	-13	200
(14, 7)	98	-27	210	-13	70	-1	25	-1	1	-0	-0	169	14	-13	400
(14, 8)	99	-27	35	22	35	-6	25	-6	5	-0	-0	-66	4	-13	200
(14, 9)	100	18	35	-14	35	-6	25	-6	1	-0	-0	143	2	-9	700
(14, 10)	101	13	70	-11	35	-1	25	-1	10	-0	1	143	2	-9	700
(14, 11)	102	-13	105	-2	35	-1	25	-1	1	-0	-0	-16	2	-13	400
(14, 12)	103	-78	35	-2	35	-6	25	-6	1	-0	-0	-16	2	-13	400
(14, 13)	104	-22	35	24	35	-6	25	-6	1	-0	-0	-16	2	-13	400
(14, 14)	105	-22	35	24	35	-6	25	-6	1	-0	-0	-16	2	-13	400
(15, 1)	106	-22	35	24	35	-6	25	-6	1	-0	-0	-16	2	-13	400
(15, 2)	107	-11	35	13	70	-1	25	-1	10	-0	-0	143	2	-13	400
(15, 3)	108	-2	35	13	35	-6	25	-6	1	-0	-0	-16	2	-13	400
(15, 4)	109	-2	35	13	35	-6	25	-6	1	-0	-0	-16	2	-13	400
(15, 5)	110	-13	70	-13	70	-1	25	-1	1	-0	-0	169	2	-13	400
(15, 6)	111	13	35	22	35	-6	25	-6	1	-0	-0	-16	2	-13	400
(15, 7)	112	13	35	22	35	-6	25	-6	1	-0	-0	-16	2	-13	400
(15, 8)	113	13	35	22	35	-6	25	-6	1	-0	-0	-16	2	-13	400
(15, 9)	114	13	35	22	35	-6	25	-6	1	-0	-0	-16	2	-13	400
(15, 10)	115	-13	70	-13	70	-1	25	-1	1	-0	-0	169	2	-13	400
(15, 11)	116	-13	70	-13	70	-1	25	-1	1	-0	-0	169	2	-13	400
(15, 12)	117	22	70	-11	35	-6	25	-6	1	-0	-0	-16	2	-13	400
(15, 13)	118	-11	35	22	35	-6	25	-6	1	-0	-0	-16	2	-13	400
(15, 14)	119	-11	35	22	35	-6	25	-6	1	-0	-0	-16	2	-13	400
(15, 15)	120	4	35	22	35	-6	25	-6	1	-0	-0	-16	2	-13	400
(16, 1)	121	11	105	-13	70	-1	25	-1	1	-0	-0	-16	2	-13	400
(16, 2)	122	11	105	-13	70	-1	25	-1	1	-0	-0	-16	2	-13	400
(16, 3)	123	2	105	-13	70	-1	25	-1	1	-0	-0	-16	2	-13	400
(16, 4)	124	13	105	-13	70	-1	25	-1	1	-0	-0	-16	2	-13	400
(16, 5)	125	13	105	-13	70	-1	25	-1	1	-0	-0	-16	2	-13	400

TABLE I DATA INFORMATION FOR QQ(I,J), QM(I,J) and QH(I,J), continued ...

(16, 6)	126	13	210	3	70	1	150	-0	1	1	2	1	001	-13	40	13200
(16, 7)	127	-12	70	-13	210	-1	150	-0	1	1	1	1	001	-13	40	13300
(16, 8)	128	-10	70	-11	70	-1	150	-0	1	1	1	1	001	-13	40	13400
(16, 9)	129	-10	70	11	35	1	150	-0	1	10	1	1	001	-13	40	13500
(16, 10)	130	-10	70	-12	35	-2	150	-0	1	1	1	1	001	-13	40	13600
(16, 11)	131	-10	70	-11	105	-2	150	-0	1	3	1	1	001	-13	40	13700
(16, 12)	132	-11	35	-12	105	-2	150	-0	1	1	1	1	001	-13	40	13800
(16, 13)	133	-11	35	-11	105	-1	150	-2	1	1	1	1	001	-13	40	13900
(16, 14)	134	-2	105	-2	105	-1	150	-2	1	1	1	1	001	-13	40	14000
(16, 15)	135	-1	105	-2	105	-1	150	-2	1	1	1	1	001	-13	40	14100
(16, 16)	136	-1	105	-2	105	-1	150	-2	1	1	1	1	001	-13	40	14200
(16, 17)	137	-1	105	-2	105	-1	150	-2	1	1	1	1	001	-13	40	14300
(16, 18)	138	-1	105	-2	105	-1	150	-2	1	1	1	1	001	-13	40	14400
(16, 19)	139	-1	105	-2	105	-1	150	-2	1	1	1	1	001	-13	40	14500
(16, 20)	140	-1	105	-2	105	-1	150	-2	1	1	1	1	001	-13	40	14600

BEST AVAILABLE COPY



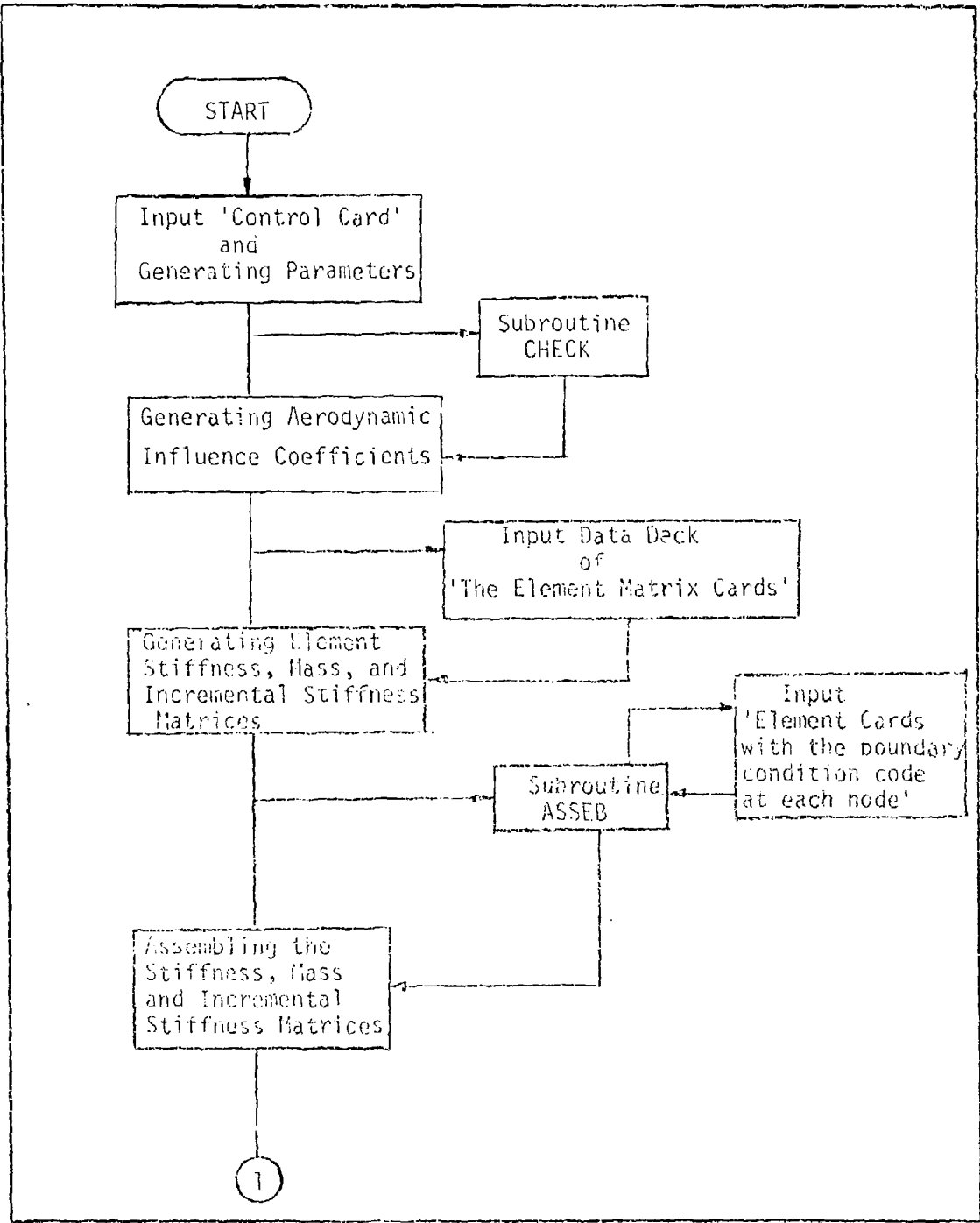
3. Element Cards with the boundary condition code at each node (2213).

Columns	1-3	The sequence number for the element	
	4-6	The starting matrix row position for the degrees of freedom at nodal point I	(ID(1))
	7-9	The starting matrix row position for the degrees of freedom at nodal point J	(ID(2))
	10-12	The starting matrix row position for the degrees of freedom at nodal point K	(ID(3))
	13-15	The starting matrix row position for the degrees of freedom at nodal point L	(ID(4))
	16-18	Boundary condition code for deflection Z at nodal point I	(w(1))
	19-21	Boundary condition code for $Z_{,x}$ at nodal point I	(w(2))
	22-24	Boundary condition code for $Z_{,y}$ at nodal point I	(w(3))
	25-27	Boundary condition code for $Z_{,xy}$ at nodal point I	(w(4))
	28-30	Boundary condition code for Z at nodal point J	(w(5))
	31-33	Boundary condition code for $Z_{,x}$ at nodal point J	(w(6))
	34-36	Boundary condition code for $Z_{,y}$ at nodal point J	(w(7))
	37-39	Boundary condition code for $Z_{,xy}$ at nodal point J	(w(8))
	40-42	Boundary condition code for Z at nodal point K	(w(9))
	43-45	Boundary condition code for $Z_{,x}$ at nodal point K	(w(10))
	46-48	Boundary condition code for $Z_{,y}$ at nodal point K	(w(11))
	49-51	Boundary condition code for $Z_{,xy}$ at nodal point K	(w(12))

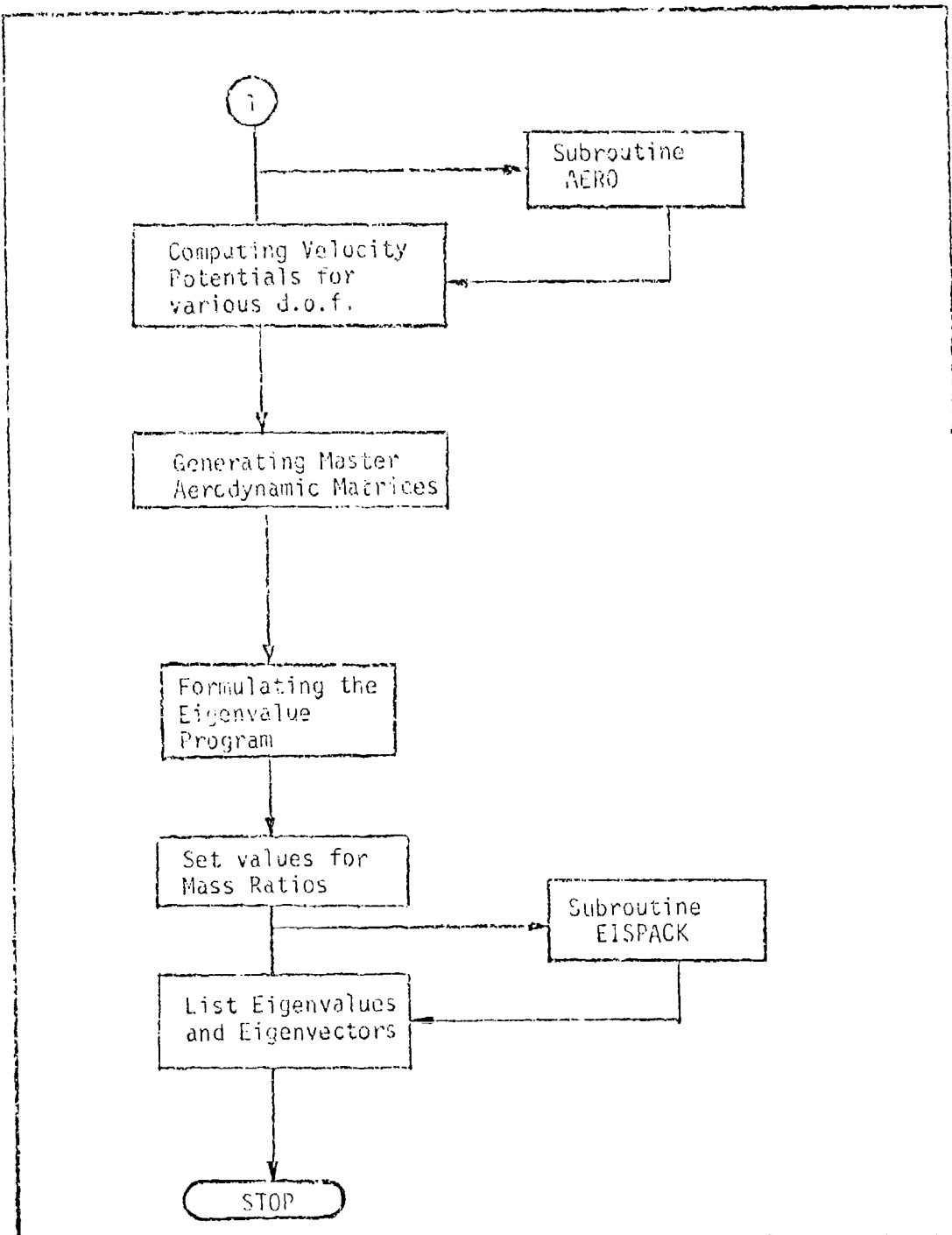
52-54	Boundary condition code for Z at nodal point L	(w(13))
55-57	Boundary condition code for Z <sub>,x</sub> at nodal point L	(w(14))
58-60	Boundary condition code for Z <sub>,y</sub> at nodal point L	(w(15))
61-63	Boundary condition code for Z <sub>,xy</sub> at nodal point L	(w(16))

The 'ID' array at I, J, K and L is assigned for each element for a specific mesh of the elements of the panel. The permutation for I, J, K and L is clockwise and I is corresponding to the origin of each local element as shown in Fig. 2. If ID(I) = 0, all the degrees of freedom at node I are zero. Same situation is applied for other nodes for the element.

The 'w' array defines the boundary condition codes for the degrees of freedom at each node. If w(I) = 0, the associated degree of freedom is zero and if w(I) ≠ 0, the associated degree of freedom is taken into account.



Program Flow Chart



Program Flow Chart continued .....



BEST AVAILABLE COPY

```

F=0.1
PRINT 139, F
C
C
C
FLOW PARAMETERS
PRINT 139, MACH
BETA=SQRT(MACH**2-1.)
DMEGA=(MACH**2)*KL*EL)/(BETA**2)
BM=ETA*OMEGA*(2.*MACH)
UD=BM*MACH
C=1./(2.*3.14159)
CB=BD
C
C
C
GENERATING AERODYNAMIC INFLUENCE COEFFICIENTS
RMAX=IX*IBX
SMAX=2*NY*IBY
DO 101 I=1,RMAX
DO 101 J=1,SMAX
GR(I,J)=0.
101 GR(I,I)=0.
DO 102 IS=1,RMAX
R=IS-1
DS=SIGMA/BETA*(EPISN/2.+EPISN*FLOAT(R))
JF=IFIX((DS-(EPISN/2.))/EPISN)+2
IF (JF.GT.SMAX) JF=SMAX
IF (DS.LT.(EPISN/2.)) JF=1
JG(IS)=JF
DO 102 J=1,JF
S=J-1
CALL CHECK (R,S,BETA,SIGMA,GR)
PI=R+1
SI=S+1
GR(R1,S1)=GR(I)
GR(PI,S1)=GR(J)
102 CONTINUE
C
C
C
GENERATING ELEMENT STIFFNESS MATRIX, ELEMENT INCREMENTAL
STIFFNESS MATRIX, AND ELEMENT MASS MATRIX
DO 103 I=1,16
DO 103 J=1,I
READ 140, (JS(L),L=1,8), IZ, IY, (JM(L),L=1,2), (JB(L),L=1,2)
OCC(I,J)=(CB**IY)*(FLOAT(JS(1))/FLOAT(JS(2))+CB**4)*FLOAT(JS(3)
1 /FLOAT(JS(4))+CB**2)*FLOAT(JS(5))/FLOAT(JS(6))+CB**2)*POICH*
2 FLOAT(JS(7))/FLOAT(JS(8))
OM(I,J)=(CB**IY)*(FLOAT(JM(1))/FLOAT(JM(2)))
ON(I,J)=(CB**IY)*(FLOAT(JB(1))/FLOAT(JB(2)))*CB)
103 CONTINUE
DO 104 I=1,16
DO 104 J=1,I
OC(I,J)=OC(J,I)
ON(I,J)=ON(J,I)
104 ON(I,J)=ON(J,I)
C
C
C
ASSEMBLE ELEMENT STIFFNESS MATRIX, ELEMENT INCREMENTAL STIFFNESS
MATRIX, AND ELEMENT MASS MATRIX
A 590
A 600
A 610
A 620
A 630
A 640
A 650
A 660
A 670
A 680
A 690
A 700
A 710
A 720
A 730
A 740
A 750
A 760
A 770
A 780
A 790
A 800
A 810
A 820
A 830
A 840
A 850
A 860
A 870
A 880
A 890
A 900
A 910
A 920
A 930
A 940
A 950
A 960
A 970
A 980
A 990
A 1000
A 1010
A 1020
A 1030
A 1040
A 1050
A 1060
A 1070
A 1080
A 1090
A 1100
A 1110
A 1120
A 1130
A 1140
A 1150

```

```

CALL ASSEB (NX,NY,ND)
A 1160
C C C GENERATING VELOCITY POTENTIAL FUNCTIONS
A 1170
A 1180
A 1190
KL=KL/FLOAT(NX)
A 1200
CALL AERO (NX,NY,ICD,IBT,ML,V,VS,EPISM,SIGMA,BETA,AD,BA,JG,NDX,NDY
A 1210
1)
A 1220
C C C GENERATING MASTER AERODYNAMIC MATRIX
A 1230
DO 123 IY=1,NDY
A 1240
DO 122 IY=1,NDY
A 1250
ND1=4
A 1260
IF (IY.EQ.NDY) ND1=2
A 1270
DO 121 ND1=1,ND1
A 1280
II=(IY-1)*4*NDX+(IY-1)*4+ND1
A 1290
IF (IY.EQ.NDY) II=(IY-1)*4*NDX+(IY-1)*2+ND1
A 1300
DO 120 JJ=1,NDX
A 1310
DO 120 JJ=1,NDY
A 1320
ND2=4
A 1330
IF (JJ.EQ.NDX) ND2=2
A 1340
DO 120 ND2=1,ND2
A 1350
JJ=(JJ-1)*4*NDX+(JJ-1)*4+ND2
A 1360
IF (JJ.EQ.NDX) JJ=(JJ-1)*4*NDX+(JJ-1)*2+ND2
A 1370
O=0.
A 1380
OO=0.
A 1390
DO 118 NL1=1,NX
A 1400
NL1=NL1-1
A 1410
IF (NL1.LT.0) GO TO 118
A 1420
IF (NL1.GT.1) GO TO 119
A 1430
DO 117 N2=1,NY
A 1440
N2=N2-1
A 1450
IF (N2.LT.0) GO TO 117
A 1460
IF (N2.GT.1) GO TO 119
A 1470
IF (N1.EQ.0) GO TO 105
A 1480
IF (N2.EQ.0) GO TO 106
A 1490
IKL=IX3*(ND1)
A 1500
GO TO 108
A 1510
IF (N2.EQ.0) GO TO 107
A 1520
IKL=IX2*(ND1)
A 1530
GO TO 108
A 1540
IKL=IX4*(ND1)
A 1550
GO TO 108
A 1560
IKL=IX1*(ND1)
A 1570
DO 116 M=1,IBX
A 1580
DO 115 N3=1,IBY
A 1590
ML=(NL2-1)*IBY+NS
A 1600
MM=(NL-1)*IBX+M
A 1610
NN=FLOAT(N-1)*IBX+BBY/2.
A 1620
YY=FLOAT(N2-1)*IBY+BBY/2.
A 1630
CALL SHAPE (FA,IFA,FL,FM,YN,EA)
A 1640
IF (JUN-NL1) 109,109,110
A 1650
JJ=(JJ-1)*4*(NDX+1)+(JJ-1)*4+ND2+(NX-NL1)
A 1660
)*4
A 1670
IF (JJ.EQ.NDY) JJ=(JJ-1)*4*(NDX+1)+(JJ-1)
A 1680
)*2+(NX-NL1)*2+ND2
A 1690
GO TO 111
A 1700
YK=0.
A 1710
A 1720
A 1730

```

BEST AVAILABLE COPY

```

VKS=0.
GO TO 114
111 IF (JUY.EQ.NDY) GO TO 113
    JJ7=JJ+2*(NDX+1)+7*(2*NDY-2)-JUY)*4*(NDX+1)
    IF (ND2.EQ.3.DM.ND2.EQ.4) GO TO 112
    VK=V(JJ,MM)+V(JJ7,MM)
    VKS=VS(JJ,MM)+VS(JJ7,MM)
    GO TO 114
112 VK=V(JJ,MM)-V(JJ7,MM)
    VKS=VS(JJ,MM)-VS(JJ7,MM)
    GO TO 114
113 VJ=V(JJ,MM)
    VKS=VS(JJ,MM)
114 O=O+(-FA*VK+DFA/KL*VKS)*(SIGMA*(EPIEN**2))
    Z=Z+O
    O=O+(-FA*VKS+DFA/KL*VK)*CSIGMA*(EPIEN**2)
    Z=Z+O
115 CONTINUE
116 CONTINUE
117 CONTINUE
118 CONTINUE
119 AK(I,J)=O
    AK(I,J)=OS
120 CONTINUE
121 CONTINUE
122 CONTINUE
123 CONTINUE
C
C FINDING EIGENVALUES AND EIGENVECTORS FOR VARIOUS RATIOS OF AIR
C MASS TO PANEL MASS
    YN=NY*2
    NN=NX
    DO 124 I=1,NN
    DO 124 J=1,NN
124 SK(I,J)=0.01*(CXN**5)/CK1*SK(I,J)+F*(CXN**2)*(YND*CNK(I,J))
    CALL GINW2 (K,ND,ND,ND,KZ)
    IF (KZ.EQ.0) GO TO 131
    PRINT 141, SG
    KL=PL*NN
    C10=NN*ND/1225.
    FACTOR=1./C10
    FACTOR=0.01*FACTOR
    DO 125 I=1,NN
    DO 125 J=1,NN
        SHK(I,J)=C10*CNK(I,J)
125 CONTINUE
    DO 126 ITER=1,9
        INO=1
        NO=NO+1
        PRINT 144, NO
        RATIO=NO/ND
        FACTOR=FACTOR/RATIO
        DO 126 I=1,NN
        DO 126 J=1,NN
            SHK(I,J)=1./RATIO*SHK(I,J)
126 CONTINUE
    DO 128 I=1,NN

```

A 1740  
A 1750  
A 1760  
A 1770  
A 1780  
A 1790  
A 1800  
A 1810  
A 1820  
A 1830  
A 1840  
A 1850  
A 1860  
A 1870  
A 1880  
A 1890  
A 1900  
A 1910  
A 1920  
A 1930  
A 1940  
A 1950  
A 1960  
A 1970  
A 1980  
A 1990  
A 2000  
A 2010  
A 2020  
A 2030  
A 2040  
A 2050  
A 2060  
A 2070  
A 2080  
A 2090  
A 2100  
A 2110  
A 2120  
A 2130  
A 2140  
A 2150  
A 2160  
A 2170  
A 2180  
A 2190  
A 2200  
A 2210  
A 2220  
A 2230  
A 2240  
A 2250  
A 2260  
A 2270  
A 2280  
A 2290  
A 2300  
A 2310



```

DO 128 J=1,NXD          A 2320
  AC=0.                 A 2330
  BC=0.                 A 2340
  DO 127 I=1,NXD       A 2350
    A11=EK(I,KI)*EMCKI,J)-AK(KI,J)) A 2360
    B11=EK(I,KI)*-AK(KI,J)) A 2370
    AC=AC+AC1+(CG*B11) A 2380
    BC=BC+(B11-(CG*AS1)) A 2390
127 CONTINUE           A 2400
  CS(I,J)=EMPLX(AC,BS) A 2410
128 CONTINUE           A 2420
  CALL CUBIG (NRD,NEID,CS,IND,NS) A 2430
  DO 129 I=1,5         A 2440
    CF=CONFLX FACTOR*0.) A 2450
    NS(I)=NS(I)*CF A 2460
    NS=EMPLX(NS(I)) A 2470
    ED=EMPLX(NS(I)) A 2480
    G=RO/ND A 2490
    RT=CONPT(NS(I)) A 2500
    SP=REAL(RT) A 2510
    TK=SR*KL A 2520
    PRINT 142, NS(I)*G,SR,TK A 2530
129 PRINT 143, (CS(J,I),J=1,NXD) A 2540
  MU=NU A 2550
130 CONTINUE           A 2560
  GO TO 132            A 2570
131 PRINT 145          A 2580
132 STOP               A 2590
C                       A 2600
133 FORMAT (34H1 PANEL FLUTTER FOR CLAMPED PANEL,////) A 2610
134 FORMAT (2F5.2,7I3,4F7.4) A 2620
135 FORMAT (2X, 20HLENGTH-WIDTH RATIO =,1F6.3/2X, 26HCHORDWISE ELEMENT A 2630
1 LENGTH =,1F6.3/3X, 24HCHORDWISE ELEMENT WIDTH =,1F6.3/) A 2640
136 FORMAT (2X, 11HBOX WIDTH =,1F6.3/3X, 34HRATIO OF BOX LENGTH TO BOX A 2650
1 WIDTH =,1F6.3/) A 2660
137 FORMAT (2X, 19HPRODUCED FREQUENCY =,1F6.3/) A 2670
138 FORMAT (2X, 23HINITIAL IN-PLANE FORCE PARAMETER=,1F6.3/) A 2680
139 FORMAT (2X, 13HANCH NUMBER =,1F5.2/) A 2690
140 FORMAT (8I4,2I3,2I4,2I6) A 2700
141 FORMAT (2X, 32HSTRUCTURAL DAMPING COEFFICIENT =,1F6.3////) A 2710
142 FORMAT ( 15H0 EIGENVALUE= ,1E12.5/1X,1E12.5/3X, 5H G = ,1F6.5/2X A 2720
1, 17HFREQUENCY RATIO =,1F6.5/2X, 22HSTIFFNESS PARAMETER = ,1F6.5) A 2730
143 FORMAT ( 14H EIGENVECTOR=,2X,10E12.5/2X,10E12.5/2X,10E12.5/2X,10 A 2740
1E12.5/2X,10E12.5/2X,10E12.5/2X,10E12.5/2X,10E12.5/2X,10E12.5) A 2750
144 FORMAT ( 20H0 DENSITY RATIO MU=,1F6.5) A 2760
145 FORMAT ( 17H SINGULAR MATRIX) A 2770
C                       A 2780
END                     A 2790

SUBROUTINE CSEB (NX,NY,NEID) B 10
  REAL (17,18),CM(18,18),DC(16,16),OM(15,16),ON(16,16),CN(18,18) B 20
  INTEGER (16),ID(4) B 30
  COMMON /BLOCK2/ OO,OM,ON B 40
  COMMON /BLOCK3/ OK,ON,OH B 50

```

DO 101 I=1,NXD	B	60
DO 101 J=1,NXD	B	70
SK(I,J)=0.	B	80
SM(I,J)=0.	B	90
SN(I,J)=0.	B	100
101 CONTINUE	B	110
NTX=GX*NY	B	120
DO 106 NEM=1,NTX	B	130
READ 107, III<(ID(I),I=1,4)>,(W(I),I=1,16)	B	140
DO 105 L=1,4	B	150
IF <(ID(L),EO,0) GO TO 105	B	160
II=ID(L)	B	170
DO 104 M=1,4	B	180
IE=4*(L-1)+M	B	190
IF <(W(IE),EO,0) GO TO 104	B	200
DO 103 LS=1,4	B	210
IF <(ID(LS),EO,0) GO TO 103	B	220
JJ=ID(LS)	B	230
DO 102 MD=1,4	B	240
IES=4*(LS-1)+MD	B	250
IF <(W(IES),EO,0) GO TO 102	B	260
SK(II,JJ)=SK(II,JJ)+QK(IE,IES)	B	270
SM(II,JJ)=SM(II,JJ)+QM(IE,IES)	B	280
SN(II,JJ)=SN(II,JJ)+QN(IE,IES)	B	290
JJ=JJ+1	B	300
CONTINUE	B	310
CONTINUE	B	320
II=II+1	B	330
CONTINUE	B	340
CONTINUE	B	350
CONTINUE	B	360
RETURN	B	370
C	B	380
107 FORMAT (22I3)	B	390
C	B	400
END	B	410
SUBROUTINE HEPO (NX,NY,NXD,IBT,KA,V,VS,EPISN,SIGMA,BETA,AD,BA,JG,M	C	10
IDX,NDY)	C	20
REAL V(40,16),VS(40,16),GRR(16,8),GRI(16,8),KA	C	30
INTEGER JG(16)	C	40
COMMON /BLDCK1/ IBX,IBY,GRR,GRI,IBY,IBY	C	50
IX1(NC)=0+IC	C	60
IX2(NC)=12+IC	C	70
IX3(NC)=IC	C	80
IX4(NC)=4+IC	C	90
NY1=NY/2	C	100
NDX1=NDX+1	C	110
NDY1=2*NDY-1	C	120
NC=IC	C	130
DO 116 NCP=1,NY	C	140
DO 115 M=1,IBX	C	150
DO 115 M=1,IBY	C	160
HM=(NE-1)*IBX+M	C	170

	NT=(NES-1)*IBY+M	C 180
	NT=(NT-1)*IBX+M	C 190
	DO 114 JJ=1,NDM1	C 200
	DO 113 II=1,NDY1	C 210
	M4=4	C 220
	IF (II.EQ,NDY) M4=2	C 230
	DO 112 ND=1,M4	C 240
	JI=(II-1)*4*NDM1+(JJ-1)*4+ND	C 250
	IF (II.EQ,NDY) JI=(II-1)*4*NDM1+(JJ-1)*2+ND	C 260
	IF (II.GT,NDY) JI=(II-2)*4*NDM1+2*NDM1+(JJ-1)*4+ND	C 270
	G=0.	C 280
	GS=0.	C 290
	DO 110 MK=1,NE	C 300
	M1=MK-JJ	C 310
	IF (M1.GT,1) GO TO 111	C 320
	IF (M1.LT,0) GO TO 110	C 330
	DO 109 N2=1,NY1	C 340
	N2=N2-II	C 350
	IF (N2.GT,1) GO TO 110	C 360
	IF (N2.LT,0) GO TO 109	C 370
	IF (M1.EQ,0) GO TO 101	C 380
	IF (N2.EQ,0) GO TO 102	C 390
	IKL=IX3(ND)	C 400
	GO TO 104	C 410
101	IF (N2.EQ,0) GO TO 103	C 420
	IKL=IX2(ND)	C 430
	GO TO 104	C 440
102	IKL=IX4(ND)	C 450
	GO TO 104	C 460
103	IKL=IX1(ND)	C 470
104	IEF=IEK	C 480
	IF (MK.EQ,NE) IEF=M	C 490
	DO 108 MN=1,IEF	C 500
	MH=(MK-1)*IBX+MK	C 510
	N2=MN-MN+1	C 520
	J2=JG(ND)	C 530
	DO 107 NL=1,187	C 540
	MEL=(MH-1)*IBY+MC	C 550
	IF (M1.GT,MEL) GO TO 105	C 560
	ISL=MEL-MT+1	C 570
	IF (ISL.GT,J2) GO TO 108	C 580
	GO TO 106	C 590
105	ISL=MT-MEL+1	C 600
	IF (ISL.GT,J2) GO TO 107	C 610
106	XX=FLOAT(MK-1)*PBX+PBX/2.	C 620
	YY=FLOAT(MC-1)*PEY+PEY/2.	C 630
	CALL SHAPE (FAL,DFAL,IFL,XX,YY,BA)	C 640
	G=G+(FAL*GPF(ND,ISL)+DFAL/KA*GRI(ND,ISL	C 650
	))*EPIEN)/ND	C 660
	GS=GS+(FAL*GRI(ND,ISL)+DFAL/KA*GRI(ND,ISL	C 670
	))*EPIEN)/ND	C 680
	CONTINUE	C 690
107	CONTINUE	C 700
108	CONTINUE	C 710
109	CONTINUE	C 720
110	CONTINUE	C 730
111	V(JI,MT)=G	C 740
112	V(JI,MT)=GS	C 750
	CONTINUE	

# BEST AVAILABLE COPY

113	CONTINUE	C 760
114	CONTINUE	C 770
115	CONTINUE	C 780
116	CONTINUE	C 790
	RETURN	C 800
C		C 810
C		C 820
	END	C 830
	SUBROUTINE CHECK (R,S,BETA,SIGMA,GR)	D 10
	DIMENSION GR(2), DN(4), DY(4)	D 20
	INTEGER P,S	D 30
	COMMON /BLUCK/ BM,UB,C,CD	D 40
	A1=2.*FLOAT(S)-1.	D 50
	A2=2.*FLOAT(S)+1.	D 60
	A3=FLOAT(S)*1.*SIGMA/BETA	D 70
	A4=FLOAT(S)+1.*SIGMA/BETA	D 80
	DO 101 I=1,2	D 90
	DK(I)=SIGMA*(FLOAT(R)+0.5)	D 100
	I2=I+2	D 110
101	DK(I2)=SIGMA*(FLOAT(R)-0.5)	D 120
	DO 102 I=1,4,3	D 130
102	DY(I)=FLOAT(S)+0.5	D 140
	DO 103 I=2,3	D 150
103	DY(I)=FLOAT(S)-0.5	D 160
	IF (S.FD.0) GO TO 113	D 170
	IF (DY(1).GT.(DK(1)/BETA)) GO TO 105	D 180
	IF (DY(4).GT.(DK(4)/BETA)) GO TO 109	D 190
	DO 104 JK=1,2	D 200
	I=JK	D 210
	CALL GIR (IK,A1,A2,A3,A4,YG3)	D 220
	GR(IK)=YG3	D 230
104	CONTINUE	D 240
	RETURN	D 250
105	IF (DY(3).GT.(DK(3)/BETA)) GO TO 107	D 260
	DO 106 IK=1,2	D 270
	CALL GIP (IK,A1,A3,A4,YG2)	D 280
	GR(IK)=YG2	D 290
106	CONTINUE	D 300
	RETURN	D 310
107	DO 108 IK=1,2	D 320
	CALL GIP (IK,A1,A1,A4,YG2)	D 330
	GR(IK)=YG2	D 340
108	CONTINUE	D 350
	RETURN	D 360
109	IF (DY(3).GT.(DK(3)/BETA)) GO TO 111	D 370
	DO 110 IK=1,2	D 380
	CALL GIP (IK,A1,A2,A2,A4,YG3)	D 390
	CALL GIP (IK,A1,A3,A2,YG2)	D 400
	GR(IK)=YG3+YG2	D 410
110	CONTINUE	D 420
	RETURN	D 430
111	DO 112 IK=1,2	D 440
	CALL GIR (IK,A1,A2,A2,A4,YG3)	D 450

DEST/...

	CALL GIPS (IK,A1,A1,A2,YG2)	D 460
	GF(IK)=YG3*YG2	D 470
112	CONTINUE	D 480
	RETURN	D 490
113	IF (P.FD.0) GO TO 120	D 500
	IF (DY(1).GT.(DN(1)/BETA)) GO TO 114	D 510
	GO TO 116	D 520
114	DO 115 II=1,2	D 530
	CALL OGSA (IK,A2,A4,YG)	D 540
	GF(IK)=YG	D 550
115	CONTINUE	D 560
	RETURN	D 570
116	IF (DY(4).GT.(DN(4)/BETA)) GO TO 118	D 580
	DO 117 II=1,2	D 590
	CALL GIR (IK,0.,1.,A3,A4,YG3)	D 600
	GF(IK)=2.*YG3	D 610
117	CONTINUE	D 620
	RETURN	D 630
118	DO 119 II=1,2	D 640
	CALL OGSA (IK,A3,1.,YG)	D 650
	CALL GIR (IK,0.,1.,1.,A4,YG3)	D 660
	GF(IK)=2.*YG3*YG	D 670
119	CONTINUE	D 680
	RETURN	D 690
120	IF (DY(1).LE.(DN(1)/BETA)) GO TO 122	D 700
	DO 121 II=1,2	D 710
	CALL OGSA (IK,0.,A4,YG)	D 720
	GF(IK)=YG	D 730
121	CONTINUE	D 740
	RETURN	D 750
122	DO 123 II=1,2	D 760
	CALL OGSA (IK,0.,1.,YG)	D 770
	CALL GIR (IK,0.,1.,1.,A4,YG3)	D 780
	GF(IK)=2.*YG3*YG	D 790
123	CONTINUE	D 800
	RETURN	D 810
C		D 820
C		D 830
	END	D 840
	SUBROUTINE GIPS (IF,Y5,MU,MU,YG2)	E 10
	COMMON /EUDKNO/ IM,UB,C,CB	E 20
	A=0.5*(MU+1)	E 30
	S=MU-1	E 40
	Y1=0.259294655*B	E 50
	Y2=0.051000983*B	E 60
	DELTA0=A	E 70
	DELTA1=Y1	E 80
	DELTA2=A-Y1	E 90
	DELTA3=Y2	E 100
	DELTA4=Y2	E 110
	Y3=C*(B-2.)*(0.568208880*FY(IF,DELTA0+YS,DELTA0)+0.47262967*(FY(I	E 120
	1)+DELTA1+YS,DELTA1)+(FY(IF,DELTA0+YS,DELTA3))+0.236026885*(FY(IK,DE	E 130
	LTAE+YS,DELTA2)+FY(IK,DELTA4+YS,DELTA4))	E 140
	RETURN	E 150
C		E 160
	END	E 190

BEST AVAILABLE COPY

```

FUNCTION FYC(IK, DELTA, YL, YU)
COMMON /BLOCK0/ BM, UB, C, CB
FK(EM, DELTA, Z) = (COS(BM * SORT(DELTA**2 - Z**2)) - 1.) / SORT(DELTA**2 - Z**2)
1)
A = 0.5 * (YU + YL)
B = YU - YL
Y1 = 0.269234605 * B
Y2 = 0.453089923 * B
DELTA0 = A
DELTA1 = A + Y1
DELTA2 = A - Y1
DELTA3 = A + Y2
DELTA4 = A - Y2
IF (IK.EQ.1) GO TO 101
FY = -SIN(CUB * DELTA) * (ACOS(YL / DELTA) + (B/2.) * (0.568888889 * FK(EM, DELTA,
1 DELTA0) + 0.47562867 * (FK(EM, DELTA, DELTA1) + FK(EM, DELTA, DELTA3)) + 0.236
226885 * (FK(EM, DELTA, DELTA2) + FK(EM, DELTA, DELTA4))))
RETURN
101 FY = CUB * (CUB * DELTA) * (ACOS(YL / DELTA) + (B/2.) * (0.568888889 * FK(EM, DELTA, D
1 ELTA0) + 0.47562867 * (FK(EM, DELTA, DELTA1) + FK(EM, DELTA, DELTA3)) + 0.236
226885 * (FK(EM, DELTA, DELTA2) + FK(EM, DELTA, DELTA4))))
RETURN
C
END

SUBROUTINE GIP (IK, YL, YU, XL, XU, YG3)
COMMON /BLOCK0/ BM, UB, C, CB
A = 0.5 * (XU + XL)
B = XU - XL
Y1 = 0.3072980346 * B
DELTA0 = A
DELTA1 = A + Y1
DELTA2 = A - Y1
YG3 = C * (B/2.) * (0.988898889 * FX(IK, DELTA0, YL, YU) + 0.555555556 * (FX(IK, D
1 ELTA1, YL, YU) + FX(IK, DELTA2, YL, YU)))
RETURN
C
END

FUNCTION FXC(IK, DELTA, YL, YU)
COMMON /BLOCK0/ BM, UB, C, CB
FS(EM, DELTA, Z) = (COS(BM * SORT(DELTA**2 - Z**2)) - 1.) / SORT(DELTA**2 - Z**2)
1)
A = 0.5 * (YU + YL)
B = YU - YL
Y1 = 0.3072980346 * B
IF (IK.EQ.1) GO TO 101
FX = -SIN(UB * DELTA) * (ACOS(YL / DELTA) - ACOS(YU / DELTA) + (B/2.) * (0.8888888
199 * FS(EM, DELTA, A) + 0.555555556 * (FS(EM, DELTA, A + Y1) + FS(EM, DELTA, A - Y1)
2))
RETURN
101 FX = COS(CUB * DELTA) * (ACOS(YL / DELTA) - ACOS(YU / DELTA) + (B/2.) * (0.8888888
199 * FS(EM, DELTA, A) + 0.555555556 * (FS(EM, DELTA, A + Y1) + FS(EM, DELTA, A - Y1)
2))
RETURN
C
END

```

BEJ

```
SUBROUTINE 063A (IK,XL,MU,YG)
COMMON /BLOCK/ BM,UB,C,CB
H=0.5*(MU+XL)
B=U-XL
Y1=0.269234655*B
Y2=0.465089323*B
Y=BM*(H+Y1)
YY=BM*(H+Y1)
Z=BM*(H+Y2)
ZZ=BM*(H+Y2)
N=BM*H
CALL BESJ (Y,0,BJ1,0.0001,IER)
CALL BESJ (YY,0,BJ2,0.0001,IER)
CALL BESJ (Z,0,BJ3,0.0001,IER)
CALL BESJ (ZZ,0,BJ4,0.0001,IER)
Y=UB*(H+Y1)
YY=UB*(H+Y1)
Z=UB*(H+Y2)
ZZ=UB*(H+Y2)
N=UB*H
IF (IK.EQ.1) GO TO 101
YG=-0.5*(B/2.)*(0.56988999*SIN(X)*BJ0+0.47862867*(SIN(Y)*BJ1+SIN(
IYY)*BJ2)+0.236926885*(SIN(Z)*BJ3+SIN(ZZ)*BJ4))
RETURN
101 YG=0.5*(B/2.)*(0.56988999*COS(X)*BJ0+0.47862867*(COS(Y)*BJ1+COS(Y
IY)*BJ2)+0.236926885*(COS(Z)*BJ3+COS(ZZ)*BJ4))
RETURN
END
```

I	10
I	20
I	30
I	40
I	50
I	60
I	70
I	80
I	90
I	100
I	110
I	120
I	130
I	140
I	150
I	160
I	170
I	180
I	190
I	200
I	210
I	220
I	230
I	240
I	250
I	260
I	270
I	280
I	290
I	300

C

# BEST COPY AVAILABLE

	SUBROUTINE BECU (X,II,BJ,D,IER)	J	10
	BJ=.0	J	20
	IF (D) 101,102,102	J	30
	101 IER=1	J	40
	RETURN	J	50
	102 IF (D) 103,103,104	J	60
	103 IER=2	J	70
	RETURN	J	80
	104 IF (X-15.) 105,105,106	J	90
	105 NTEST=90.+10.*X-X**2/3.	J	100
	GO TO 107	J	110
	106 NTEST=90.+X/2.	J	120
	107 IF (N-NTEST) 109,108,108	J	130
	108 IER=4	J	140
	RETURN	J	150
	109 IEP=0	J	160
	II=II+1	J	170
	BPREV=.0	J	180
C		J	190
C	COMPUTE STARTING VALUE OF M	J	200
C		J	210
	IF (X-5.) 110,111,111	J	220
	110 MA=X/C.	J	230
	GO TO 112	J	240
	111 MA=1.177+60./X	J	250
	112 MB=II+IF(IAC)/4+2	J	260
	MZEPD=MZEPD+(MA*MB)	J	270
C		J	280
C	SET UPPER LIMIT OF M	J	290
C		J	300
	MMAI=NTEST	J	310
	DO 121 M=MZEPD+MMAI*3	J	320
C		J	330
C	SET F(N)=F(N-1)	J	340
C		J	350
	FMI=1.0E-28	J	360
	FM=.0	J	370
	ALPHA=.0	J	380
	IF (M-(M/2)**2) 114,113,114	J	390
113	JT=-1	J	400
	GO TO 115	J	410
114	JT=1	J	420
115	M2=M-2	J	430
	DO 118 N=1,M2	J	440
	MK=M-K	J	450
	BPK=2.*FLOAT(MK)*FMI/X-FM	J	460
	FM=FM1	J	470
	FMI=BPK	J	480
	IF (MK-N-1) 117,116,117	J	490
116	EJ=FMK	J	500
117	JT=JT	J	510
	C=1+JT	J	520
118	ALPHA=ALPHA+BPK**2	J	530
	BPK=C.*FMI/X-FM	J	540
	IF (N) 120,119,120	J	550
119	BJ=FMK	J	560
120	ALPHA=ALPHA+BPK	J	570
	BJ=BJ/ALPHA	J	580
	IF (ABS(BJ-BPREV)-ABS(D*BJ)) 122,122,121	J	590
121	BPREV=BJ	J	600
	IER=3	J	610
	122 RETURN	J	620
C	END	J	630
		J	640



# BEST AVAILABLE COPY

```

SUBROUTINE SHAPE (FA,DTA,IK,X,Y,BA)
F1(Z)=1.+2.*(Z**3)-3.*(Z**2)
F2(Z)=2*(Z-1.)**2
F3(Z)=(Z**3)-(Z**2)
DF1(Z)=6.*(Z**2)-6.*Z
DF2(Z)=3.*(Z**2)-4.*Z+1.
DF4(Z)=3.*(Z**2)-2.*Z
IF (IK.EQ.0) GO TO 106
IF (IK.EQ.1.OR.IK.EQ.3.OR.IK.EQ.5.OR.IK.EQ.7) GO TO 101
IF (IK.EQ.2.OR.IK.EQ.4.OR.IK.EQ.6.OR.IK.EQ.8) GO TO 102
IF (IK.EQ.9.OR.IK.EQ.11.OR.IK.EQ.13.OR.IK.EQ.15) GO TO 103
IF (IK.EQ.10.OR.IK.EQ.12.OR.IK.EQ.14.OR.IK.EQ.16) GO TO 104
101 AA=F1(X)
    CC=DF1(X)
    GO TO 105
102 AA=F2(X)
    CC=DF2(X)
    GO TO 105
103 AA=1.-F1(X)
    CC=-DF1(X)
    GO TO 105
104 AA=F4(X)
    CC=DF4(X)
105 IF (IK.EQ.1.OR.IK.EQ.2.OR.IK.EQ.13.OR.IK.EQ.14) BB=F1(Y)
    IF (IK.EQ.3.OR.IK.EQ.4.OR.IK.EQ.15.OR.IK.EQ.16) BB=F2(Y)*BA
    IF (IK.EQ.5.OR.IK.EQ.6.OR.IK.EQ.9.OR.IK.EQ.10) BB=1.-F1(Y)
    IF (IK.EQ.7.OR.IK.EQ.8.OR.IK.EQ.11.OR.IK.EQ.12) BB=F4(Y)*BA
    FA=AA*BB
    DFA=CC*BB
    RETURN
106 FA=0.
    DFA=0.
    RETURN
C
END

```

K 10  
K 20  
K 30  
K 40  
K 56  
K 66  
K 70  
K 80  
K 90  
Y 100  
K 110  
K 120  
K 130  
K 140  
K 150  
K 160  
K 170  
K 180  
K 190  
K 200  
K 210  
Y 220  
K 230  
K 240  
K 250  
K 260  
K 270  
K 280  
K 290  
K 300  
K 310  
K 320  
K 330  
K 340  
K 350

PANEL FLUTTER FOR CLAMPED PANEL

LENGTH-WIDTH RATIO = 1.000 SPANWISE ELEMENT WIDTH = 1.000  
CHORDWISE ELEMENT LENGTH = 1.000  
BOX WIDTH = .500 RATIO OF BOX LENGTH TO BOX WIDTH = .500  
REDUCED FREQUENCY = .500  
INITIAL IN-PLANE FORCE PARAMETER = .100  
MACH NUMBER = 1.20  
STRUCTURAL DAMPING COEFFICIENT = 0.000

DENSITY RATIO MU = .01500

EIGENVALUE = 5.09752E-01 -1.44227E-02 0 - .02829 FREQUENCY RATIO = .71404 STIFFNESS PARAMETER = .35702  
EIGENVECTOR  
2.71201E-01 1.73227E-03 3.49503E-01 -6.74931E-04 3.81089E-01 -1.28203E-03 4.54907E-01 -5.78048E-03 5.15697E-01 -5.75731E-03  
7.94799E-02 -1.14777E-02 6.93758E-01 -1.03775E-02 2.26185E-02 -3.87557E-03 3.60910E-01 -1.24987E-02 3.70264E-01 3.21762E-03  
4.70592E-01 -1.05057E-02 5.11406E-01 1.27015E-02 5.00000E-01 8. 6.26550E-01 -4.83439E-03 9.23917E-01 -1.21921E-02  
1.12643E-01 -1.48363E-02 6.32644E-01 -1.74833E-02 -6.32218E-01 9.42035E-03  
EIGENVALUE = 1.31424E-01 5.67010E-04 U = .00471 FREQUENCY RATIO = .32252 STIFFNESS PARAMETER = .18125  
EIGENVECTOR  
-1.60339E-01 -1.27951E-02 -1.36713E-01 -5.06322E-03 -1.24742E-01 -1.56964E-02 -1.16354E-01 -9.20402E-03 -9.96963E-03 4.70427E-02  
4.24146E-01 2.70765E-02 7.05061E-02 -1.60734E-02 6.51616E-01 -2.97705E-03 3.58316E-01 3.21471E-03 6.65137E-03 -1.87387E-02  
5.24153E-01 3.02880E-02 -1.84923E-01 1.33035E-02 -2.63591E-01 -2.33017E-02 -1.76307E-01 -1.40153E-02 6.40618E-02 -1.49576E-01  
9.15823E-01 1.43044E-02 6.92169E-01 -2.27189E-02 -5.56703E-02 -1.23074E-02  
EIGENVALUE = 7.18589E-02 -7.13719E-04 G = -.00993 FREQUENCY RATIO = .26807 STIFFNESS PARAMETER = .13403  
EIGENVECTOR  
3.70582E-01 -7.89265E-03 4.15737E-01 6.45275E-04 -3.41736E-01 -7.91461E-03 -4.82366E-01 -7.69072E-03 5.69237E-01 2.40733E-02  
-3.52513E-02 5.61880E-02 -6.12743E-01 -2.82033E-02 -2.65645E-01 -1.18713E-02 2.97272E-01 6.31790E-02 -4.00539E-01 -2.24810E-03  
-5.77016E-01 4.70239E-03 4.13103E-01 2.84316E-02 -2.93596E-01 -1.34512E-02 -3.40582E-01 -2.06160E-02 -5.51195E-01 -2.77798E-02  
-1.63210E-01 1.93235E-02 -5.31106E-01 2.46294E-02 3.20200E-01 4.10567E-02  
EIGENVALUE = 5.16318E-02 1.32179E-03 U = .03722 FREQUENCY RATIO = .22727 STIFFNESS PARAMETER = .11363  
EIGENVECTOR  
-1.17236E-01 5.26891E-02 -1.65143E-02 6.54495E-02 3.03007E-02 -1.24284E-01 1.72478E-01 -5.95032E-02 9.16949E-02 7.12945E-02  
2.09345E-01 -1.70091E-01 2.62433E-01 5.52933E-02 -1.56885E-01 2.05447E-01 -1.70349E-01 -2.79492E-01 -4.28421E-01 -2.13032E-01  
-6.26794E-01 -2.76931E-02 -2.88932E-01 -1.71884E-01 -5.08649E-02 -1.27787E-01 1.55512E-01 3.37365E-03 2.58932E-01 1.03506E-01  
-1.05595E-01 1.80141E-01 -7.06735E-01 -1.45935E-01 -9.52394E-01 -3.63004E-01

EIGENVALUE= 4.90984E-02 -2.70008E-03 G = -.05500 FREQUENCY RATIO = .22165 STIFFNESS PARAMETER = .11093  
 EIGENVECTOR  
 -1.62754E-01 2.58694E-01 -1.30407E-01 1.10518E-01 2.57932E-01 -2.15037E-01 1.84875E-01 -3.37512E-01 -2.51695E-02 -2.32032E-02  
 4.35613E-01 -5.33176E-01 -5.8703E-02 -2.04364E-01 -5.63618E-01 5.35784E-01 4.60522E-01 -9.16288E-02 1.67870E-01 4.03644E-01  
 -1.85898E-01 6.52873E-01 2.36530E-01 6.31718E-01 2.19078E-01 -1.39609E-01 7.43524E-02 -2.13394E-01 -1.06067E-01 -2.17761E-01  
 -4.53715E-01 3.40671E-01 -3.02150E-02 6.15561E-01 4.61568E-01 6.10616E-01

DENSITY RATIO MU= .02500

EIGENVALUE= 5.32935E-01 -2.16467E-02 G = -.04062 FREQUENCY RATIO = .73017 STIFFNESS PARAMETER = .36508

EIGENVECTOR  
 2.50000E-01 0. 3.41448E-01 -3.51760E-03 3.61033E-01 -5.53808E-03 4.56446E-01 -1.23192E-02 5.20538E-01 -1.24326E-02  
 1.25275E-01 -1.74406E-02 7.07136E-01 -2.16722E-02 2.88874E-02 -1.38357E-02 3.96015E-01 -2.21433E-02 -2.76765E-01 7.79475E-03  
 5.10147E-01 -2.03298E-02 -5.41673E-01 2.31675E-02 4.69374E-01 -4.82735E-03 6.22640E-01 -1.21634E-02 9.36408E-01 -2.59452E-02  
 1.84783E-01 -2.23647E-02 6.84759E-01 -3.27375E-02 -6.68778E-01 1.85861E-02

EIGENVALUE= 1.38812E-01 1.04935E-03 G = .00756 FREQUENCY RATIO = .37258 STIFFNESS PARAMETER = .18629

EIGENVECTOR  
 -1.04603E-01 -6.89992E-03 -1.16775E-01 -2.49426E-03 -1.23101E-01 -1.31556E-02 -8.71043E-02 -9.96728E-03 -3.76974E-03 9.18527E-03  
 3.75455E-01 2.41705E-02 1.10173E-01 -2.36345E-02 6.18405E-01 -2.38567E-02 4.03265E-01 7.76814E-05 5.77230E-02 -3.10560E-02  
 6.26505E-01 -6.61053E-02 -9.69051E-02 -2.79283E-02 -1.64549E-01 -1.93815E-02 -1.35186E-01 -1.59207E-02 1.06455E-01 -2.17587E-02  
 7.45558E-01 -6.43066E-03 8.15534E-01 -5.92423E-02 5.56574E-02 -2.93602E-02

EIGENVALUE= 7.65897E-02 -2.53252E-03 G = -.03307 FREQUENCY RATIO = .27679 STIFFNESS PARAMETER = .13939

EIGENVECTOR  
 4.12027E-01 -1.95277E-01 6.65881E-01 -2.99352E-01 -4.14071E-01 1.57604E-01 -6.30450E-01 2.42194E-01 9.68508E-01 -3.81281E-01  
 7.40915E-02 1.04675E-01 -8.69439E-01 3.72827E-01 -7.93337E-01 4.36014E-01 2.24850E-01 1.43233E-01 -1.06373E+00 5.65499E-01  
 -1.53347E+00 9.92652E-01 6.75830E-02 2.74023E-01 -3.81301E-01 1.32272E-01 -4.28051E-01 1.25333E-01 -7.43764E-01 2.73503E-01  
 -5.60018E-01 -4.05961E-01 -1.61438E+00 1.07450E+00 -2.268128E-01 4.43503E-01

EIGENVALUE= 6.29235E-02 2.92551E-03 G = .04649 FREQUENCY RATIO = .25092 STIFFNESS PARAMETER = .12546

EIGENVECTOR  
 -1.06237E-02 2.48302E-02 -3.42033E-03 2.35291E-02 -0.76617E-03 -2.01850E-02 1.77626E-02 -3.92211E-02 5.77140E-03 3.09169E-03  
 -1.23227E-03 -5.63873E-02 4.29342E-02 -4.21253E-02 2.70701E-03 3.84318E-02 -1.09462E-01 1.50242E-02 -1.14810E-01 6.89337E-02  
 -1.19270E-01 1.46425E-01 -1.87302E-01 2.20100E-01 -5.45281E-03 -1.51556E-02 1.89388E-02 -2.47087E-02 5.00192E-02 -3.71391E-02  
 1.54123E-03 3.17613E-02 -1.59034E-01 1.47531E-01 -2.39997E-01 2.00764E-01

EIGENVALUE= 5.60590E-02 -5.09009E-03 G = -.09080 FREQUENCY RATIO = .23701 STIFFNESS PARAMETER = .11851

EIGENVECTOR  
 -1.55215E-01 -6.35883E-02 -1.24132E-01 -7.18035E-01 -7.19035E-02 1.34613E-01 1.19970E-01 2.43910E-01 1.35685E-01 2.84460E-02  
 4.04032E-01 3.31513E-01 1.89025E-01 -2.16774E-02 -3.12504E-01 -3.62932E-01 1.07862E-02 4.01859E-01 -4.18115E-01 1.12930E-01  
 -6.33614E-01 -2.30812E-01 -8.84097E-01 3.72895E-02 9.51827E-02 9.89495E-02 1.36316E-01 6.32020E-02 1.78155E-01 -5.39036E-02  
 -1.97373E-01 -2.03916E-01 -6.62807E-01 -9.57312E-02 -8.41283E-01 2.48088E-01

DENSITY RATIO MU= .03500

EIGENVALUE= 5.48314E-01 2.174249E-02 G = -.05002 FREQUENCY RATIO = .74071 STIFFNESS PARAMETER = .37036

EIGENVECTOR

1.30488E-01 1.86381E-03 1.80838E-01 6.2281E-04 1.94158E-01 1.26498E-03 2.59137E-01 4.89550E-03 2.97829E-01 4.06782E-03

9.75207E-02 1.08278E-02 4.08435E-01 2.62385E-03 4.76252E-02 9.85934E-03 2.45424E-01 1.25471E-02 2.15796E-01 1.42145E-03

3.11389E-01 1.1287E-02 3.25394E-01 1.16760E-02 2.50000E-01 9. 3.50007E-01 3.26934E-03 5.41070E-01 1.04382E-02

1.47464E-01 1.44788E-02 4.27525E-01 1.80838E-03 3.86304E-01 6.76592E-03

EIGENVALUE= 1.46696E-01 9.67734E-04 G = .00650 FREQUENCY RATIO = .36301 STIFFNESS PARAMETER = .19151

EIGENVECTOR

-1.00595E-01 4.54388E-03 1.37439E-01 4.11745E-03 1.04070E-01 1.61930E-02 7.07381E-02 1.29360E-02 1.70118E-02 1.59682E-02

3.04615E-01 1.65880E-02 2.27403E-01 5.84057E-02 9.08478E-01 9.15125E-02 7.03397E-01 3.24541E-02 2.57293E-01 7.89166E-02

1.15589E+00 1.95723E-01 5.16180E-03 7.68747E-02 1.39487E-01 2.12439E-02 1.20344E-01 2.53449E-02 2.45304E-01 5.47607E-02

1.07992E+00 7.06030E-02 1.46338E+00 1.98238E-01 2.66887E-01 2.96891E-02

EIGENVALUE= 8.67425E-02 5.55596E-03 G = -.06405 FREQUENCY RATIO = .29167 STIFFNESS PARAMETER = .14734

EIGENVECTOR

-2.65342E-02 7.17894E-03 6.30713E-02 7.39838E-03 2.65028E-02 1.56747E-04 4.16831E-02 6.01985E-03 1.01876E-01 7.78799E-04

-2.28429E-02 1.7439E-02 9.25134E-02 1.92859E-02 1.89510E-01 2.29039E-02 1.02493E-01 8.84133E-04 2.81115E-01 1.47933E-02

4.72593E-01 3.3514E-02 2.81332E-01 5.12334E-03 3.03508E-02 2.13242E-03 2.87082E-02 2.07017E-03 6.96916E-02 2.02392E-02

1.63096E-01 3.47374E-02 5.13339E-01 2.77407E-02 3.56760E-01 2.27551E-02

EIGENVALUE= 7.20165E-02 3.63030E-03 G = .05041 FREQUENCY RATIO = .26844 STIFFNESS PARAMETER = .13422

EIGENVECTOR

2.07262E-01 7.79365E-03 2.86757E-01 2.15588E-02 8.09229E-02 2.52058E-02 2.66863E-01 9.92767E-03 2.05389E-01 1.49992E-01

-2.14332E-01 3.67896E-01 5.01234E-01 1.56515E-01 7.61090E-02 3.00814E-01 9.21890E-01 6.68092E-01 1.10741E+00 9.23564E-02

1.49016E+00 5.20238E-01 2.78452E+00 4.78847E-01 5.43011E-02 2.01282E-02 1.62893E-01 4.69472E-02 4.59507E-01 1.94382E-01

-2.50828E-02 2.30386E-01 1.60659E+00 2.79203E-01 2.97406E+00 4.91414E-04

EIGENVALUE= 6.19934E-02 6.25723E-03 G = -.10103 FREQUENCY RATIO = .24912 STIFFNESS PARAMETER = .12456

EIGENVECTOR

-2.06859E-01 9.02497E-02 2.15529E-01 1.31835E-01 2.96822E-01 2.01705E-02 4.06735E-01 5.2814E-02 1.19085E-01 1.07294E-01

9.42497E-01 2.85386E-02 1.61907E-01 2.51738E-01 7.65737E-01 2.18991E-01 7.27124E-01 6.31490E-01 3.02301E-01 7.73834E-01

-1.54335E+00 4.21525E-01 1.43855E+00 1.2234E+00 1.88821E-01 7.25743E-03 2.94225E-01 3.94037E-02 8.8036E-02 2.53365E-01

-6.17539E-01 2.59016E-01 1.25677E+00 6.21582E-01 1.09660E+00 1.52773E+00

DENSITY RATIO MU= .04500

EIGENVALUE= 5.54946E-01 3.18754E-02 G = -.05744 FREQUENCY RATIO = .74525 STIFFNESS PARAMETER = .37263

EIGENVECTOR

1.27399E-01 2.36880E-03 1.95585E-01 1.52735E-03 1.96111E-01 1.54294E-03 2.76377E-01 5.42729E-03 2.20769E-01 3.72462E-03

1.34285E-01 1.25494E-02 4.47525E-01 1.12895E-01 8.94213E-02 1.24174E-02 2.89749E-01 1.50521E-02 2.31148E-01 8.35919E-03

3.58810E-01 1.30102E-02 3.61675E-01 1.32038E-02 2.50000E-01 0. 3.69389E-01 3.11457E-03 5.83894E-01 1.15392E-02

2.07382E-01 1.71204E-02 5.01989E-01 2.21037E-02 4.20157E-01 6.27684E-03

DENSITY RATIO MU= .03500

EIGENVALUE= 5.48314E-01 G = -.05002 FREQUENCY RATIO = .74071 STIFFNESS PARAMETER = .37036

EIGENVECTOR

1.30488E-01 1.85381E-03 1.89838E-01 6.2281E-04 1.94158E-01 1.26495E-03 2.59137E-01 4.89590E-03 2.97825E-01 4.66382E-03

2.75207E-02 1.08578E-01 9.65381E-03 4.76328E-03 9.85994E-03 2.45428E-01 1.25471E-02 2.15796E-01 1.42145E-03

3.11388E-01 1.1587E-02 3.2330E-01 1.16780E-02 2.50003E-01 0. 3.50007E-01 3.26934E-03 5.41078E-01 1.0432E-02

1.47464E-01 1.44788E-02 4.27525E-01 1.80833E-02 3.86284E-01 6.75952E-03

EIGENVALUE= 1.46690E-01 G = .00660 FREQUENCY RATIO = .36301 STIFFNESS PARAMETER = .19151

EIGENVECTOR

-1.00385E-01 4.54288E-03 1.37433E-01 1.11745E-03 1.04370E-01 1.61905E-02 7.07381E-03 1.99360E-02 1.76118E-02 1.59652E-02

5.04615E-01 1.65500E-02 2.37433E-01 5.84057E-02 9.08978E-01 9.15125E-02 7.03387E-01 3.74541E-02 2.51283E-01 7.81663E-02

1.15589E+00 1.95233E-01 5.16128E-03 7.68747E-02 1.39487E-01 2.24390E-02 1.20345E-01 2.53445E-02 2.45304E-01 5.47607E-02

1.07959E+00 7.06036E-02 1.46338E+00 1.98238E-01 2.66987E-01 3.98881E-02

EIGENVALUE= 8.67425E-02 G = -.06405 FREQUENCY RATIO = .29167 STIFFNESS PARAMETER = .14734

EIGENVECTOR

-2.65345E-02 7.17694E-03 6.30731E-02 7.39838E-03 2.65026E-02 1.56747E-04 4.16231E-02 6.01935E-03 1.01876E-01 7.78799E-01

-2.28428E-02 1.74339E-02 9.57134E-02 1.92659E-02 1.89510E-01 2.90393E-02 1.02492E-01 8.8133E-04 2.81115E-01 1.47355E-02

4.72893E-01 3.35144E-02 2.81382E-01 5.12334E-03 3.00309E-02 2.13245E-03 2.87032E-02 2.07017E-03 6.98916E-02 2.00226E-02

1.63050E-01 3.47374E-02 5.13339E-01 2.177407E-02 3.58760E-01 2.27531E-02

EIGENVALUE= 7.20165E-02 G = .05041 FREQUENCY RATIO = .26844 STIFFNESS PARAMETER = .13422

EIGENVECTOR

2.07282E-01 7.79355E-03 2.86757E-01 2.15588E-02 8.09229E-02 2.52056E-02 2.65363E-01 9.99767E-03 2.06329E-01 1.49992E-01

-2.14332E-01 3.67896E-01 5.01226E-01 1.56515E-01 7.61090E-02 3.00845E-01 9.21890E-01 6.03055E-01 1.10741E+00 9.23564E-02

1.49016E+00 5.30238E-01 2.78452E+00 4.78647E-01 5.44011E-02 2.01325E-02 1.62893E-01 4.63047E-02 4.59207E-01 1.84380E-01

-2.30232E-02 2.30368E-01 1.80659E+00 2.79289E-01 2.97406E+00 4.91414E-04

EIGENVALUE= 6.19034E-02 G = -.10103 FREQUENCY RATIO = .24912 STIFFNESS PARAMETER = .12456

EIGENVECTOR

-2.06525E-01 9.02497E-02 2.15522E-01 1.31835E-01 2.36222E-01 2.01705E-02 4.08739E-01 5.32614E-02 1.19062E-01 1.07894E-01

9.49497E-01 2.85326E-02 1.81907E-01 2.51733E-01 7.65137E-01 2.18991E-01 7.27124E-01 6.81490E-01 3.32301E-01 7.75839E-01

-1.54335E+00 4.21525E-01 1.49351E+00 1.22345E+00 1.82821E-01 7.25743E-03 2.94225E-01 3.94087E-02 8.80376E-02 2.53365E-01

-6.17539E-01 2.59016E-01 1.85672E+00 6.21682E-01 1.05660E+00 1.52778E+00

DENSITY RATIO MU= .04500

EIGENVALUE= 5.54946E-01 G = -.05744 FREQUENCY RATIO = .74525 STIFFNESS PARAMETER = .37263

EIGENVECTOR

1.27329E-01 2.36930E-03 1.97585E-01 1.52735E-03 1.96111E-01 1.54294E-03 2.76377E-01 5.49729E-03 3.20769E-01 3.72462E-03

1.34285E-01 1.25434E-02 4.47522E-01 1.12655E-02 8.84213E-02 1.24174E-02 2.89449E-01 1.50521E-02 2.31148E-01 8.35919E-03

3.58810E-01 1.30102E-02 3.61675E-01 1.33086E-02 2.50000E-01 0. 3.69389E-01 3.11457E-03 5.88394E-01 1.15392E-02

2.07382E-01 1.71204E-02 5.01989E-01 2.21037E-02 4.20157E-01 6.27684E-03

EIGENVALUE= 8.48193E-02 2.74160E-02 G = .32912 FREQUENCY RATIO = .29505 STIFFNESS PARAMETER = .14753  
 EIGENVECTOR  
 2.73838E-02 3.08450E-02 6.87357E-02 1.86095E-02 5.64523E-02 1.08934E-02 9.36030E-02 7.34521E-02 9.79277E-03 5.22807E-02  
 -1.06543E-01 4.49240E-01 4.53610E-02 5.25170E-02 4.51720E-02 1.09227E-01 3.61157E-01 1.95836E-01 6.09093E-01 1.26203E-01  
 6.08063E-01 -1.34233E-01 8.03825E-01 5.47811E-01 6.39462E-02 3.19843E-03 1.28536E-01 5.98964E-02 4.01070E-02 5.04236E-02  
 -8.19423E-02 1.33127E-01 7.37270E-01 3.91096E-02 1.03655E+00 3.98229E-01

EIGENVALUE= 9.44164E-02 -1.12974E-02 G = -.11966 FREQUENCY RATIO = .30782 STIFFNESS PARAMETER = .13321  
 EIGENVECTOR  
 -6.50417E-02 2.67698E-03 -1.47682E-01 3.19603E-02 1.29629E-01 1.02455E-01 2.78463E-01 2.37004E-01 2.81163E-01 3.24131E-01  
 -1.45058E-01 5.69548E-01 5.22790E-01 4.32275E-01 6.32014E-01 5.71655E-01 3.14075E-01 1.76762E-01 9.66593E-01 1.41018E+00  
 1.72823E+00 2.38668E+00 1.10025E+00 2.37102E+00 1.46164E-01 1.40600E-01 2.62813E-01 3.03762E-01 4.65034E-01 4.22376E-01  
 3.07297E-01 3.96329E-01 1.81207E+00 2.46367E+00 1.22857E+00 2.13933E+00

EIGENVALUE= 7.07209E-02 -2.57349E-02 G = -.36389 FREQUENCY RATIO = .27017 STIFFNESS PARAMETER = .13508  
 EIGENVECTOR  
 -2.16520E-02 7.39874E-02 5.42405E-02 -1.29479E-01 9.87010E-02 3.02939E-02 2.35089E-01 2.51194E-02 2.24018E-02 1.03205E-01  
 -2.62905E-01 4.87816E-03 7.57333E-02 8.53730E-02 3.49689E-01 3.16834E-02 2.04445E-01 1.68265E-01 8.66318E-01 3.53353E-01  
 9.34458E-01 4.67458E-01 2.05382E+00 4.36255E-01 9.20345E-02 3.59456E-02 2.24342E-01 1.80030E-02 8.45523E-02 6.22851E-02  
 -3.45990E-01 -4.83319E-02 9.89420E-01 6.11273E-01 2.05250E+00 5.98348E-01

DENSITY RATIO MU= .06500

EIGENVALUE= 5.27270E-01 -3.58407E-02 G = -.06792 FREQUENCY RATIO = .72683 STIFFNESS PARAMETER = .36341  
 EIGENVECTOR  
 1.17861E-01 3.74064E-03 2.09554E-01 4.78855E-03 2.01613E-01 2.15845E-03 2.28816E-01 6.11582E-03 3.87713E-01 1.67734E-04  
 2.15066E-01 1.29055E-02 5.57428E-01 1.30575E-02 2.34814E-01 1.71986E-02 4.39393E-01 1.77942E-02 2.64798E-01 7.61677E-03  
 5.62943E-01 -1.86250E-03 4.75881E-01 1.34238E-02 3.50000E-01 0.  
 4.12510E-01 -1.91731E-02 7.65900E-01 2.81871E-02 5.06411E-01 2.99491E-04

EIGENVALUE= 2.64673E-01 -1.71390E-02 G = -.06476 FREQUENCY RATIO = .51473 STIFFNESS PARAMETER = .25737  
 EIGENVECTOR  
 4.37902E-02 -1.74077E-03 5.37372E-02 2.68016E-03 7.65742E-02 1.31182E-02 2.11678E-01 3.34171E-02 2.39309E-01 7.69874E-03  
 5.56061E-01 4.77464E-03 6.17164E-01 6.15873E-02 8.24343E-01 4.75925E-02 8.71207E-01 2.55735E-02 4.16554E-02 1.58835E-02  
 1.28023E+00 -3.57442E-02 3.32455E-01 1.78597E-02 8.07261E-03 1.97224E-02 2.39315E-01 3.43112E-02 7.36350E-01 6.13420E-02  
 1.07183E+00 3.9371E-02 1.66740E+00 3.01435E-02 1.1817E-01 9.10428E-03

EIGENVALUE= 9.43066E-02 4.74660E-02 G = .50332 FREQUENCY RATIO = .31614 STIFFNESS PARAMETER = .15807  
 EIGENVECTOR  
 3.75712E-02 3.20938E-02 8.54917E-02 2.39622E-03 7.13685E-02 6.41912E-03 1.11777E-01 8.48976E-02 1.11161E-02 4.19844E-02  
 -1.10614E-01 1.83143E-01 6.38045E-02 2.17715E-02 3.13850E-02 2.07451E-01 3.60966E-01 1.63741E-01 5.67708E-01 2.30429E-01  
 5.86131E-01 8.42902E-02 6.32171E-01 6.69974E-01 8.33220E-02 6.13506E-03 1.53548E-01 7.25543E-02 6.85757E-02 1.90434E-02  
 -8.03509E-02 2.44447E-01 7.18105E-01 5.82397E-03 8.75860E-01 5.69090E-01

EIGENVALUE= 8.23575E-02 -4.36470E-02 G = -.52997 FREQUENCY RATIO = .29628 STIFFNESS PARAMETER = .14814  
 EIGENVECTOR  
 -5.53250E-02 3.29323E-02 3.08282E-02 -1.23946E-01 1.23157E-02 -1.53127E-01 1.67850E-01 2.58841E-01 5.31677E-02 8.61495E-03  
 -2.67324E-01 2.10478E-01 8.41301E-02 1.22755E-01 3.57774E-01 1.98189E-01 2.49966E-01 5.54818E-01 4.23183E-01 4.27957E-01  
 8.02353E-02 1.15114E+00 1.03143E+00 1.61394E+00 1.61394E+00 1.61394E+00 1.43947E-01 2.33617E-01 6.91950E-02 1.28770E-01  
 -4.18761E-01 2.28633E-01 -1.55191E-02 3.1363E+00 9.67506E-01 1.83965E+00

11-11-68

EIGENVALUE= 3.39877E-02 -2.07312E-02 G = -.82270 FREQUENCY RATIO = .30845 STIFFNESS PARAMETER = .15432  
EIGENVECTOR  
1.13344E-01 4.51435E-02 1.73492E-01 1.76752E-01 -1.52124E-01 -7.48931E-02 -2.89453E-01 -2.09110E-01 9.35826E-03 5.93171E-01  
-5.97415E-01 7.17416E-01 -3.51151E-01 8.24277E-01 1.84193E-01 -1.05392E+00 -8.71865E-01 2.37371E-02 3.61143E-01 -1.23093E+00  
5.34947E-01 -2.16125E+00 1.21557E+00 -1.15457E+00 -1.77697E-01 -1.36906E-01 -2.57572E-01 -3.96383E-01 -3.23149E-01 7.65664E-01  
2.12438E-01 -5.99033E-01 1.80346E-01 -2.05634E+00 4.10725E-01 -1.45633E+00

DENSITY RATIO MU= .07500

EIGENVALUE= 4.26697E-01 -1.53055E-02 G = -.03570 FREQUENCY RATIO = .65495 STIFFNESS PARAMETER = .32743  
EIGENVECTOR  
9.51578E-02 9.90697E-03 2.19330E-01 1.14132E-01 2.10363E-01 -4.01199E-03 4.01410E-01 -1.56515E-02 5.09921E-01 -1.42673E-03  
5.14823E-01 3.31335E-02 3.11325E-01 3.62170E-02 5.88003E-01 -7.34897E-02 7.91202E-01 -6.88831E-02 2.78251E-01 -2.06925E-02  
1.04781E+00 -2.65312E-02 -9.64743E-01 2.42663E-02 2.50009E-01 0.  
8.81577E-01 -7.65575E-02 1.41101E+00 -1.23976E-01 -6.07375E-01 -1.20143E-02

EIGENVALUE= 4.00318E-01 -4.62301E-02 G = -.11356 FREQUENCY RATIO = .63885 STIFFNESS PARAMETER = .31942  
EIGENVECTOR  
1.5612E-01 -3.31363E-01 2.50745E-01 -7.49090E-01 3.05105E-01 7.53539E-01 7.05247E-01 -1.47234E+00 9.57612E-01 -1.73519E+00  
1.15010E+00 -1.87362E+00 1.56239E+00 -2.99974E+00 1.86144E+00 -3.22837E+00 1.70938E+00 -2.89987E+00 -5.0544E-01 9.05852E-01  
2.29079E+00 -3.90012E+00 -1.24198E+00 2.37998E+00 3.99183E-01 -8.85854E-01 8.92579E-01 -1.78411E+00 1.92059E+00 -3.63477E+00  
2.00456E+00 -3.25574E+00 3.07231E+00 -5.22387E+00 -1.08923E+00 2.10410E+00

EIGENVALUE= 1.01304E-01 6.58202E-02 G = .64363 FREQUENCY RATIO = .32300 STIFFNESS PARAMETER = .16650  
EIGENVECTOR  
4.70295E-02 2.62435E-02 1.02330E-01 -1.48487E-02 8.30209E-02 -2.57373E-03 1.82437E-01 -9.69425E-02 1.57972E-02 3.75457E-02  
-1.23680E-01 2.07696E-02 6.87366E-02 6.04737E-03 3.40679E-02 2.65953E-01 3.68183E-01 1.45533E-01 5.28127E-01 -2.93572E-01  
5.60526E-01 -5.71075E-02 6.13376E-01 -7.93005E-01 9.63163E-02 1.45418E-02 1.77531E-01 -8.51455E-02 7.61216E-02 -3.19236E-03  
-9.02799E-02 3.03431E-01 6.94334E-01 1.96797E-02 7.63207E-01 -5.73596E-01

EIGENVALUE= 9.93725E-02 -6.11555E-02 G = -.69297 FREQUENCY RATIO = .31474 STIFFNESS PARAMETER = .15737  
EIGENVECTOR  
-6.05221E-02 -2.77372E-02 -1.21066E-02 -1.31507E-01 -2.20041E-02 -1.46294E-01 1.82695E-01 -2.65333E-01 -5.90163E-02 -1.02352E-01  
-2.43573E-01 2.51025E-01 1.82635E-02 -1.21737E-01 -3.81049E-01 2.09476E-01 -2.71748E-01 -4.43333E-01 3.14133E-01 -8.28831E-01  
-1.19456E-01 -8.07420E-01 8.21763E-01 -1.26642E+00 3.84333E-02 -1.57331E-01 3.14712E-02 -3.05455E-01 3.53133E-03 -1.27335E-01  
-4.31203E-01 2.61327E-01 -2.32374E-01 -1.05822E-02 7.46103E-01 -1.47328E+00

EIGENVALUE= 1.00312E-01 -2.73917E-02 G = -.27334 FREQUENCY RATIO = .31945 STIFFNESS PARAMETER = .15973  
EIGENVECTOR  
1.17842E-01 5.19437E-02 1.51406E-01 2.04656E-01 -1.89757E-01 -3.48161E-02 -3.87223E-01 -2.36925E-01 -1.05352E-01 4.61636E-01  
-7.26005E-01 3.59766E-01 -1.67419E-01 -7.51566E-01 5.97041E-01 -9.30031E-01 -7.74589E-01 -1.83602E-01 9.29666E-02 -1.23174E+00  
-1.02042E+00 -3.12195E-01 1.15032E+00 7.55451E-01 -1.60316E-01 -8.92751E-03 -2.17433E-01 -3.00125E-01 -5.77106E-02 -6.04771E-01  
4.95292E-01 -4.40633E-01 6.52073E-01 -8.33513E-01 4.69093E-01 1.63958E-02

DENSITY RATIO MU= .08500

EIGENVALUE= 4.53302E-01 1.12032E-01 G = .24715 FREQUENCY RATIO = .67832 STIFFNESS PARAMETER = .33916  
EIGENVECTOR  
-5.14835E-02 2.64032E-02 -8.94550E-02 7.87637E-02 -7.29095E-02 7.40772E-02 -1.07523E-01 1.63074E-01 -1.31170E-01 2.14023E-01  
-2.95795E-02 2.59275E-01 -1.58723E-01 3.50530E-01 3.14726E-01 -9.38216E-01 -5.40799E-02 3.70376E-01 1.37722E-01 -1.15778E-01  
-4.15239E-02 4.77348E-01 1.55132E-01 -3.07168E-02 8.33732E-02 -1.49746E-01 1.95971E-01 -2.09430E-01 4.37918E-01  
-1.60196E-02 4.36390E-01 -6.02967E-02 6.49731E-01 2.14071E-01 -2.63945E-01

EIGENVALUE= 4.8065E-01 -1.9170E-01 G = -.12596 FREQUENCY RATIO = .60724 STIFFNESS PARAMETER = .33262  
EIGENVECTOR  
1.9633E-02 1.2211E-01 2.0481E-01 2.2693E-01 1.8594E-01 2.1265E-01 4.1027E-01 2.8299E-01 5.3132E-01 3.4291E-01  
6.3911E-01 1.0400E-01 8.9330E-01 1.7294E-01 1.4384E-01 3.8439E-02 3.2143E-01 2.1863E-01 2.8725E-01 3.1279E-01  
1.2052E+00 2.1343E-01 7.4389E-01 4.1118E-01 2.1390E-01 3.7123E-01 7.0322E-01 1.2931E-01 1.8457E+00 5.2479E-01  
1.0722E+00 0.7592E-01 1.6145E+00 3.3479E-01 3.5506E-01 5.5922E-01  
EIGENVALUE= 1.0749E-01 9.1677E-02 G = .75939 FREQUENCY RATIO = .34820 STIFFNESS PARAMETER = .17410  
EIGENVECTOR  
-3.2274E-02 3.1963E-02 1.3722E-01 7.3164E-02 1.1518E-01 3.0293E-02 1.2701E-01 1.2292E-01 1.7531E-02 3.5971E-02  
7.9271E-02 3.2234E-01 9.5271E-02 2.1232E-02 5.4545E-02 3.2150E-01 2.3079E-01 2.9079E-01 3.5112E-02 1.5292E-01  
-6.5113E-01 2.1249E-01 3.4393E-01 1.1555E+00 1.4536E-01 1.3043E-02 2.9792E-01 1.9153E-01 1.6390E-01 3.1120E-02  
-6.4052E-03 3.7479E-01 6.5031E-01 2.1773E-01 5.7204E-01 1.1692E+00  
EIGENVALUE= 9.4701E-02 -7.2755E-02 G = -.83124 FREQUENCY RATIO = .33018 STIFFNESS PARAMETER = .16509  
EIGENVECTOR  
1.9633E-02 5.0202E-02 5.4722E-02 9.6002E-02 2.3183E-02 2.9235E-02 1.6135E-01 1.1380E-01 2.5292E-02 2.1512E-01  
-2.2972E-01 4.2237E-02 1.5112E-01 3.2003E-01 3.2003E-01 3.2003E-01 9.6385E-02 9.6385E-02 9.6385E-02 3.6923E-01  
3.0577E-01 5.2110E-01 8.7493E-01 3.5025E-01 3.8232E-02 1.7402E-01 1.1294E-01 1.5292E-01 3.4135E-02 7.6531E-02  
3.8883E-01 6.0755E-01 1.3173E-01 6.4204E-01 9.0270E-01 4.5944E-01  
EIGENVALUE= 1.0302E-01 -3.3471E-02 G = -.30571 FREQUENCY RATIO = .33237 STIFFNESS PARAMETER = .16623  
EIGENVECTOR  
-5.4517E-02 4.7229E-02 5.4694E-02 1.4937E-01 1.1007E-01 3.8232E-02 2.0451E-01 1.2287E-01 1.2741E-01 2.3172E-01  
4.7229E-01 1.2287E-02 5.2114E-02 3.3262E-01 5.2552E-01 3.3262E-01 3.4084E-01 2.6212E-01 2.5112E-01 2.8749E-01  
-3.5232E-01 1.2287E-02 3.3262E-01 3.7032E-01 3.7032E-01 3.7032E-01 8.4737E-02 6.4737E-02 6.4737E-02 3.2003E-01  
-1.0342E-01 1.2287E-01 1.2287E-01 1.2287E-01 1.2287E-01 1.2287E-01 1.2287E-01 1.2287E-01 1.2287E-01 1.2287E-01  
EIGENVALUE= 4.2334E-01 -2.5359E-01 G = -.57592 FREQUENCY RATIO = .69103 STIFFNESS PARAMETER = .34532  
EIGENVECTOR  
9.2412E-03 9.7007E-02 3.4911E-02 1.6359E-01 2.6217E-02 1.7292E-01 1.1226E-01 1.2287E-01 1.7292E-01 1.7292E-01  
1.7292E-01 1.7292E-01 4.2334E-01 4.2334E-01 4.2334E-01 1.1226E-01 1.1226E-01 1.1226E-01 1.1226E-01 2.3200E-01  
-5.5713E-01 3.2334E-01 2.7922E-01 4.3433E-01 2.1226E-01 2.1226E-01 2.1226E-01 2.1226E-01 2.1226E-01 2.1226E-01  
-5.5713E-01 3.2334E-01 2.7922E-01 4.3433E-01 2.1226E-01 2.1226E-01 2.1226E-01 2.1226E-01 2.1226E-01 2.1226E-01  
EIGENVALUE= 4.8169E-01 1.2722E-01 G = .36976 FREQUENCY RATIO = .75337 STIFFNESS PARAMETER = .35263  
EIGENVECTOR  
1.5413E-02 1.0749E-02 1.6332E-01 3.1482E-02 1.4102E-01 3.2303E-02 2.2968E-01 1.2291E-01 2.2968E-01 1.7452E-01  
1.5413E-01 2.1226E-01 3.2334E-01 3.2445E-01 7.4389E-01 3.2334E-01 3.2334E-01 3.2334E-01 3.2334E-01 3.2334E-01  
3.5430E-01 5.4034E-01 3.7323E-01 2.2968E-01 1.7452E-01 1.7452E-01 1.7452E-01 1.7452E-01 1.7452E-01 1.7452E-01  
2.0629E-01 3.2334E-01 3.4311E-01 5.0292E-01 4.4745E-01 2.0173E-01  
EIGENVALUE= 4.2334E-01 -2.5359E-01 G = -.57592 FREQUENCY RATIO = .69103 STIFFNESS PARAMETER = .34532  
EIGENVECTOR  
9.2412E-03 9.7007E-02 3.4911E-02 1.6359E-01 2.6217E-02 1.7292E-01 1.1226E-01 1.2287E-01 1.7292E-01 1.7292E-01  
1.7292E-01 1.7292E-01 4.2334E-01 4.2334E-01 4.2334E-01 1.1226E-01 1.1226E-01 1.1226E-01 1.1226E-01 2.3200E-01  
-5.5713E-01 3.2334E-01 2.7922E-01 4.3433E-01 2.1226E-01 2.1226E-01 2.1226E-01 2.1226E-01 2.1226E-01 2.1226E-01  
-5.5713E-01 3.2334E-01 2.7922E-01 4.3433E-01 2.1226E-01 2.1226E-01 2.1226E-01 2.1226E-01 2.1226E-01 2.1226E-01  
EIGENVALUE= 4.8169E-01 1.2722E-01 G = .36976 FREQUENCY RATIO = .75337 STIFFNESS PARAMETER = .35263  
EIGENVECTOR  
1.5413E-02 1.0749E-02 1.6332E-01 3.1482E-02 1.4102E-01 3.2303E-02 2.2968E-01 1.2291E-01 2.2968E-01 1.7452E-01  
1.5413E-01 2.1226E-01 3.2334E-01 3.2445E-01 7.4389E-01 3.2334E-01 3.2334E-01 3.2334E-01 3.2334E-01 3.2334E-01  
3.5430E-01 5.4034E-01 3.7323E-01 2.2968E-01 1.7452E-01 1.7452E-01 1.7452E-01 1.7452E-01 1.7452E-01 1.7452E-01  
2.0629E-01 3.2334E-01 3.4311E-01 5.0292E-01 4.4745E-01 2.0173E-01



EIGENVALUE= 1.1920E-01 9.73798E-02 G = .85933 FREQUENCY RATIO = .36245 STIFFNESS PARAMETER = .18122  
 EIGENVECTOR  
 5.48869E-03 1.08205E-01 1.08205E-01 9.55197E-02 5.69047E-02 6.11975E-02 1.9493E-01 1.20105E-02 1.93474E-02  
 1.78282E-02 3.01015E-01 7.42489E-02 3.36714E-02 1.63080E-01 3.36714E-02 4.02715E-01 9.70877E-02 2.01375E-01 6.20985E-01  
 4.96965E-01 3.69276E-01 1.53614E-01 9.77652E-01 1.29405E-01 4.59769E-02 1.34628E-01 6.67412E-01 8.67385E-02 3.78187E-02  
 1.33796E-01 4.21306E-01 6.33033E-01 3.75537E-01 9.62203E-02 1.10091E+00  
 EIGENVALUE= 9.96124E-02 -9.47821E-02 G = -.95131 FREQUENCY RATIO = .34431 STIFFNESS PARAMETER = .17215  
 EIGENVECTOR  
 7.18216E-03 9.84635E-02 -1.44047E-01 1.19257E-01 9.94265E-02 1.51773E-01 -3.14130E-01 1.12931E-01 2.20222E-02 4.47209E-02  
 3.97760E-01 2.67795E-02 -7.1434E-02 9.85882E-02 2.31931E-01 1.85082E-01 -1.34685E-01 5.05616E-01 9.81353E-01 2.43942E-01  
 -4.92530E-01 7.0066E-01 -1.4494E+00 2.79293E-02 9.11395E-02 1.93752E-01 -3.49093E-01 1.78914E-01 7.53332E-02 1.14093E-01  
 6.19214E-01 1.74497E-01 -3.17388E-01 9.06208E-01 -1.55782E+00 2.36340E-01  
 EIGENVALUE= 1.16445E-01 -3.94212E-02 G = -.33354 FREQUENCY RATIO = .34595 STIFFNESS PARAMETER = .17298  
 EIGENVECTOR  
 4.47053E-02 1.24245E-01 1.89924E-01 -1.62443E-01 -1.23907E-02 -3.51517E-01 -1.81345E-01 -1.43195E-01 3.43248E-01  
 -5.50410E-01 8.69978E-02 -2.01115E-03 5.96301E-01 7.50455E-01 6.78313E-01 -3.73423E-01 -3.07315E-01 4.34327E-01 -5.78655E-01  
 9.59234E-01 1.08947E-02 3.82782E-01 1.53176E+00 -1.22887E-01 5.6833E-02 -1.72834E-01 -3.15110E-01 4.53044E-02 -4.39431E-01  
 5.67783E-01 -2.95022E-01 5.83937E-01 -6.94748E-02 8.05735E-02 5.55670E-01

DO NOT WRITE ON THIS COPY